Enhancement of Optical Wireless Communications Using Hybrid and Multiple Access Techniques

Hesham Sadat Badran Ibrahim

COLLEGES SCIENCES
BRETAGNE POUR L'INGENIEUR
LOIRE ET LE NUMERIQUE

ENSTA BRETAGNE

THÈSE DE DOCTORAT DE

L'ÉCOLE NATIONALE SUPÉRIEURE
DE TECHNIQUES AVANCÉES BRETAGNE

ÉCOLE DOCTORALE N° 648
Sciences pour l'Ingénieur et le Numérique
Spécialité : *Télécommunications*

Par

Hesham Sadat BADRAN IBRAHIM

Enhancement of Optical Wireless Communications Using Hybrid and Multiple Access Techniques

Thèse présentée et soutenue à Brest, le 2 Décembre 2024
Unité de recherche : Lab-STICC

Rapporteurs avant soutenance :

Karim ABED-MERAIM	Professeur, University of Orléans, Orléans, France
Cornel IOANA	Maître de conférences (HDR), INP Grenoble, France

Composition du Jury :

Président :	Christophe MOY	Professeur, Université de Rennes, Rennes, France
Examinateurs :	Karim ABED-MERAIM	Professeur, University of Orléans, Orléans, France
	Cornel IOANA	Maître de conférences (HDR), INP Grenoble, France
	Christophe MOY	Professeur, Université de Rennes, Rennes, France
	Roua YOUSSEF	Maître de conférences, Université de Rennes, Rennes, France
Dir. de thèse :	Ali MANSOUR	Professeur, ENSTA Bretagne, Brest, France
Co-dir. de thèse :	Ayman AL FALOU	Professeur, Yncréa Ouest/ISEN, Brest, France
Encadrant :	Mohamed ABAZA	Professeur, AASTMT, Cairo, Egypt

Invité(s) :

Koffi-Clément YAO	Maître de conférences (HDR), UBO, Brest, France
Marwa EL-BOUZ	Enseignant-Chercheuse (HDR), Yncréa Ouest/ISEN, Brest, France

Acknowledgement

I am deeply grateful to ALLAH for His countless blessings. I would also like to extend my heartfelt thanks to my parents and my brother for their contributions to my education. Their unwavering love, constant support, wise advice, and prayers over the years are more than I can ever fully express my gratitude for. The thought that completing my Ph.D. would bring them happiness motivated me to work even harder.

I am deeply indebted to my thesis director Prof. Ali MANSOUR, for his support, encouragement, the opportunity he provided for me to learn and grow, and his valuable comments. I thank him for always being available and helpful. I must also thank my supervisor Prof. Ayman Al FALOU, for the time he devoted to evaluating my work, identifying challenges, and engaging in discussions that helped me make significant progress in my research. I am sincerely thankful to my thesis supervisor, Prof. Mohamed ABAZA, for his invaluable feedback, insightful discussions, and constant encouragement.

I want to thank Prof. Christophe MOY from the University of Université de Rennes for being the president of my Ph.D. committee. Also, My sincere thanks go to the reviewers, Prof. Karim ABED-MERAIM from the University of Orléans and Dr. Cornel IOANA from the University of INP Grenoble, for honoring me by accepting to be rapporteurs of my dissertation. Additionally, I thank Dr. Roua YOUSSEF from Université de Bretagne Occidentale for accepting to be the examiner of my dissertation. Moreover, I would like to express my hearty thanks to my Comité de Suivi Individuel (CSI) members Dr. Koffi-Clément YAO from Université de Bretagne Occidentale and Occidentale and Dr. Marwa El BOUZ from ISEN Brest for the valuable discussions. Also, I am deeply thankful for my friends, especially Dr. Kahina BENSAFIA, Eng. Hocine MAHNI and Eng. Nour RIZK, whose encouragement helped me overcome challenges.

Finally, I would like to thank my colleagues for the enriching discussions we had during my thesis preparation: Prof. Chen CHEN from Chongqing University, Dr. Khaled METWALLY from Aix Marseille University, France, Dr. Jad ABOU CHAAYA from ENIB, France, Dr. Azza MAHDY from AASTMT, Egypt, Dr. Mohamed ABBAS from AASTMT, Egypt.

Table of Contents

Acknowledgement i

List of Figures vii

List of Tables xi

Abbreviations xiii

List of Symbols xvii

Mathematical Notation xxi

1 Introduction 1

1.1 Background . . . 1
1.2 Thesis Contributions . . . 4
1.3 Thesis Organization . . . 5

2 State of the Art 7

2.1 Introduction . . . 7
2.2 Radio Communications . . . 7
2.3 Free Space Optical Communication . . . 9
2.4 Ultraviolet Communication . . . 10
2.5 Underwater Optical Wireless Communication . . . 11
2.6 Infrared Communication . . . 11
2.7 Visible Light Communications (VLC) . . . 11
2.7.1 Features of VLC . . . 12
2.7.2 VLC architecture . . . 13
2.7.3 VLC applications . . . 13
2.7.4 Light-emitting diode . . . 16
2.8 Challenges and Motivation . . . 17
2.9 Multiple Access Techniques in VLC . . . 18

2.9.1 Time division multiple access . . . 19
2.9.2 Code division multiple access . . . 19
2.9.3 Wavelength division multiple access . . . 20
2.9.4 Orthogonal frequency division multiple access . . . 20
2.9.5 Space division multiple access . . . 22
2.9.6 Non-orthogonal multiple access . . . 23
2.9.7 Comparison of multiple access techniques . . . 25
2.10 Power Allocation Techniques in NOMA-based VLC Systems . . . 25
2.10.1 Static power allocation (SPA) . . . 27
2.10.2 Strategic design techniques . . . 28
2.10.3 Numerical search techniques . . . 31
2.11 MIMO in VLC Systems . . . 34
2.12 MIMO in NOMA-VLC Systems . . . 35
2.13 User Pairing in NOMA-VLC Systems . . . 38
2.13.1 Random user pairing . . . 39
2.13.2 Next-largest-difference-based user pairing algorithm . . . 39
2.13.3 Divide-and-NLUPA . . . 40
2.13.4 Distributed-NOMA . . . 42
2.13.5 Uniform channel gain difference . . . 42
2.13.6 Hybrid user pairing . . . 43
2.13.7 User pairing optimization algorithms . . . 44
2.14 Summary . . . 44

3 Achievable Rate Performance of NOMA-MIMO-VLC Systems 47
3.1 Introduction . . . 47
3.2 System and Channel Models . . . 47
3.3 Power Allocation Techniques and User-Pairing Algorithms . . . 52
3.3.1 Power allocation techniques . . . 53
3.3.2 User-Pairing Algorithms . . . 54
3.4 Numerical Results and Discussions . . . 56
3.4.1 Two-User Scenario . . . 57
3.4.2 Five-User Scenario . . . 64
3.4.3 Six-User Scenario . . . 71
3.4.4 Performance Comparison . . . 75

3.5 Summary 77

4 Bit Error Rate Performance of NOMA-MIMO-VLC Systems 79

4.1 Introduction 79
4.2 System Model 79
4.3 Diversity Combining Techniques 81
4.3.1 Selection combining 81
4.3.2 Equal gain combining 82
4.3.3 Maximum ratio combining 82
4.4 BER Analytical Expression 82
4.4.1 Perfect SIC 85
4.4.2 Imperfect SIC 86
4.5 Numerical Results and Discussions 87
4.5.1 Two-User Scenario 87
4.5.2 Three-User Scenario 90
4.5.3 Four-User Scenario 94
4.6 Summary 100

5 Conclusions and Future Work 101

5.1 Conclusions 101
5.2 Recommendations for Future Work 102

List of Publications 105

Bibliography 107

List of Figures

1.1 The main directions of the thesis. 4

2.1 Electromagnetic spectrum. 9
2.2 Various application scenarios of FSO systems. 10
2.3 VLC architecture. 13
2.4 Example of VLC applications platforms. 15
2.5 Number of publications on different VLC environments from several organizations (IEEE, MDPI, Elsevier and OSA) from 2000 to 2023. 15
2.6 Schematic of two main White LED architectures (a) phosphor-based, (b) RGB. 16
2.7 Comparison between TDMA, CDMA, OFDMA, and NOMA techniques concerning time, frequency, and power domains, for a 3-user example. . . . 18
2.8 Block diagram of optical OFDM transmitter and receiver. 21
2.9 An illustration of a two-user downlink NOMA scheme in the VLC system with superposition coding and SIC. 24
2.10 Block diagram of 2 × 2 MIMO-based NOMA-VLC system with N users. . 36
2.11 Random user pairing. 39
2.12 NLUPA pairing. 39
2.13 D-NLUPA pairing. 40
2.14 D-NOMA pairing. 41
2.15 UCGD pairing. 43
2.16 Hybrid pairing. 43

3.1 The downlink 2 × 2 NOMA-MIMO-VLC system serving N users. 48
3.2 VLC channel model. 50
3.3 Schematic of a 2 × 2 NOMA-MIMO-VLC system with N users. 51
3.4 Illustration of user grouping and pairing for even and odd number of users using NLUPA and UCGD. 55

3.5 Achievable rate vs. normalized offset based NOMA using FPA with two users ($N = 2$): (**a**) LED 1, (**b**) LED 2. 58
3.6 Achievable rate vs. normalized offset-based NOMA and OFDMA with two users ($N = 2$) (**a**) LED 1, (**b**) LED 2. 59
3.7 Achievable rate vs. normalized offset based NOMA using NGDPA, GRPA and FPA with two users ($N = 2$). 61
3.8 Sum rate vs. normalized offset based NOMA using NGDPA, GRPA and FPA with two users ($N = 2$). 62
3.9 Sum rate gain vs. normalized offset based NOMA using NGDPA, GRPA and FPA with two users ($N = 2$). 63
3.10 Achievable rate vs. normalized offset-based NOMA with five users ($N = 5$) for LED 1 using (**a**) FPA, (**b**) GRPA, (**c**) NGDPA, and for LED 2 using (**d**) FPA, (**e**) GRPA, (**f**) NGDPA. 64
3.11 Achievable rate vs. normalized offset-based NOMA with five users ($N = 5$) with Strategy 1 NLUPA/UCGD user pairing of LED 1 using (**a**) FPA, (**b**) GRPA, (**c**) NGDPA, and of LED 2 using (**d**) FPA, (**e**) GRPA, (**f**) NGDPA. 66
3.12 Achievable rate vs. normalized offset-based NOMA with five users ($N = 5$) with Strategy 2 NLUPA user pairing of LED 1 using (**a**) FPA, (**b**) GRPA, (**c**) NGDPA, and of LED 2 using (**d**) FPA, (**e**) GRPA, (**f**) NGDPA. . . . 68
3.13 Achievable rate vs. normalized offset-based NOMA with five users ($N = 5$) with Strategy 2 UCGD user pairing of LED 1 using (**a**) FPA, (**b**) GRPA, (**c**) NGDPA, and of LED 2 using (**d**) FPA, (**e**) GRPA, (**f**) NGDPA. . . . 70
3.14 Achievable rate vs. normalized offset-based NOMA with six users ($N = 6$) for LED 1 using (**a**) FPA, (**b**) GRPA, (**c**) NGDPA, and for LED 2 using (**d**) FPA, (**e**) GRPA, (**f**) NGDPA. 71
3.15 Achievable rate vs. normalized offset-based NOMA with six users ($N = 6$) with NLUPA user-pairing of LED 1 using (**a**) FPA, (**b**) GRPA, (**c**) NGDPA, and of LED 2 using (**d**) FPA, (**e**) GRPA, (**f**) NGDPA. 72
3.16 Achievable rate vs. normalized offset-based NOMA with six users ($N = 6$) with UCGD user-pairing of LED 1 using (**a**) FPA, (**b**) GRPA, (**c**) NGDPA, and of LED 2 using (**d**) FPA, (**e**) GRPA, (**f**) NGDPA. 74
3.17 Sum rate vs. normalized offset-based OFDMA and NOMA with five users ($N = 5$) (**a**) without grouping, (**b**) NLUPA/UCGD Strategy 1, (**c**) NLUPA Strategy 2, (**d**) UCGD Strategy 2. 75

3.18 Sum rate vs. normalized offset-based OFDMA and NOMA with six users ($N = 6$) (**a**) without grouping, (**b**) NLUPA, (**c**) UCGD. 76

4.1 Illustration of a downlink NOMA-MIMO-VLC system accommodating N users. 80
4.2 Multi-user NOMA-MIMO-VLC downlink system. 81
4.3 BER vs. power allocation factor (α) of FPA. 88
4.4 BER vs. transmit SNR utilizing SC with NGDPA, GRPA and FPA with two users ($N = 2$). 88
4.5 BER vs. transmit SNR utilizing EGC with NGDPA, GRPA and FPA with two users ($N = 2$). 89
4.6 BER vs. transmit SNR utilizing MRC with NGDPA, GRPA and FPA with two users ($N = 2$). 90
4.7 BER vs. transmit SNR employing NGDPA, GRPA and FPA with three users ($N = 3$) using (**a**) SC, (**b**) EGC, (**c**) MRC. 91
4.8 BER vs. transmit SNR employing NGDPA, GRPA and FPA with three users ($N = 3$) applying user pairing using (**a**) SC, (**b**) EGC, (**c**) MRC. . . 93
4.9 BER vs. transmit SNR employing NGDPA, GRPA and FPA with four users ($N = 4$) using (**a**) SC, (**b**) EGC, (**c**) MRC. 95
4.10 BER vs. transmit SNR employing NGDPA, GRPA and FPA with four users ($N = 4$) applying NLUPA using (**a**) SC, (**b**) EGC, (**c**) MRC. 97
4.11 BER vs. transmit SNR employing NGDPA, GRPA and FPA with four users ($N = 4$) applying UCGD using (**a**) SC, (**b**) EGC, (**c**) MRC. 99

List of Tables

2.1 Comparison between different multiple access techniques 25
2.2 A summary of power allocation optimization in NOMA downlink VLC systems. 32
2.3 Comparison of different power allocation methods. 33
2.4 An overview of MIMO-based NOMA-VLC systems. 37

3.1 Simulation parameters 57
3.2 User ordering of two-user scenario for both LEDs at different Q values. . . 58
3.3 User ordering of five-user scenario for both LEDs at different Q values. . . 65
3.4 User ordering of five-user scenario with Strategy 1 NLUPA/UCGD user pairing for both LEDs at different Q values. 67
3.5 User ordering of five-user scenario with Strategy 2 NLUPA user pairing for both LEDs at different Q values. 69
3.6 User ordering of five-user scenario with Strategy 2 UCGD user pairing for both LEDs at different Q values. 70
3.7 User ordering of six-user scenario for both LEDs at different Q values. . . . 72
3.8 User ordering of six-user scenario with NLUPA for both LEDs at different Q values. 73
3.9 User ordering of six-user scenario with UCGD user pairing for both LEDs at different Q values. 74

4.1 The power distribution in three-user scenario: p_n is the power assigned to the nth user. 91
4.2 Summary of SNR values at a BER of 10^{-5} for SC, EGC, and MRC employing NGDPA, GRPA, and FPA techniques in a three-user scenario. . . . 92
4.3 The power distribution in three-user scenario with user pairing. 94
4.4 Summary of SNR values at a BER of 10^{-5} for SC, EGC, and MRC employing NGDPA, GRPA, and FPA techniques in a three-user scenario with user pairing. 94

4.5 The power distribution in four-user scenario. 96
4.6 Summary of SNR values at a BER of 10^{-5} for SC, EGC, and MRC employing NGDPA, GRPA, and FPA techniques in a four-user scenario. . . . 96
4.7 The power distribution in four-user scenario with NLUPA. 97
4.8 Summary of SNR values at a BER of 10^{-5} for SC, EGC, and MRC employing NGDPA, GRPA, and FPA techniques in a four-user scenario with NLUPA. 98
4.9 The power distribution in four-user scenario with UCGD. 99
4.10 Summary of SNR values at a BER of 10^{-5} for SC, EGC, and MRC employing NGDPA, GRPA, and FPA techniques in a four-user scenario with UCGD. 100

Abbreviations

2G	Second Generation
3G	Third Generation
4G	Fourth Generation
5G	Fifth Generation
6G	Sixth Generation
ACO-OFDM	Asymmetrically Clipped Optical OFDM
ADC	Analog to Digital Converter
ANFR	Agence Nationale des Fréquences
AP	Access Point
APA	Arbitrary Power Allocation
AUV	Autonomous Underwater Vehicle
BD	Block Diagonalization
BER	Bit Error Rate
BMUP	Bipartite Matching based User Pairing
CDMA	Code Division Multiple Access
CD-NOMA	Code-Domain NOMA
CP	Cyclic Prefix
CS	Cuckoo Search
CSI	Channel State Information
CSIPA	CSI-based Power Allocation
DAC	Digital to Analog Converter
DC	Direct Current
DCO-OFDM	Direct Current biased Optical OFDM
DD	Direct Detection
DE	Differential Evolution
D-NOMA	Distributed-NOMA
D-NLUPA	Divide and-NLUPA
DPA	Dynamic Power Allocation
EGC	Equal Gain Combining

EMI	Electromagnetic Interference
EPA	Enhanced Power Allocation
ES	Exhaustive Search
FCC	Federal Communications Commission
FDMA	Frequency Division Multiple Access
FFT	Fast Fourier Transform
FoV	Field of View
FPA	Fixed Power Allocation
FSO	Free Space Optical
FTPA	Fractional Transmit Power Allocation
GP	Gradient Projection
GPA	General Power Allocation
GPS	Global Positioning System
GRPA	Gain Ratio Power Allocation
HPV	Hybrid Power line VLC
ICI	Inter-Cell Interference
IFFT	Inverse FFT
IFS	Improved Fractional Strategy
IFTPA	Improved FTPA
IM	Intensity Modulation
IoT	Internet of Things
IPA	Inverse Power Allocation
IPLS	Inverse Power Law Strategy
IPLSPA	Improved Power Law Strategy Power Allocation
IR	Infrared
ISFA	Intra Symbol Frequency Averaging
ISI	Inter-Symbol Interference
ITS	Intelligent Transportation Systems
ITU	International Telecommunication Union
IUI	Inter-User Interference
LAN	Local Area Network
LASER	Light Amplification by Stimulated Emission of Radiation
LD	Laser Diode
LED	Light-Emitting Diode

LOS	Line of Sight
MADM	Multi-Attribute Decision Making
MED	Minimum Euclidean Distance
MFOPA	Multi-Factor control Optimal Power Allocation
MIMO	Multiple-Input Multiple-Output
MISO	Multiple-Input Single-Output
ML	Maximum-Likelihood
MM	Majorization-Minimization
MMSE	Minimum Mean Square Error
mmWave	Millimeter-Wave
MRC	Maximum Ratio Combining
NGDPA	Normalized Gain Difference Power Allocation
NLGRPA	Normalized Logarithmic Gain Ratio Power Allocation
NLOS	Non-Line of Sight
NLUPA	Next-Largest-Difference User-Pairing Algorithm
NMPA	Nonlinear Marine Predator Algorithm
NOMA	Non-Orthogonal Multiple Access
OCDMA	Optical Code Division Multiple Access
OFDM	Orthogonal Frequency Division Multiplexing
OFDMA	Orthogonal Frequency Division Multiple Access
OMA	Orthogonal Multiple Access
OOC	Optical Orthogonal Codes
OOK	On-Off Keying
OPA	Optimal Power Allocation
OQAM	Offset Quadrature Amplitude Modulation
OSDMA	Optical SDMA
OSTBC	Orthogonal Space-Time Block Coding
OTDMA	Optical Time-Division Multiple Access
OWC	Optical Wireless Communication
PAPR	Peak-to-Average Power Ratio
PD	Photodetector
PDF	Probability Density Function
PLC	Power Line Communication
PLS	Power Law Strategy

P/S	Parallel-to-Serial
PSO	Particle Swarm Optimization
QoS	Quality of Service
RB	Resource Block
RC	Repetition Coding
RF	Radio Frequency
RGB	Red-Green-Blue
ROC	Random Optical Codes
SC	Selection Combining
SDMA	Space Division Multiple Access
S-GRPA	Simplified Gain Ratio Power Allocation
SIC	Successive Interference Cancellation
SINR	Signal-to-Interference Plus Noise Ratio
SISO	Single-Input Single-Output
SM	Spatial Modulation
SMP	Spatial Multiplexing
SNR	Signal to Noise Ratio
S/P	Series-to-Parallel
SPA	Static Power Allocation
SS	Signature Sequences
TDMA	Time Division Multiple Access
UCGD	Uniform Channel Gain Difference
UOC	Underwater Optical Communication
UV	Ultraviolet
UVC	Ultraviolet Communication
VL	Visible Light
VLC	Visible Light Communication
WDMA	Wavelength Division Multiple Access
Wi-Fi	Wireless Fidelity
ZF	Zero Forcing

List of Symbols

α	Power allocation factor
$\alpha_{i,n}$	Power allocation factor of the nth user at ith LED
α_n^{FTPA}	Power allocation factor of the nth user utilizing FTPA
α_n^{IFS}	Power allocation factor of the nth user utilizing IFS
α_n^{IPLS}	Power allocation factor of the nth user utilizing IPLS
α_n^{PLS}	Power allocation factor of the nth user utilizing PLS
Γ	FET channel noise factor
$\gamma_{i,n}$	ith element of vector $\boldsymbol{\gamma}_n$
κ	Boltzmann's constant $\kappa = 1.38 * 10^{-23}$ J$/K$
$\mho_{i,m}$	mth user pair for the ith LED
μ_n	Mean of the received signal at the nth user
$\Phi_{1/2}$	Semi-angle at half power
ϕ_n	Angle of irradiance
ψ_c	Field of view
ψ_n	Angle of incidence
ρ_{n_k}	Threshold for detecting the kth user's signal at U_n
$\sigma^2_{sh_n}$	Variance of the shot noise at the nth user
$\sigma^2_{th_n}$	Variance of the thermal noise at the nth user
$\sigma^2_{z_n}$	Total variance at the nth user
ζ	Modulation index
A	Detection area of PD
B	Bandwidth
c	Possible symbol combinations
C_{pd}	Fixed capacitance of the photodetector
D	Distance between user 1 and user N
$d_{ji,n}$	Distance between the ith LED and the jth PD of the nth user
d_l	Spacing between the LEDs
d_{lu}	Vertical spacing between the users and LEDs
d_{pd}	Distance between PDs of each user
G_{ol}	Open-loop voltage gain
$g(\psi_n)$	Gain of the optical concentrator
g_m	FET transconductance
$\mathbf{H}_n$	Channel gain matrix of the nth user
$h_{ji,n}$	Channel gain between the jth PD of the nth user and the ith LED
I	Total number of LEDs

I_2	Noise bandwidth factor
I_3	Weighting function
I_{bg}	Photocurrent due to background radiation
I_{DC}	DC bias current provided for the LED
J	Total number of PDs
l	Potential error combinations at the nth user
L	Distance between user 1 and the room edge
m	Order of Lambertian emission
N	Total number of users
$\mathcal{N}(\mu, \sigma^2)$	PDF of a Gaussian distribution with mean μ and variance σ^2.
n_c	Reflective index of the optical concentrator
p_{elec}	Total electrical power
P_{e_n}	Overall error probability for the nth user
$P_{e_{n\to k}}$	Error probability at the nth user in decoding the signal intended for the kth user
$P_{e_{n\to k\|s_k=0}}$	Conditional probability of error at the nth user in decoding the signal intended for the kth user when $s_k = 0$
$P_{e_{n\to k\|s_k=1}}$	Conditional probability of error at the nth user in decoding the signal intended for the kth user when $s_k = 1$
$P(e_n^l \mid e_{n+1}^l e_{n+2}^l \dots e_N^l)$	Error probability for the lth error combination at the nth user
$P_{e_{n_{im}}}$	Error probability for the nth user for Imperfect SIC decoding
$P_{e_{n_{per}}}$	Error probability for the nth user for Perfect SIC decoding
$P_{e_{n\to k\|n=k}}$	Error probability associated with self-decoding
$P_{e_{n_v}}$	Error probability of the vth user as decoded at the nth user
$p_{i,n}$	Power allocated at the ith LED for the nth user
P_o	Output optical power of the LED
P_{r_n}	Received optical power for the nth user
q	Electronic charge $q = 1.6 * 10^{-19}$
Q	Normalized offset of user n relative to user 1
$R_{i,n}$	Achievable data rate for the nth user
R_p	Responsivity of PD
$s_{i,n}$	Signal modulated in the ith LED for the nth user
$\widehat{s}_v$	Decoded symbol corresponding to the vth user
$\mathbf{T}$	Potential interference combinations matrix
T_k	Absolute temperature
$T_s(\psi_n)$	Gain of the optical filter
U_n	User n
w_{jn}	Allocated weight at jth PD at the nth user
$\mathbf{x}$	Transmitted signal vector
$\widetilde{\mathbf{x}}$	Estimated signal vector
x_i	Superimposed input signal to the ith LED
$\mathbf{y}_n$	Received signal vector at the nth user

y_n	Output signal at the nth user
$\widehat{y}_n$	Decoded signal at the nth user
$\mathbf{z}_n$	Additive white Gaussian noise vector
z_n	Additive white Gaussian noise

Mathematical Notation

$(\cdot)^{-1}$	The inverse of a matrix
$(\cdot)^T$	The transpose of a matrix
$Q(\cdot)$	Gaussian-Q function

Chapter 1

Introduction

1.1 Background

Visible light communication (VLC) is an ancient method that utilizes visible light for the transmission of messages between different locations. In ancient China, the use of flames for communication proved to be an efficient means of relaying signals from border sentry stations to remote command offices along the Great Wall. Similarly, lighthouses were strategically positioned along coastlines and islands to guide cargo ships navigating the seas. The Romans employed polished metallic plates to reflect sunlight for long-distance signaling purposes. Optical communication systems based on semaphore lines were pioneered in the 1790s. The initial visual telegraphy system, established by Claude Chappe in 1792 in France, facilitated information exchange between cities [1].

During the late 19th and early 20th centuries, the heliograph, a wireless solar telegraph developed by the US military in the early 1800s, relied on Morse code flashes produced by reflecting sunlight with a mirror [2]. These flashes were generated through the interruption of the light beam using a shutter or momentarily pivoting the mirror. In 1880, Alexander Graham Bell introduced the photophone, a device that transmitted voice signals via a light beam [3]. The voice signals were directed towards a mirror, causing vibrations that were then reflected by sunlight; upon reception, the sunlight vibrations were converted back into a voice signal. Bell's experiment involved modulating the voice signal onto sunlight, enabling information transmission over a distance of approximately 213 m. However, a significant drawback of this device was its poor performance in cloudy weather. Although this experiment did not lead to a commercial product, Bell regarded this optical technology as his most significant invention, surpassing even his invention of the modern telephone which uses electricity to transmit voice. This breakthrough paved the way for illustrating the fundamental principle of optical wireless communication (OWC).

The inception of optical communication garnered substantial attention following the emergence of light amplification by stimulated emission of radiation (LASER) and the

laser diode (LD) during the 1960s. This progress continued with the introduction of low-loss optical fibers as a means of information transmission utilizing light in the 1970s, the invention of the optical fiber amplifier in the 1980s, and the development of the in-fiber Bragg grating in the 1990s. These technological advancements laid the foundation for the telecommunications revolution of the late 20th century and established the infrastructure for the Internet. Consequently, research largely shifted its focus toward optical fiber transmission rather than free-space transmission [4].

Despite their high data transmission rates and reliable performance, fiber optics have several limitations. A key drawback is the necessity for physical cabling, which can result in high costs and labor-intensive installation and maintenance procedures. This infrastructure constraint also limits the flexibility and scalability of fiber optic networks, especially in dynamic environments where frequent changes or expansions are necessary. In addition, fiber optic systems are vulnerable to bending losses and physical impairment, leading to signal degradation and necessitating repairs. Furthermore, fiber optics encounter difficulties in penetrating buildings and other obstructions. In contrast, VLC offers wireless connectivity without extensive cabling, providing a versatile and cost-effective solution for modern communication needs.

In the 1980s, the emergence of high-efficiency red and yellow light emitting diodes (LEDs) spurred the idea of using solid-state lighting for the purpose of illumination. The inception of the first white LED for commercial purposes occurred in 1996, marking a significant milestone in the lighting industry [5]. LED lights are recognized for their high energy efficiency, minimal carbon emissions, absence of mercury, long-lasting durability, and production of superior quality illumination. Comparative studies have shown that LED lights consume 75% less power and have a lifespan that is 25% longer than traditional incandescent lamps [6].

In the early 1990s, mobile phones were primarily utilized for voice calls and text messaging. Nowadays, smartphones are equipped with a variety of sensors and applications aimed at facilitating health monitoring, video conferencing, online media streaming, as well as financial transactions and utilization of cloud services. Additionally, the proliferation of Internet of Things (IoT) devices, such as smart home systems, wearable technology, industrial sensors, and autonomous vehicles [7]. Expanding wireless communication necessitates a wider bandwidth to ensure uninterrupted connectivity and increased data rates. Nevertheless, the frequency spectrum below 6.5 GHz is currently heavily utilized, leaving no space for allocating additional spectrum for mobile applications and IoT services.

This challenge has prompted researchers to explore novel wireless technologies capable of meeting the requirements for higher data rates at a reduced cost. One promising solution in this regard is the utilization of the visible light spectrum, which offers advantages such as the availability of LED lights, enhanced security, greater bandwidth, and the potential for frequency reuse. The advancement of cost-effective optoelectronic devices, such as LEDs, LDs, photodiodes (PDs), and various optical components, has led to significant improvements in VLC systems. Moreover, the demand for data is particularly high in indoor environments, given that individuals spend approximately 80% of their time indoors [8]. Therefore, employing VLC in indoor environments for high data rate applications could potentially alleviate strain on the limited radio frequency (RF) spectrum, thereby paving the way for other applications like smart cities and autonomous vehicles. In 2003, the term VLC was initially introduced by Nakagawa Laboratory. A series of foundational investigations were conducted by S. Haruyama and M. Nakagawa at Keio University in Japan. They explored the potential of using white LEDs to provide simultaneous illumination and communication in VLC systems [9], [10].

Despite the numerous advantages of VLC, several factors impose significant challenges to fully realizing its potential. One of the primary challenges is the line-of-sight (LOS) requirement for optimal communication, as physical obstructions can severely degrade signal quality. Additionally, ambient light interference can introduce noise and reduce the reliability of VLC systems. The limited coverage area of LED transmitters necessitates a dense deployment of transmitters to ensure seamless connectivity. Moreover, the modulation bandwidth of LEDs is typically constrained to a few MHz, potentially limiting the achievable data rates. Addressing these challenges is crucial for the widespread adoption and efficient operation of VLC systems [11]–[13].

Despite the aforementioned challenges, the integration of advanced technologies such as Multiple-Input Multiple-Output (MIMO) and Non-Orthogonal Multiple Access (NOMA) presents promising solutions to enhance the performance of VLC systems. MIMO technology, by utilizing multiple LED transmitters and PD receivers, can increase both system capacity and reliability. This approach helps mitigate the limitations imposed by the narrow coverage area and the LOS requirement, as it enables more robust communication in dynamic environments [14], [15].

On the other hand, NOMA improves spectral efficiency by allowing multiple users to share the same frequency and time resources through power-domain multiplexing. By allocating power based on the users' channel conditions, NOMA enhances the system's

capacity and user fairness, addressing the limited bandwidth of LEDs. In this thesis, we focus on leveraging MIMO and NOMA to overcome the constraints of VLC, investigating their combined impact on enhancing overall system performance [16], [17].

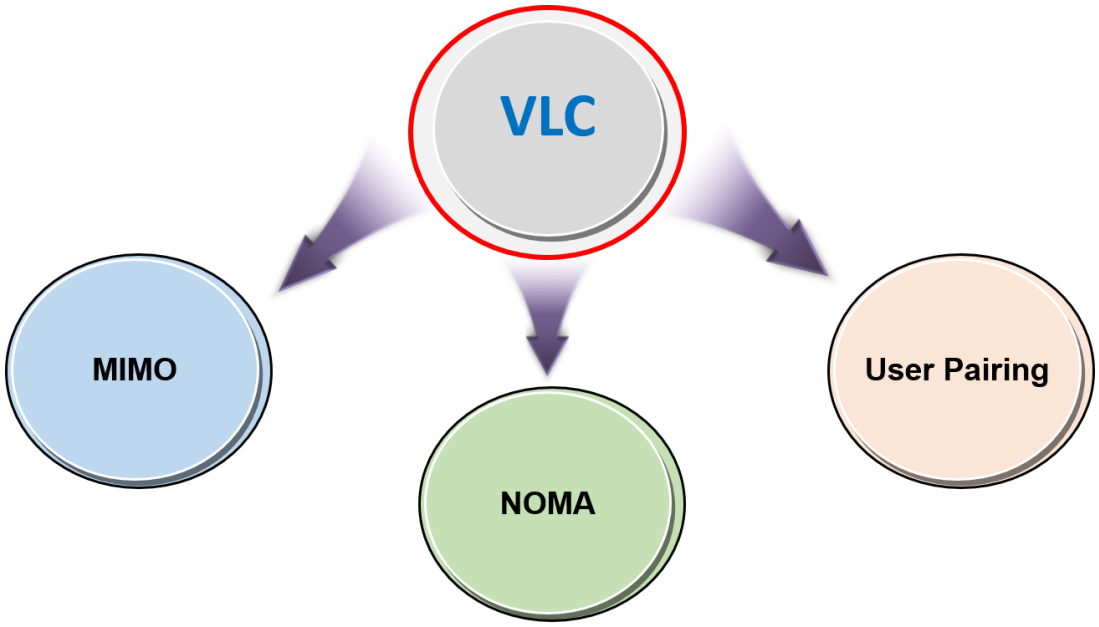

Figure 1.1 – The main directions of the thesis.

1.2 Thesis Contributions

The primary objective of this thesis is to offer reliable solutions to the aforementioned challenges of VLC. Figure 1.1 shows the main directions considered in the thesis. In summary, the key contributions of this thesis are listed as follows:

1. Power allocation plays a crucial role in the performance of NOMA. For the practical implementation of MIMO-NOMA-VLC systems, it is essential to employ efficient power allocation methods with low computational complexity. The performance of various low-complexity power allocation techniques such as: fixed power allocation (FPA), gain ratio power allocation (GRPA), normalized gain difference power allocation (NGDPA) is investigated in MIMO-NOMA-based VLC systems. Moreover, We evaluated the value of the power allocation coefficient that attains the best achievable rate for the FPA technique.

2. User pairing algorithms: Two low complexity user pairing algorithms, uniform channel gain difference (UCGD) and next largest difference user pairing algorithm (NLUPA), are utilized to manage the complexity of NOMA's successive interference cancellation (SIC) process in MIMO-NOMA-VLC systems. These algorithms are crucial in grouping users in a way that maximizes overall system performance.
3. Evaluation of achievable rate: this thesis provides a comprehensive assessment of the achievable rate in MIMO-NOMA-VLC systems employing the suggested power allocation techniques and user pairing algorithms. Comparative analyses are conducted to demonstrate the superiority of NOMA utilizing different power allocation techniques over orthogonal frequency division multiple access (OFDMA). Additionally, the performance of user pairing algorithms is evaluated in scenarios with even numbers of users, as well as in odd-numbered user scenarios where two different strategies are applied.
4. Assessment of bit error rate (BER): The error rate performance of two efficient user-pairing algorithms in conjunction with three low-complexity power allocation techniques in MIMO-NOMA-VLC systems, utilizing various diversity combining techniques, is investigated. An analytic expression for the BER is derived for an arbitrary number of users, assuming perfect channel state information (CSI).

1.3 Thesis Organization

This thesis includes the presented research work in five chapters. First, the state-of-the-art techniques and a literature review are covered in Chapter 2. Chapter 3 presents the achievable rate performance of MIMO-NOMA-VLC system. The evaluation of the BER performance of the system is discussed in Chapter 4 and the conclusions with the future work are drawn in Chapter 5. In particular, this thesis is organized as follows:

Chapter 2 reviews the state of the art in VLC communication systems, covering key technologies, the features and architecture of VLC systems, and their applications. It also discusses the motivation behind VLC and the major challenges it faces. Furthermore, this chapter introduces offered solutions, including various multiple access techniques, NOMA with different power allocation strategies, MIMO, and diverse user grouping algorithms.

Chapter 3 presents an achievable rate analysis of MIMO communication systems in a NOMA-based indoor VLC environment. Three low-complexity power allocation techniques are examined alongside two efficient user-pairing algorithms for NOMA-VLC, considering scenarios with both even and odd numbers of users. The system's performance is compared to NOMA without user pairing and to OFDMA, demonstrating significant enhancements in achievable rate.

Chapter 4 discusses the BER performance of MIMO-NOMA-VLC systems, incorporating various diversity combining techniques and the derivation of the corresponding analytical expression.

Chapter 5 provides the conclusions of the presented research work and gives some prospects for further investigations related to the scope of the thesis.

Chapter 2

State of the Art

2.1 Introduction

This chapter delves into a key technology of modern wireless communication. Indeed, visible light communication (VLC) has emerged as a promising solution by leveraging the visible light spectrum. However, to fully harness the potential of VLC, several challenges must be addressed, which motivates the need for advanced techniques and strategies. We also explore critical and essential aspects for overcoming challenges in VLC systems. We begin by discussing multiple access techniques, focusing on non-orthogonal Multiple Access (NOMA). Next, we discuss power allocation techniques, which are crucial for enhancing the performance of NOMA-based VLC systems. Following this, we investigate the integration of multiple-input multiple-output (MIMO) technology with VLC. Lastly, we study user pairing algorithms, essential for managing the complexity of NOMA.

2.2 Radio Communications

Wireless communication is essential in the modern era of information technology, supporting many everyday applications, such as: cellular telecommunications and global positioning system (GPS) localization [18]–[20]. The COVID-19 pandemic, along with measures like curfews, teleworking, and remote education, has increased internet traffic and strained wireless local area networks (LANs) [21], [22]. Additionally, the exponential growth of multimedia applications and wireless connected devices, driven by mobile applications and the Internet of Things (IoT), has created an extraordinary demand for high-data-rate wireless connectivity [17], [23]. In this respect, next generations (beyond 5G) of wireless networks are expected to provide high system capacity, high quality of service (QoS), massive device connectivity, low latency, and high energy efficiency. Unfortunately, radio frequency (RF) communication in wireless networks suffers from limited spectrum resources, defined globally by the International Telecommunication Union (ITU), and

licensed locally by regulatory bodies as the Agence Nationale des Fréquences (ANFR) in France. Most of the applications and services are congested in traditional RF bandwidth sub 6.5 GHz [24], [25]. Figure 2.1 highlights the wideness of the electromagnetic spectrum that can be utilized effectively. Several features and technologies have opened up many possibilities to fulfill the anticipated requirement of 5G and beyond wireless networks [26], [27]. To address the growing demand for wireless data traffic, the main approaches include: (i) improving the spectral efficiency of existing RF solutions; (ii) utilizing the entire RF bandwidth from 3 kHz to 300 GHz; and (iii) exploiting the available spectrum beyond 300 GHz [28]–[30].

The first approach involves enabling techniques such as advanced multiple access methods, new modulation schemes, and massive multiple-input multiple-output (MIMO) to enhance the spectral efficiency of conventional RF communication. The second approach leverages the wide spectrum of millimeter-wave (mmWave) bands (20–100 GHz) to meet capacity requirements and alleviate spectrum shortages [31], [32]. However, mmWave communications face challenges due to their sensitivity to blockages and high propagation loss at high carrier frequencies [33]. Spectrum extension by utilizing unoccupied frequency bands, as proposed in the second and third approaches, provides a direct solution for wireless mobile networks, with global mobile data traffic expected to reach up to 5 zettabytes by 2030 [34], [35]. The frequency band (95 GHz–3 THz) has been designated for sixth-generation (6G) research to meet future data traffic demands according to the Federal Communications Commission (FCC) [36], [37]. However, deploying 6G systems presents technical challenges, such as overcoming the high propagation and atmospheric absorption of THz frequencies, which requires new transceiver designs [38], [39]. By considering the third approach, many researchers are exploring optical wireless communication (OWC), including ultraviolet (UV), infrared (IR), and visible light (VL), as a promising complementary and alternative technique to RF. Utilizing optical frequency bands for wireless data transmission is an attractive solution due to its vast unlicensed bandwidth and advancements in solid-state optical technology [40]–[42]. OWC systems encompass outdoor systems such as free space optical (FSO), ultraviolet communication (UVC), and underwater communications [43], [44]. Additionally, IR communication and visible light communication (VLC) systems are widely used in indoor environments [45]–[49].

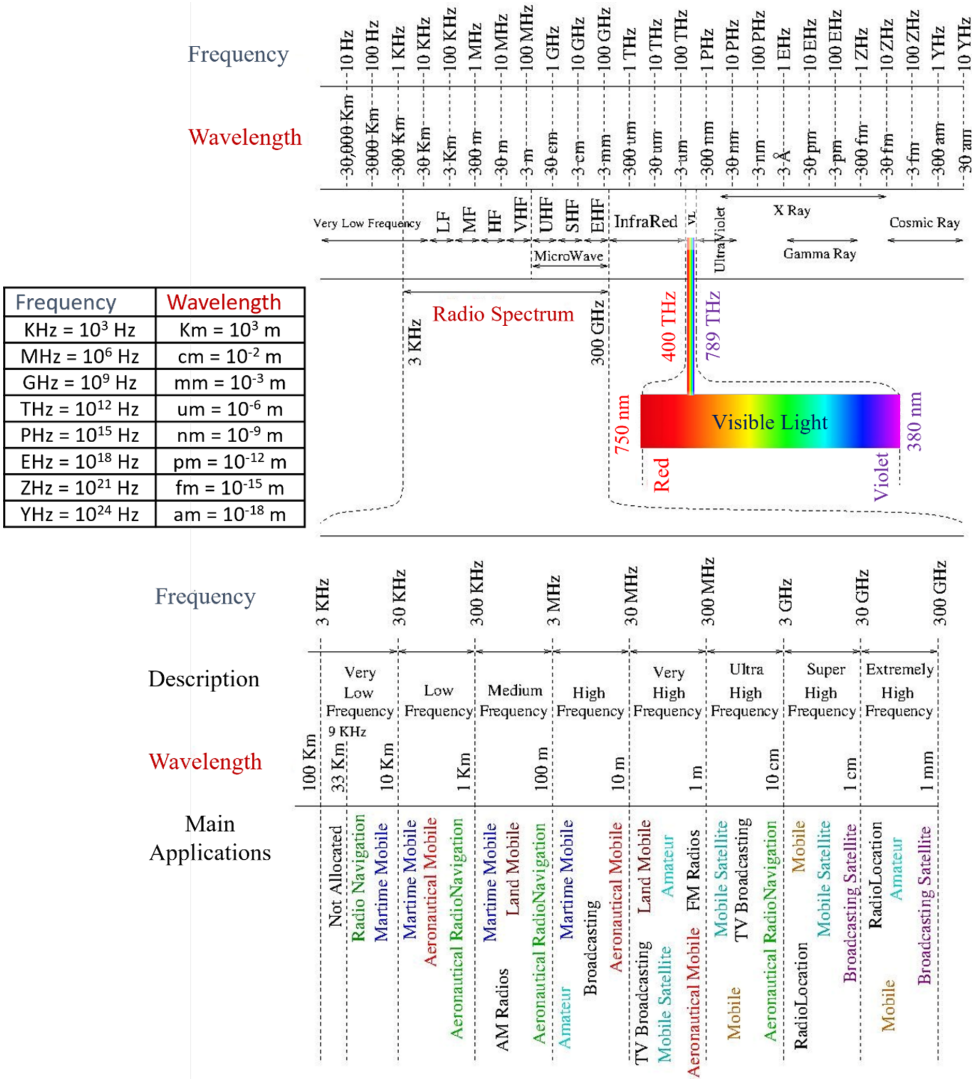

Frequency	Wavelength
KHz = 10^3 Hz	Km = 10^3 m
MHz = 10^6 Hz	cm = 10^{-2} m
GHz = 10^9 Hz	mm = 10^{-3} m
THz = 10^{12} Hz	um = 10^{-6} m
PHz = 10^{15} Hz	nm = 10^{-9} m
EHz = 10^{18} Hz	pm = 10^{-12} m
ZHz = 10^{21} Hz	fm = 10^{-15} m
YHz = 10^{24} Hz	am = 10^{-18} m

Figure 2.1 – Electromagnetic spectrum [24].

2.3 Free Space Optical Communication

As a subset of OWC, FSO is generally operates using the near IR spectrum. It can also utilize VL and UV spectra, though IR is preferred due to its lower attenuation levels. FSO commonly employs laser diodes (LDs) rather than light-emitting diodes (LEDs) for transmission. LDs produce narrow beams that facilitate high data rate communication between two fixed points over distances ranging from a few nanometers to several thousand kilometers [50], [51]. Figure 2.2 illustrates various application scenarios of FSO systems.

Despite its many advantages across a broad range of applications, FSO faces challenges with link reliability, especially in long-range communications. This is due to its high sensitivity to several factors, including weather conditions (e.g., fog, rain, haze, snow, and scintillation), atmospheric turbulence (which causes fluctuations in air density and changes in the air's refractive index), and physical obstructions (e.g., flying birds, trees, and tall buildings that can temporarily block the signal beam) [52], [53].

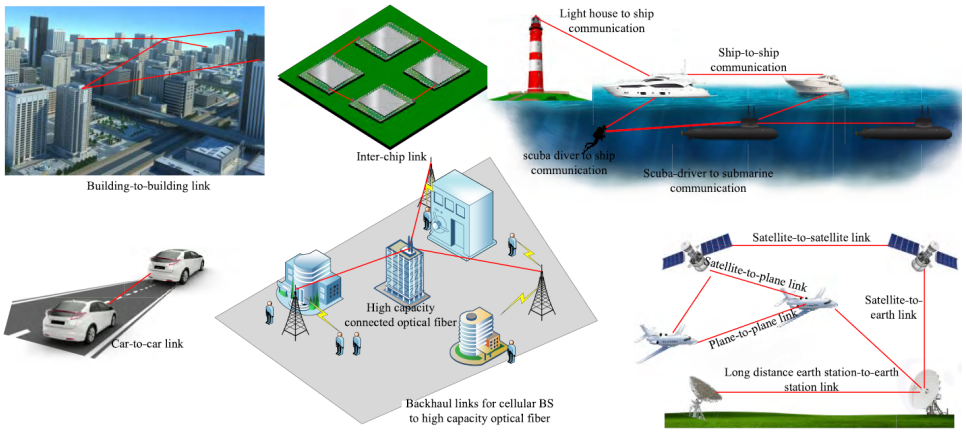

Figure 2.2 – Various application scenarios of FSO systems [54].

2.4 Ultraviolet Communication

As a form of OWC, UVC utilizes the UV spectrum, specifically the solar blind waveband in the wavelength range of 200 to 280 nm [55]. This technology leverages the unique properties of UV light to enable non-line-of-sight (NLOS) communication, making it highly effective in environments where direct line-of-sight (LOS) cannot be maintained. UVC is particularly advantageous in outdoor and harsh conditions as it can penetrate through dust, fog, and smoke, providing robust and reliable communication links. Additionally, due to the strong atmospheric scattering and absorption characteristics of UV light, UVC offers inherent security and resistance to eavesdropping, as the signals do not travel far and are difficult to intercept [56], [57]. Applications of UVC include secure military communications, disaster recovery operations, and sensor networks in environments with obstacles or particulate matter. Despite its benefits, UVC faces challenges such as limited transmission range and potential health hazards due to prolonged exposure to UV light, necessitating careful consideration in its deployment [58].

2.5 Underwater Optical Wireless Communication

Seawater exhibits low absorption for blue-green light, making underwater optical communication (UOC) superior to RF or acoustic alternatives in terms of data rate and transmission bandwidth. High-speed connections are achievable by utilizing optical wavelengths in the blue-green spectrum (typically between 450 to 550 nm) [59], [60]. UOWC systems are applicable in disaster precaution, offshore exploration, environmental monitoring, autonomous underwater vehicle (AUV) operations, as well as military operations. However, UOWC systems are susceptible to absorption and scattering caused by underwater channels, which lead to severe attenuation of optical waves and eventually hinder system performance [61], [62].

2.6 Infrared Communication

As a form of OWC, IR communication utilizes the infrared spectrum, typically within the wavelength range of 700 nanometers to 1 millimeter, for transmitting data. It offers several advantages, including high data rates, low power consumption, and immunity to electromagnetic interference. It is widely used in various applications such as remote controls, short-range communication devices, and secure data links [63], [64]. The LOS nature of IR communication enhances its security, making it difficult for unauthorized users to intercept the signal. However, IR communication is sensitive to physical obstructions and requires a clear path between the transmitter and receiver. Additionally, ambient light and weather conditions can impact the performance of IR communication systems. Despite these challenges, IR remains a valuable technology for indoor and short-range communication applications due to its high bandwidth and reliability [65], [66].

2.7 Visible Light Communications (VLC)

Using VLC to transmit information through visible light is an emerging approach in optical wireless data transmission that utilizes white or colored LEDs. Operating within the frequency range of 400 THz (750 nm) to 789 THz (380 nm), as shown in Figure 2.1, VLC transmits data by intensity modulating light sources faster than the persistence of the human eye [67], [68]. As a subset of OWC, VLC stands out because the signal carrier is visible to the human eye. Unlike traditional OWC, which focuses solely on

communication, VLC can provide dual functionality of communication and illumination. VLC systems must adhere to eye safety constraints and ensure communication even when the illuminating light is dimmed or turned off [69], [70]. Moreover, the investment already devoted to providing illumination is reused to facilitate high data rate communication between light sources and users. LED luminaires act as network access points, making VLC a direct competitor to broadband radio technologies such as Wireless Fidelity (Wi-Fi) and 5G systems.

2.7.1 Features of VLC

Hereinafter, we highlight some distinguishing features and important aspects of VLC [71]–[75].

- **Unlicensed Spectrum:** Visible light operates in an unrestricted, very large spectrum (389 THz wide) available worldwide. This contrasts with RF technology, limited and has restricted bands; many RF frequencies are reserved for specific applications, such as: military or aviation.
- **Health Safety:** Wavelengths corresponding to VL frequencies are safe for the human body, which makes it possible in some applications to transmit with high power, compared to RF and IR which have power constraints for skin and eye safety.
- **Electromagnetic Interference (EMI):** The invulnerability of VLC to RF interference makes it suitable for places that are susceptible to EMI as hospitals, aircraft, mines and petrochemical plants.
- **Security and Quality of Service (QoS):** VLC mainly requires a LOS communication, the nature of VL does not penetrate walls that provide small cells with high spatial reuse, high QoS and a secure system that hide data from potential eavesdroppers.
- **Ubiquitous Computing:** VLC is well-suited for ubiquitous computing, as light-producing devices, such as: indoor lamps, commercial displays, traffic lights, and outdoor lamps are omnipresent.
- **Compatibility with other technologies:** VLC is not supposed to replace RF, but rather complement it where VLC networks can be connected to the existing optical fiber networks and integrated as part of 5G wireless communication systems

2.7.2 VLC architecture

Leveraging the widespread presence of LED lighting infrastructure for both illumination and data transmission positions VLC as a green and energy-efficient technology [76], [77]. Typical VLC systems use relatively simple and off-the-shelf components, LED as a transmitter and photodiode (PD) as a receiver, which constitute inexpensive systems [73]. The block diagram of the end-to-end VLC system is illustrated in Figure 2.3. In an intensity modulation (IM) process, LEDs can transmit data by varying the light intensity at a very high frequency without being observed by the human eye [78], [79]. PDs or image sensors at the receiver end, in a process known as direct detection (DD), are used to generate an electrical current proportional to the variation in the received optical power [80].

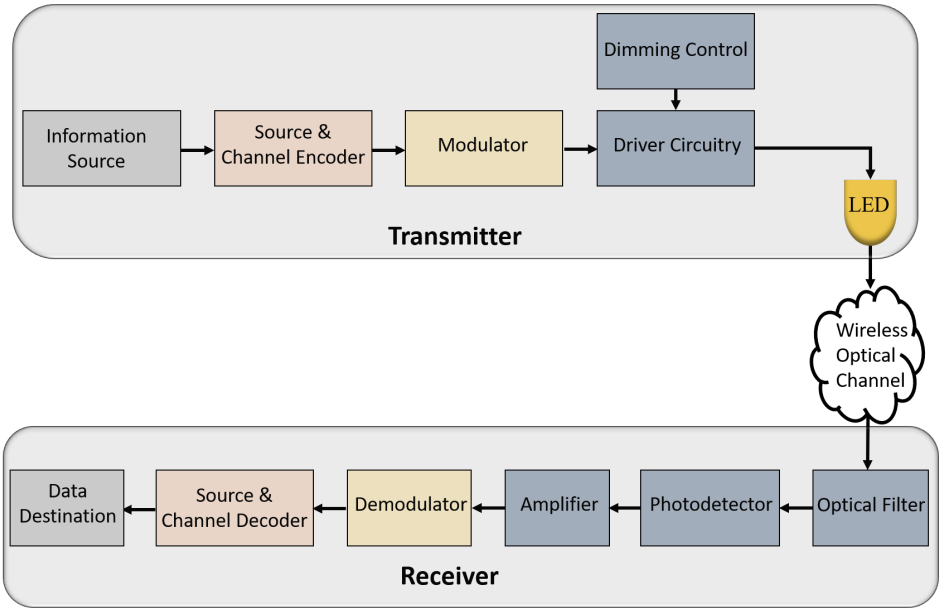

Figure 2.3 – VLC architecture [81].

2.7.3 VLC applications

The VLC technology is still in its early stages and requires significant development before being widely adopted for practical applications. Nonetheless, various large-scale applications are expected to emerge in the coming years across several research areas, as outlined below [82]–[86]:

— **Aviation and Hospitals:** Radio waves should not be used by passengers in aircraft, especially during landing and takeoff. LED-based lights, which are already used in aircraft cabins, could function as VLC transmitters, providing both illumination and media services for passengers. In hospitals, some equipment is susceptible to interference from radio waves, making VLC particularly advantageous in these settings.
— **Smart Lighting:** Smart buildings require both aesthetic and functional lighting. Smart lighting with VLC offers infrastructure for both lighting and communication, reducing the need for additional circuitry and lowering energy consumption within the building.
— **Hazardous Environments:** In environments such as petrochemical plants and mines, RF communication poses explosion risks. VLC, being a safer alternative, can be used for both illumination and communication in these hazardous settings.
— **Underwater Communications:** VLC supports high data rates underwater, where other technologies like RF are limited to distances of less than a meter. This capability enables communication between divers or remote-operated vehicles.
— **Vehicle and Transportation:** Intelligent transportation systems (ITS) use LED-based lights in traffic lights and vehicles to communicate with each other, preventing accidents and ensuring road safety.
— **Positioning:** While outdoor location-based services rely on GPS, its accuracy degrades indoors and in dense urban areas. Using white LEDs in indoor environments can effectively estimate user location. For example, indoor spaces illuminated by LEDs with unique IDs can assist visually impaired people in navigating buildings.

Figure 2.4 illustrates several examples of VLC applications platform. VLC can be exploited in different communication environments, such as indoors, outdoors, underwater, and underground. Extensive research has been conducted on visible light communications and Figure 2.5 presents the number of VLC publications on different environments from highly reputed journals in various organizations such as: IEEE Xplore (https://ieeeplore.ieee.org/, accessed on 28 July 2024), MDPI (https://www.mdpi.com/, accessed on 28 July 2024), ScienceDirect-Elsevier (https://www.elsevier.com/, accessed on 28 July 2024) and OSA (https://www.osapublishing.org/, accessed on 28 July 2024). It is notable that approximately 79% of the research focuses on indoor environments. Consequently, this thesis primarily addresses indoor VLC system models, challenges, and solutions.

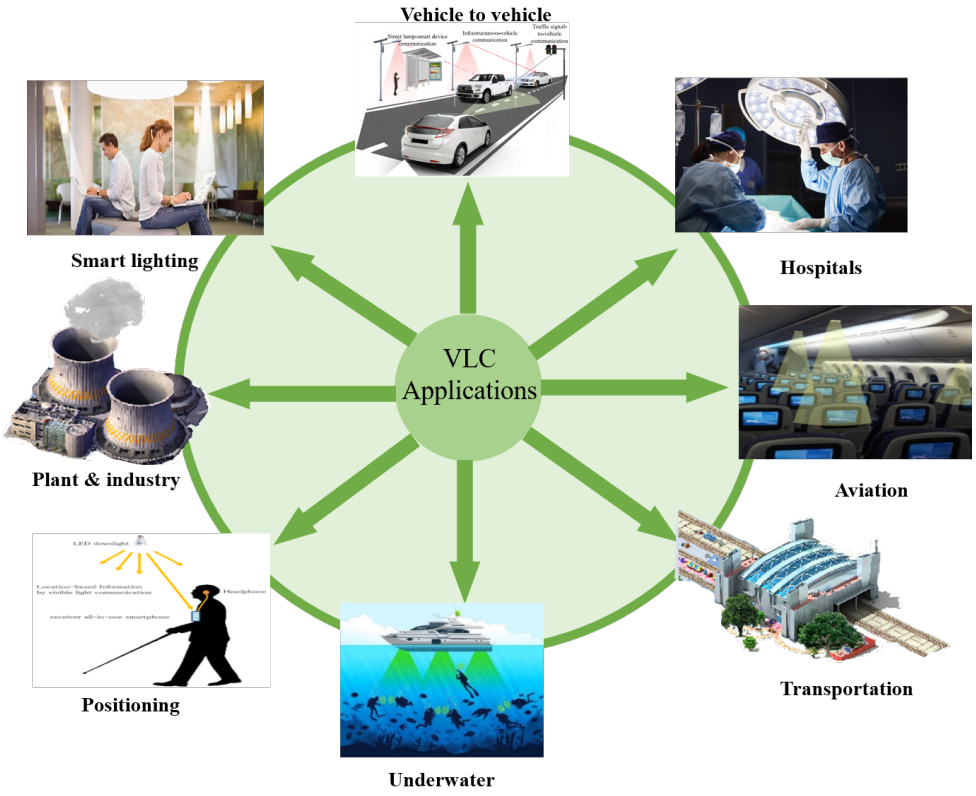

Figure 2.4 – Example of VLC applications platforms [84].

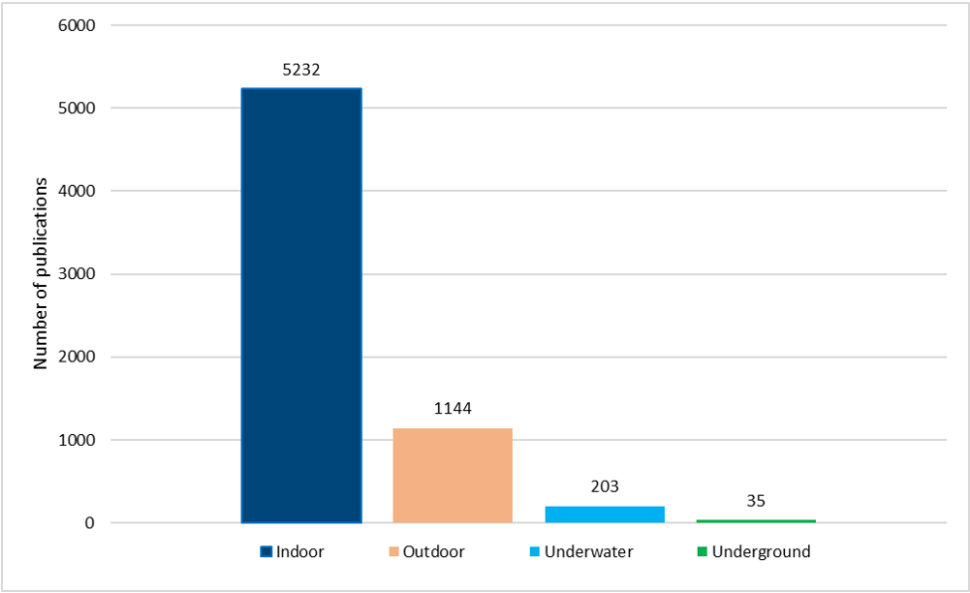

Figure 2.5 – Number of publications on different VLC environments from several organizations (IEEE, MDPI, Elsevier and OSA) from 2000 to 2023.

2.7.4 Light-emitting diode

In recent years, advancements in LED switching speed, brightness, and large-scale diffusion have drawn significant attention from both industry and academia towards VLC. Researchers have started to view visible light as an effective complement to traditional RF communications, which are becoming increasingly congested [87]. High-power LED devices offer numerous advantages, including long lifespan, energy efficiency, low maintenance costs, low heat generation, improved visibility, and superior illumination compared to incandescent and fluorescent lighting. The dual functionality of LEDs for lighting and switching holds substantial innovative potential and is expected to lead to significant applications [88].

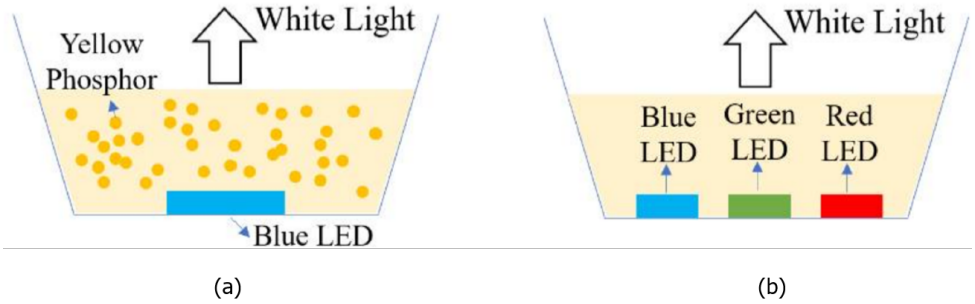

Figure 2.6 – Schematic of two main White LED architectures (a) phosphor-based, (b) RGB.

LEDs are preferred over LDs when the application requires both illumination and communication, as is the case with VLC [89]. There are two primary types of visible LEDs: single-color LEDs (e.g., red, green, or blue) and white LEDs. White light is the most commonly used form of illumination in typical communication applications [90]. Currently, there are two technologies for generating white light using LEDs, as illustrated in Figure 2.6. The more popular method for illumination, which is low in complexity, energy-efficient, and cost-effective, involves using a blue LED with a yellow phosphor coating. However, due to the slow relaxation time of the phosphor coating, the modulation bandwidth is limited to the range of 2-5 MHz [91]. Another more attractive method involves using separate red-green-blue (RGB) emitters. The RGB LED is the most common multi-chip LED, consisting of three jointly packaged LED chips (red, green, and blue) to produce white light [71]. By adjusting the light intensities of the different chips, the color of the output light can be modified. Since this type of LED does not use

phosphor and its associated slow relaxation time, it achieves a higher modulation bandwidth of 10-20 MHz, making it more suitable for communication. However, multi-chip LEDs still have drawbacks, such as a more complex structure and higher costs compared to traditional phosphor-based LEDs [92].

2.8 Challenges and Motivation

VLC faces several challenges that need to be addressed to fully realize its potential. Adverse weather conditions like rain, fog, and snow can severely attenuate the light signals, further complicating reliable communication. However, since this thesis focuses on indoor environments, one primary challenge is the requirement for a LOS between the transmitter and receiver, which can be easily disrupted by obstacles or device mobility, leading to communication interruptions [93]. Moreover, the major challenge to developing VLC systems with high achievable data rates, is the limited modulation bandwidth of LEDs, typically constrained to a few MHz depending on the type of LED [94]. Addressing these challenges is crucial for the widespread adoption and deployment of VLC technology in practical applications. To overcome the modulation bandwidth issue, efficient development of high-order modulation techniques, frequency reuse, MIMO, and advanced multiple access schemes are proposed.

Visible Light Communication (VLC) is emerging as a promising solution for next-generation wireless communication systems, offering high data rates, enhanced security, and energy efficiency by leveraging the visible light spectrum. However, to fully realize the potential of VLC, it is essential to address the aforementioned challenges. Incorporating advanced multiple access schemes such as non-orthogonal multiple access (NOMA) into VLC systems presents a significant advancement, as NOMA can enhance system capacity and user fairness by allowing multiple users to share the same frequency resources. Additionally, effective power allocation strategies are crucial for optimizing the performance of NOMA-based VLC systems, ensuring efficient utilization of available power, and improving overall system performance. The integration of MIMO technology further augments VLC by enhancing spatial diversity and mitigating interference. Finally, user pairing algorithms play a vital role in managing the complexity of NOMA's successive interference cancellation (SIC) process, ensuring that users are grouped in a manner that maximizes system performance. By combining these advanced techniques, we can significantly enhance the performance of VLC systems, making them a viable and efficient option for future wireless communication networks.

2.9 Multiple Access Techniques in VLC

Several orthogonal and non-orthogonal RF multiple access techniques have demonstrated the effective sharing of network valuable resources among a large number of users. Multiple access techniques used in VLC systems are adopted from their counterparts in RF communication systems [95]. For example, time division multiple access (TDMA), used in second-generation (2G) cellular technology, allows multiple users to share the same frequency band by dividing it into different time slots. Conversely, third-generation (3G) cellular technology implemented code division multiple access (CDMA), allocating frequencies and time intervals to different users with distinct codes to prevent interference. In fourth-generation (4G) networks, orthogonal frequency division multiple access (OFDMA) is used, assigning different frequency subcarriers to different users [96], [97]. Similarly, several orthogonal multiple access (OMA) techniques are studied in VLC systems, such as optical TDMA (OTDMA), optical CDMA (OCDMA), wavelength division multiple access (WDMA), and OFDMA. In the aforementioned OMA techniques, different users are allocated orthogonal resources such as frequency, time, and code [98].

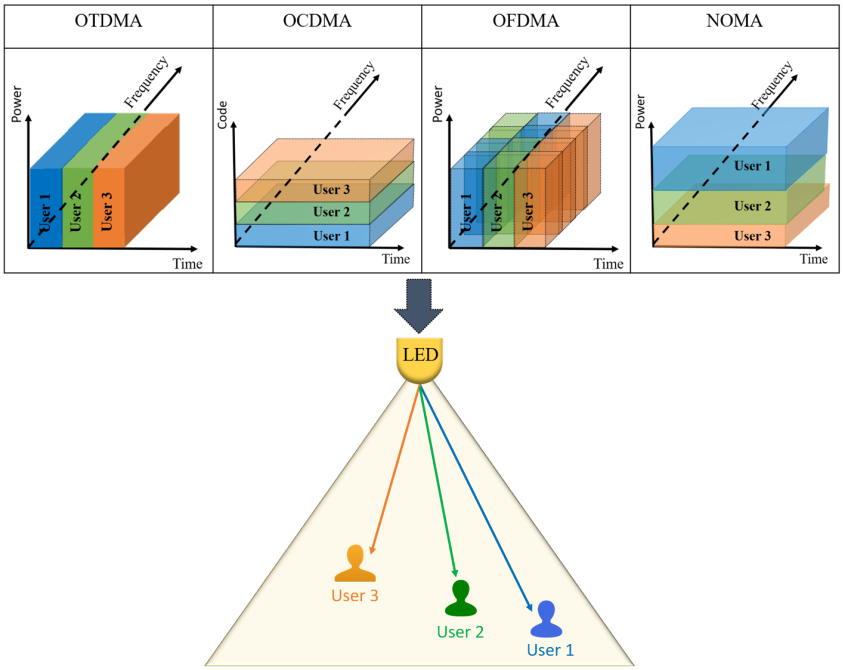

Figure 2.7 – Comparison between TDMA, CDMA, OFDMA, and NOMA techniques concerning time, frequency, and power domains, for a 3-user example.

On the other hand, 5G networks and beyond need to provide services for a large number of high-data-rate users [99], [100]. Unlike OMA, non-orthogonal multiple access (NOMA) allows multiple users to share the same frequency band simultaneously, thereby significantly increasing the system's spectral efficiency. NOMA comprises two main types: power-domain NOMA and code-domain NOMA (CD-NOMA) [101], [102]. power-domain NOMA, the more widely adopted and less complex system, is a promising candidate for beyond 5G networks. In power-domain NOMA, multiple users transmit and receive over the entire available frequency and time resources using different power levels [103], [104]. Figure 2.7 illustrates a comparison between different multiple access techniques concerning the time, code, frequency, and power domains.

2.9.1 Time division multiple access

In OTDMA, the temporal resources of the channel are shared among users by assigning each a specific time slot. While indoor applications typically involve relatively low user mobility, the need for precise synchronization at user terminals and LEDs as access points (APs) can become challenging due to very high data rates, especially with an increased number of users [105]. Furthermore, TDMA suffers from inter-cell interference (ICI) in multicell scenarios at overlapping areas between cells, which can lead to significant degradation in VLC system performance [106].

2.9.2 Code division multiple access

Simultaneous transmission over the available spectral resources at the same time by allocating a unique code to each user can be achieved using CDMA. Each user correlates the received signals with its assigned code to suppress inter-user interference (IUI) [105]. The concept of OCDMA is similar to RF-based CDMA, but it uses optical codes called optical orthogonal codes (OOCs). The performance of OCDMA is greatly affected by the choice of high-rate signature sequences (SS). At the receiver, each SS code must be distinguishable from a shifted version of itself as well as a possibly shifted version of every other sequence in the set to provide optimal recovery. However, generating these codes becomes more challenging with a larger number of users. Although random optical codes (ROCs) are simpler to generate than OOCs [107], they provide sub-optimal performance. Generally, to accommodate a larger number of users, longer OOCs are required, which impacts achievable data rates and increases system complexity [108]. This can be a significant disadvantage for a relatively dense VLC network in a typical large-space scenario.

2.9.3 Wavelength division multiple access

To enhance data transmission efficiency by assigning distinct wavelengths to individual data streams, WDMA is employed in wireless communication. This technique is similar to frequency division multiple access (FDMA), but it leverages the optical spectrum rather than radio frequencies. The primary advantage of WDMA is its ability to significantly increase the capacity and efficiency of data transmission. By facilitating the simultaneous transmission of multiple data streams across different wavelengths, WDMA has the potential to elevate the overall throughput and reduce latency [109].

Nevertheless, WDMA also presents several disadvantages in wireless communication. The implementation of WDMA systems requires advanced and often costly equipment, including wavelength-specific transmitters and receivers. Additionally, managing and maintaining these systems can be complex due to the need for precise wavelength control and potential interference issues between closely spaced wavelengths [110].

2.9.4 Orthogonal frequency division multiple access

Orthogonal frequency division multiplexing (OFDM) has been presented as a key enabler for high data rate communications [111]. In the context of VLC systems, as data rates increase, the limited bandwidth of LEDs leads to inter-symbol interference (ISI) [112], [113]. This can be minimized using effective equalization-enabled techniques. OFDM is efficient in terms of ISI reduction, as it uses a large number of low-rate orthogonal subcarriers to acquire increased throughput. OFDM-based receivers require only a simple one-tap equalizer, which reduces system complexity [114]. However, there are certain limitations in realizing OFDM within VLC systems. Specifically, conventional OFDM generates complex and bipolar waveforms, which are incompatible with the IM/DD schemes employed in VLC. This issue can be effectively resolved by exploiting Hermitian symmetry on the subcarriers in the frequency domain to produce a real OFDM signal suitable for VLC systems. Figure 2.8 illustrates the transceiver structure of a typical OFDM system. Firstly, at the transmitting end, a group of transmitted bits are mapped to corresponding constellation points. The serial and complex-mapped data are then converted into several low-rate parallel data streams using a serial-to-parallel (S/P) converter. The utilization of Hermitian Symmetry serves the purpose of deriving signals with real values, thereby discarding the complex component of an OFDM signal, which cannot be transmitted through a single LED. The output of Hermitian Symmetry

is passed through the inverse fast Fourier transform (IFFT) to generate the time-domain signal, which is then subjected to parallel-to-serial (P/S) conversion. A cyclic prefix (CP) is then added to eliminate ISI. The output from the CP block is fed directly into a digital-to-analog converter (DAC), translating the discrete IFFT sample points into continuous time-varying signals. To ensure the OFDM time-domain signal is both real and positive, DC biasing is introduced. Subsequently, double-sided clipping is applied to fit the signal within the dynamic range of the LED. The resulting signal is then used to modulate the LED intensity.

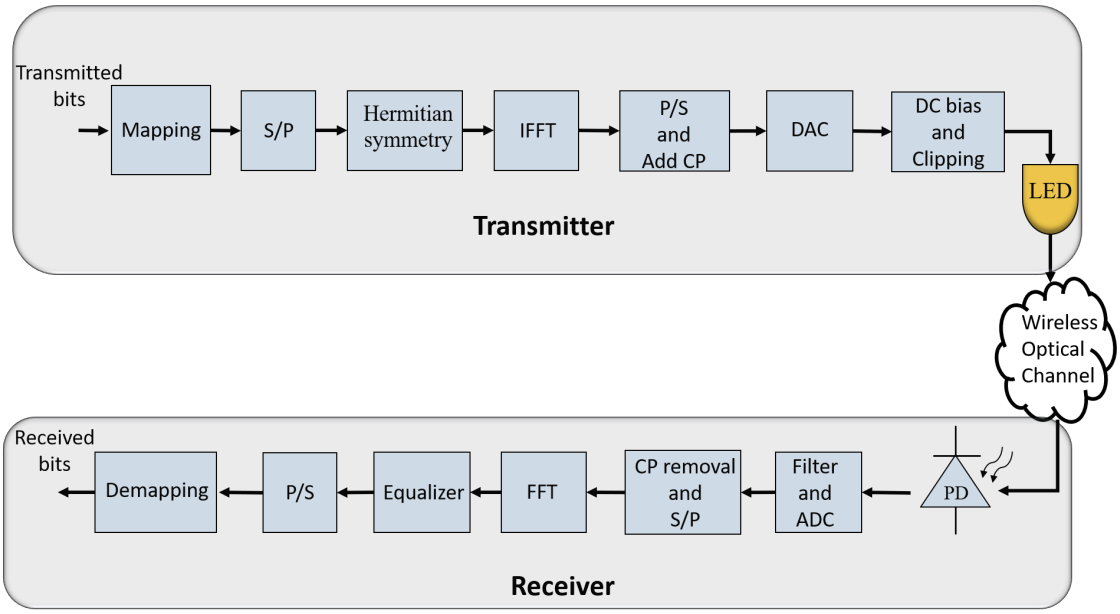

Figure 2.8 – Block diagram of optical OFDM transmitter and receiver.

At the receiver, the optical signals received through the channel are converted to proportional electrical signals by the PD. These signals are then filtered and processed by an analog-to-digital converter (ADC). The CP extension of each OFDM symbol is removed after series-to-parallel (S/P) conversion. Next, the fast Fourier transform (FFT) algorithm is applied, followed by one-tap frequency domain equalization to compensate for channel effects. Finally, P/S conversion and demapping are conducted to retrieve the originally transmitted bits.

Several new schemes that provide unipolar and real time-domain OFDM signals have been proposed to ensure compatibility with VLC systems. Direct-current biased optical OFDM (DCO-OFDM) and asymmetrically clipped optical OFDM (ACO-OFDM) were

developed to generate real unipolar OFDM signals. In DCO-OFDM, a DC bias is added to the signal before clipping to obtain a unipolar signal [115], [116]. For ACO-OFDM, only odd-numbered subcarriers are modulated before zero-level clipping, which does not result in any loss of information [117]. Owing to employing Hermitian symmetry in optical OFDM to obtain real signals, there is a loss in spectral efficiency by a factor of two for DCO-OFDM and a factor of 4 for ACO-OFDM [118]. Therefore, DCO-OFDM remains particularly advantageous in terms of spectral efficiency. While multipath propagation is negligible in VLC systems due to their predominantly LOS nature, OFDM still plays a significant role in combating channel impairments such as the low-pass effect caused by the limited modulation bandwidth of LEDs [119]. Moreover, OFDM's adaptive bit loading allows efficient utilization of the channel by assigning higher-order modulation schemes to subcarriers with better SNR. Additionally, OFDM enables high spectral efficiency by transmitting multiple orthogonal subcarriers simultaneously, making it suitable for high-data-rate VLC systems. Hermitian symmetry ensures the OFDM signal is real-valued, which is necessary for intensity modulation in VLC. However, this comes at the cost of a reduction in throughput caused by reducing the effective number of subcarriers available for data transmission. However, this limitation can be mitigated through techniques like MIMO systems or advanced modulation schemes, which improve overall data rates and spectral efficiency [120]. It is worth noting that OFDMA is essentially an extension of OFDM, where each user is assigned a group of subcarriers within each time slot based on their specific traffic requirements and channel conditions [121]. Among these OMA techniques, researchers have focused on OFDMA as an efficient scheme for VLC networks due to its distinct advantages such as low implementation complexity and high spectral efficiency.

2.9.5 Space division multiple access

Space division multiple access (SDMA) involves separating users in the spatial domain. In addition to OMA, various NOMA techniques are applied to VLC systems. Optical SDMA (OSDMA) is a NOMA technique that uses multiple directional optical beams at the transmitter to separate users in the spatial domain [122]. However, this approach requires either special LEDs or specialized optics with off-the-shelf LEDs, which increases the implementation complexity of the system, making OSDMA less practical for VLC networks in general. Nonetheless, combining TDMA with SDMA has been shown to significantly improve network performance compared to the simple TDMA approach [122].

2.9.6 Non-orthogonal multiple access

Power-domain NOMA (simply referred to as "NOMA") significantly enhances the capacity and efficiency of 5G networks, making it a promising candidate for meeting the high data rate and connectivity demands of future wireless communication systems. NOMA utilizes the power domain to serve multiple users simultaneously in the same frequency band and time slot using the same code. To ensure fairness and effective resource distribution, NOMA allocates higher power to users with a lower signal-to-noise ratio (SNR) [103]. Unlike OFDMA, which maintains the transmitted power of all users at a certain level and divides the available resource blocks (RBs), NOMA assigns different power levels to each user while all users share the available RBs. Therefore, OFDMA has a frequency constraint on subcarrier separation for orthogonality, whereas NOMA utilizes the entire bandwidth without separations [123]. At the transmitter end, superposition coding is applied, and a multiuser detection algorithm such as SIC is performed at the receiver end. Several features of NOMA are outlined below [124]–[128]:

- **Massive connectivity:** While OMA is limited by the number of orthogonal resources, NOMA does not face such limitations. Theoretically, can accommodate a considerable number of users. However, it is limited to the performance of SIC.
- **Lower latency:** OMA waits for available resource blocks to transmit, which requires waiting for an access grant. In contrast, NOMA supports flexible scheduling and grant-free transmission.
- **High spectral efficiency:** Spectral efficiency is a critical performance metric in wireless systems. Every NOMA user can utilize the entire bandwidth, whereas an OMA user can utilize only a limited amount. Properly grouped NOMA users can achieve higher data rates compared to OMA.
- **Good compatibility:** Theoretically, NOMA can be integrated with any existing OMA technique due to its novel power dimension.
- **Fairness:** A key attribute of NOMA is assigning higher power to users with lower SINR. Consequently, NOMA can ensure an excellent trade-off between user fairness and system throughput.

In addition, optical NOMA has recently gained significant attention as a promising technique capable of addressing key challenges in VLC systems and outperforming conventional multiple access techniques. Simultaneous communication of information from one transmitter to different receivers in a downlink broadcast channel is known as superposition coding [129].

The main concept of a two-user NOMA in a VLC system with superposition coding at the transmitter and SIC at the receivers is illustrated in Figure 2.9. The transmitter applies superposition coding to the signals of both users and compares the channel gains to determine the required power coefficients. User 1, who has a weak received signal, is farther from the LED (weak user with worse channel gain), while User 2, who has a strong received signal, is closer to the LED (strong user with better channel gain) [130], [131]. The transmitter assigns higher power to the weak user's signal compared to the strong user's signal, then superimposes both signals and conveys them simultaneously. The concept of superposition coding can be applied to a large number of users, with power allocation based on each user's channel gain. At the receiver end, NOMA employs SIC for detection. User 1 can directly detect its message from the superimposed received signal, treating interference from User 2's signal as noise. In contrast, User 2 must apply SIC by first detecting User 1's signal, subtracting it from the received signal, and then detecting its own signal. For a large number of users, each user (except the farthest one) needs to apply SIC to all stronger signals before detecting its own signal [132].

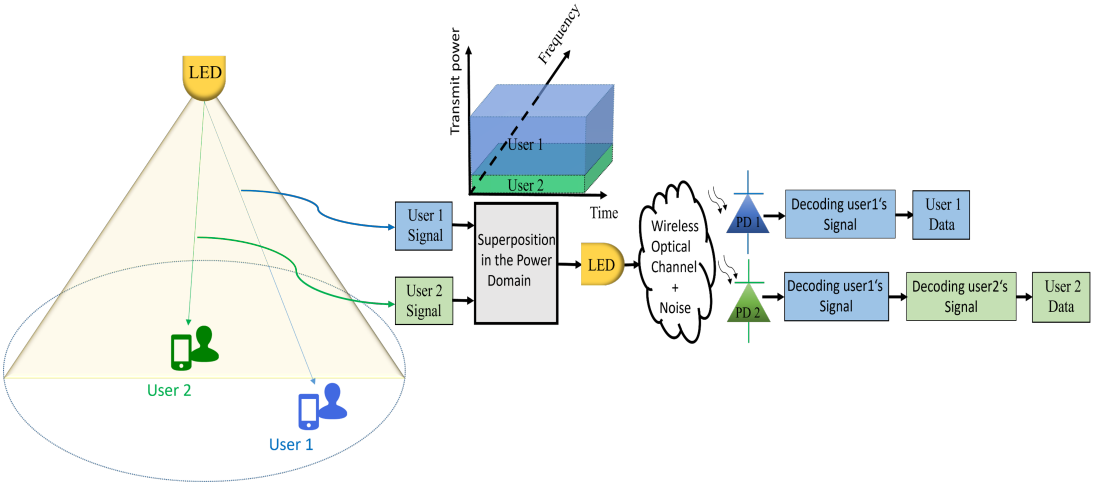

Figure 2.9 – An illustration of a two-user downlink NOMA scheme in the VLC system with superposition coding and SIC.

Although the NOMA scheme offers several benefits in RF, the unique characteristics of VLC networks further enhance NOMA's performance compared to RF for the following reasons [133]–[135]:

1. NOMA performance is enhanced at high SNR levels, which is typical in VLC

networks that consist of small cells with short propagation distances and strong LOS. NOMA is particularly efficient in multiplexing a small number of users, which is advantageous in indoor VLC systems.

2. Accurate channel state information (CSI) at the transmitter can enhance the power allocation for each user in NOMA. The quasistatic nature of the channel due to low mobility in indoor VLC systems allows for more reliable CSI estimation.
3. Adjusting the semiangles of the LEDs and the FoVs of the PD can improve NOMA performance in VLC by controlling the channel gain difference between users.

2.9.7 Comparison of multiple access techniques

Following the above discussions, OFDMA and NOMA are the most suitable schemes for high-rate VLC networks [106]. Table 2.1 provides a brief comparison of the multiple access schemes discussed earlier, focusing on three key features of large-space scenarios: inter-cell interference (ICI), the potential for a large number of users, and the requirement for high data rates. A more detailed performance comparison between OFDMA and NOMA will be discussed later.

Table 2.1 – Comparison between different multiple access techniques [106].

	OTDMA	SDMA	OFDMA	NOMA
ICI	✓	✓	✓	
Large no. users			✓	✓
High data rate		✓		✓

2.10 Power Allocation Techniques in NOMA-based VLC Systems

Power allocation involves assigning different power levels to users sharing the same resources. As previously mentioned, the NOMA concept relies on allocating higher power to users with poorer channel gains and lower power to users with better channel gains. Therefore, selecting an effective power allocation technique is crucial to ensure appropriate power levels for each user, thereby enhancing the performance of the NOMA system [136],

[137]. In the realms of RF and VLC, the power distribution in NOMA broadens the scope of research objectives significantly. This expansion includes considerations such as allocation of channel resources [138], [139], fairness among users [140], [141], improving energy efficiency [142], [143], user scheduling [139], [144], sum rate [145], [146], and meeting QoS requirements [147], [148].

Power allocation techniques in NOMA can generally be classified into static power allocation (SPA) and dynamic power allocation (DPA) methods. SPA assigns a fixed power level to each user for every connection. Conversely, DPA techniques adjust the power level for each user based on the instantaneous channel state information (CSI). While DPA techniques are more effective in mobile environments due to their adaptability, SPA techniques are simpler to implement [149].

DPA techniques fall into two main categories: numerical search techniques and strategic design techniques. Numerical search techniques aim to find an analytical solution to the optimization problem but are computationally intensive and not suitable for real-time processing. Conversely, strategic design techniques provide simple closed-form solutions that are more suitable for real-time processing [150], [151].

There are a limited number of SPA techniques in literature. The first SPA technique proposed was the user's index-based fixed power allocation (FPA) [133]. Moreover, equal power allocation (EPA) was presented and compared to FPA [152]. Another FPA technique, arbitrary power allocation (APA), was proposed without direct comparison to previous SPA methods [153]. Additionally, an FPA technique was developed to maximize the minimum Euclidean distance (MED) of the resultant constellation in both uplink and downlink scenarios [154], [155].

Conversely, there are numerous DPA strategic design techniques in the literature. The first DPA strategic design method, fractional transmit power allocation (FTPA), was proposed to mimic the channel power allocation in LTE [156]. In [157], the authors proposed CSI-based power allocation (CSIPA) where power allocation is inversely proportional to the state of the channel. Motivated by cognitive radio, general power allocation (GPA), is another DPA strategic design method that seeks to achieve better spectrum efficiency than FPA [158]. Furthermore, in [135], the authors proposed a gain ratio power allocation (GRPA) technique, particularly for NOMA-based VLC systems.

Recently, new DPA strategic design techniques have been introduced to enhance the performance of previous strategies. The improved fractional transmit power allocation (IFTPA) technique was introduced and compared with FTPA, allowing independent

power control parameters for each user in a NOMA-based multicarrier system [159]. In [151], the authors proposed an improved fractional strategy (IFS), a modified version of GRPA, and compared it with GRPA from the perspective of sum-rate capacity. Without a control parameter a similar DPA technique, the improved power law strategy power allocation (IPLSPA), was proposed and compared with FTPA in terms of sum-rate capacity [160]. An adjusted version of GRPA, named normalized gain difference power allocation (NGDPA), was also presented and compared with GRPA from a sum-rate capacity perspective [161], [162]. Lastly, anormalized logarithmic gain ratio power allocation (NLGRPA) was developed and compared with both GRPA and NGDPA in terms of sum-rate capacity [163]. The most widely used power allocation schemes in NOMA-based VLC systems will be discussed in the following subsections.

2.10.1 Static power allocation (SPA)

The benefit of SPA lies in its low computational complexity at the transmitter side, whereas its drawback is that it neglects the channel quality of the users, leading to unsatisfactory performance in mobile environments compared to DPA techniques [164], [165]. Only a few SPA techniques have been outlined in the literature. APA, the simplest SPA technique, allocates power without any specific logic. There is no established mechanism for assigning power to users, but the requirement that the total power assigned to users equals the total transmit power is mandatory. However, as the number of users increases, APA becomes increasingly intricate [153], [166].

Fixed power allocation (FPA)

The FPA technique, widely recognized as the most popular SPA scheme, is renowned for its straightforward nature and suboptimal power allocation approach. This technique, which is channel-independent, involves assigning predetermined power ratios to individual users. In a scenario involving two users, a portion of the overall power is designated to one user, while the residual power is allocated to the second user [167]. Despite its simplicity, FPA is considered inefficient, especially in dynamic mobile settings, due to its lack of consideration for channel conditions during power allocation. The allocation of power to the nth can be expressed as

$$p_n = \alpha p_{n+1} \tag{2.1}$$

where $0 < \alpha < 1$ is the power allocation coefficient, while p_{n-1} represents the static power allocated to the user positioned prior to the nth selected user in accordance with the decoding process [135]. The power allocation coefficient plays a crucial role in overseeing the efficiency of the system and ensuring fairness among users.

2.10.2 Strategic design techniques

In this subsection, the strategies for dynamic power allocation (DPA) are presented, encompassing both strategic design techniques and numerical search techniques. The discussion begins with an overview of the strategic design methods.

Gain ratio power allocation (GRPA)

This allocation technique was proposed as an efficient power allocation technique aimed at improving the throughput and user fairness of the VLC system [135]. As per GRPA, the allocation of power is influenced by the gain of each user in relation to the gain of the user sorted first, along with the decoding order n. The power designated to the n-th user in the sorted sequence is given as in [135]

$$p_n = \left(\frac{h_1}{h_n}\right)^{n+1} p_{n+1} \tag{2.2}$$

Therefore, the power allocated diminishes as the channel gain of the n-th user, denoted as h_n, increases. This is because users with favorable channel conditions require lower power levels to successfully decode their signals, especially after eliminating the signals from users with lower decoding priority. Additionally, the ratio $\frac{h_1}{h_n}$ is raised to an exponent related to the decoding order to ensure fairness. Users with lower decoding orders will necessitate significantly higher power levels due to the substantial interference they encounter.

Power law strategy (PLS)

As a power allocation technique based on GRPA, PLS was developed to address the challenge posed by the similarity of channel gains among users and to support a dynamic range of users in a MIMO-VLC system [147]. Several studies on the GRPA strategy design are mostly based on the inverse ratio, with an increasing order of channel gain

distribution. The power allocation factor based on PLS is expressed as in [151]

$$\alpha_n^{PLS} = \frac{\prod_{i=1}^{n}\left(\frac{h_1}{h_i}\right)^n}{\sum_{n=1}^{N}\left(\prod_{i=1}^{n}\left(\frac{h_1}{h_i}\right)^n\right)} \tag{2.3}$$

where N is the total number of users. The power counting of $\frac{h_1}{h_i}$ is subject to the user's order, which varies exponentially.

An enhanced version of the PLS, known as the inverse power law strategy (IPLS), was introduced in [150], [160]. The power allocation coefficient of the n-th in a group employing the IPLS technique is expressed as [150]

$$\alpha_n^{IPLS} = \begin{cases} \frac{1}{1+\left(\frac{h_1}{h_2}\right)+\cdots+\left(\frac{h_1}{h_n}\right)}, n = 1 \\ \frac{\left(\frac{h_1}{h_n}\right)}{1+\left(\frac{h_1}{h_2}\right)+\cdots+\left(\frac{h_1}{h_n}\right)}, 2 \leq n \leq N \end{cases} \tag{2.4}$$

Fractional Transmit Power Allocation (FTPA)

This power allocation strategy assesses users' power ratios based on each user's channel qualities. The power allocation coefficient of the nth user utilizing FTPA can be represented as [151]

$$\alpha_n^{FTPA} = \frac{(h_n^2)^{-\alpha}}{\sum_{i=1}^{N}(h_i^2)^{-\alpha}} \tag{2.5}$$

where $0 \leq \alpha \leq 1$.

The revised FTPA introduced in [151] is referred to as the improved fractional strategy (IFS). Under this power allocation scheme, the channel proportions are reframed, and the constraint of $(0 \leq \alpha \leq 1)$ is eliminated. The power allocation coefficient of the n-th user is given by [151]

$$\alpha_n^{IFS} = \frac{\left(\frac{h_1}{h_n}\right)^\beta}{\sum_{i=1}^{N}\left(\frac{h_1}{h_i}\right)^\beta} \tag{2.6}$$

In this technique, β is not confined to the range [0, 1], and is not only relevant to the users' order. Moreover, the authors proved that it is possible to attain a locally optimum

solution for the system throughput in NOMA-based VLC systems by imposing a specific $\beta > 0$ in the aforementioned equation.

Simplified gain ratio power allocation (S-GRPA)

The authors of [168] introduce a low complexity power allocation scheme for NOMA-based indoor VLC systems, referred to as the simplified gain ratio power allocation (S-GRPA) scheme. The S-GRPA scheme employs look-up tables instead of calculation methods to allocate power, addressing the challenge of incomplete CSI.

Normalized gain difference power allocation (NGDPA)

The NGDPA was presented in [162] to improve the sum rate of MIMO-based multi-user indoor VLC systems. Simulation results have demonstrated that employing NGDPA in NOMA-enabled MIMO-VLC setups leads to a notable increase in the sum rate compared to the traditional GRPA technique. Similarly, a corresponding framework utilizing NGDPA was presented in [169] with the aim of improving the achievable data transmission rate and throughput under lower BER conditions and peak-to-average power ratio (PAPR).

For the 2×2 MIMO-NOMA-VLC system using NGDPA for power allocation, the electrical power assigned at the i-th LED to the user n and user $n+1$ is expressed as [162]

$$p_{i,n} = \left(\frac{h_{1i,1} + h_{2i,1} - h_{1i,n+1} - h_{2i,n+1}}{h_{1i,1} + h_{2i,1}} \right)^{n} p_{i,n+1} \tag{2.7}$$

where $h_{1i,n+1}$, $h_{2i,n+1}$ are the channel gains of the user $n+1$, associated to the i-th LED, at its PDs 1 and 2, respectively, while $h_{1i,1}$, $h_{2i,1}$ are the channel gains of the first sorted user, corresponding to the i LED, at its PDs 1 and 2, respectively.

Furthermore, the authors of [170] proposed a QoS-guaranteed optimal power allocation (OPA) strategy to enhance the energy efficiency and outage probability of NOMA-VLC systems. It has been demonstrated that NOMA with OPA results in superior energy efficiency compared to NOMA with GRPA and NGDPA schemes.

Normalized logarithmic gain ratio power allocation (NLGRPA)

For MIMO-VLC networks, a normalized logarithmic GRPA technique, referred to as NLGRPA, was introduced in [163] as an efficient technique to improve the achievable sum

rate of NOMA-based indoor MIMO-VLC systems. This scheme is particularly efficient for systems with a large number of users, offering low computational complexity. The NLGRPA scheme has yielded significant improvements in the sum rate for indoor NOMA-based VLC systems compared to GRPA and NGDPA. In particular, for the $I \times J$ NOMA-aided MIMO-VLC networks, the relationship between the power allocated to the nth user and $(n+1)$th user in the i-th LED can be described as [163]

$$p_{i,n} = \left| \frac{\log\left(\sum_{j=1}^{J} h_{ji,n+1}\right)}{\frac{1}{2}\log\left(\left(\sum_{j=1}^{J} h_{ji,1}\right)^2 - \left(\sum_{j=1}^{J} h_{ji,n+1}\right)^2\right)} \right| p_{i,n+1} \tag{2.8}$$

2.10.3 Numerical search techniques

Numerical search techniques can be viewed as optimization problems with various objective functions, such as maximizing sum-rate capacity or energy efficiency. Numerous studies have suggested various optimization techniques for enhancing the performance of NOMA-VLC networks [171]–[176]. Nevertheless, the enhancement in performance achieved through the optimization of power allocation is accompanied by a rise in network complexity. In [171], the Cuckoo Search (CS) meta-heuristic optimization algorithm was employed to address a multi-objective optimization issue concerning the users' received power and achievable rate. The optimized approach demonstrated a superior sum rate compared to the FPA in the NOMA-VLC system. An iterative algorithm was employed to select the optimal NOMA pairs and subsequently, determine their allocated powers utilizing the majorization-minimization (MM) technique in [172] to maximize the sum rate for NOMA-VLC with steerable beams. In [173], the authors suggested the particle swarm optimization (PSO) applied to the power allocation coefficients in multi-cell NOMA-VLC networks. The performance was compared with the non-optimized power allocation NOMA scenario and the results showed improved performance in terms of sum rate and fairness. In [174], the nonlinear marine predator algorithm (NMPA) was utilized for addressing the fair power allocation problem, optimizing the sum rate efficiently. Moreover, an intelligent user association approach for multi-user scenarios in the NOMA-VLC system was proposed in [175] along with an adaptive optimal power allocation scheme. This strategy takes into account the error propagation at the receiver, seeking maximiza-

tion of the system throughput. Various optimization techniques that are applied to the power allocation schemes to improve the overall system performance are summarized in Table 2.2 (all references in the next tables are sorted chronologically).

Table 2.2 – A summary of power allocation optimization in NOMA downlink VLC systems.

System Model	**Optimization Method**	**Maximization**	**Contribution**	**Ref.**
4 VLC AP + N users	Gradient projection (GP) algorithm	Sum rate + User rate	A power allocation scheme under QoS constraint and user grouping that achieves a higher sum rate performance than OMA	[176]
1 VLC AP + 2 users	GP algorithm	Sum rate + Fairness	An optimal power allocation that outperforms the OMA scheme taking into consideration practical optical power and QoS constraints	[146]
4 VLC AP + N users	Analytical method	Sum rate	The sum rate performance of the proposed enhanced power allocation (EPA) algorithm outperforms the FPA and GRPA in terms of sum rate	[177]
1 VLC AP with I LEDs + N users	Interior-point algorithm	Achievable rate	Propose optimal power allocation schemes for both static and mobile users and derived a closed form expression for achievable rates of static users	[178]
1 VLC AP + N users	Analytical method	Achievable rate	Introduce an adaptive power allocation scheme that chooses between GRPA or inverse power allocation (IPA) and the optimal power allocation factor to increase the achievable rate using multi-attribute decision making (MADM)	[179]

System Model	Optimization Method	Maximization	Contribution	Ref.
1 VLC AP + N users	KKT conditions for optimality	Sum rate	Introduce a joint power line communications (PLC)-VLC power allocation scheme that outperforms FPA and NGDPA in terms of sum rate	[180]
1 VLC AP + N users	Interior-point algorithm	Sum rate	The sum rate performance of the proposed multi-factor control optimal power allocation (MFOPA) outperforms FPA and GRPA	[181]
4 VLC AP + N users	KKT conditions for optimality	Sum rate	Present an optimal power allocation for a downlink hybrid power line VLC (HPV) system that maximizes sum rate compared to FPA and GRPA	[182]
1 VLC AP + N users	Differential evolution (DE) based heuristic algorithm	Sum rate	Verify the superiority of two proposed power allocation schemes over the conventional FPA and GRPA in terms of sum rate and user fairness using simulation	[183]

Table 2.3 – Comparison of different power allocation methods.

	SPA	Strategic design techniques	Numerical search techniques
Scheme's nature	Fixed	Dynamic	Dynamic
Channel Gain	Independent	Dependent	Dependent
Solution	Suboptimal	Suboptimal	Optimal
Complexity	Low	Low - Intermediate	Computationally Complex

The aforementioned power allocation methods, including SPA, strategic design techniques, and numerical search techniques, exhibit varying performance across metrics such as sum rate, fairness, BER, etc. Moreover, the effectiveness of power allocation is primarily influenced by system model parameters, such as the distance between users, LED positions, etc. Table 2.3 provides a general comparison of different power allocation methods.

Due to their low implementation complexity, DPA-based strategic design methods and SPA techniques are more appropriate for the practical implementation of NOMA-VLC systems. Therefore, this thesis focuses on DPA-based strategic design and SPA methods.

2.11 MIMO in VLC Systems

It has been assumed that the aforementioned VLC system consists of a single transmitter and receiver. Nevertheless, a typical room in a home or office contains several LEDs to provide adequate lighting. Accordingly, MIMO can be implemented in VLC scenarios due to the presence of multiple transmitters [90]. Introducing MIMO in VLC systems can enhance both the reliability and bit rate, which are currently constrained by the bandwidth of the transmitters [184]. Unlike RF MIMO systems, which have multiple distinct channels between the transmitter and receiver, VLC systems often exhibit high channel correlation due to the similarities of the channels and the confinement of transmitters and receivers to a single room [90]. To address this, the angular diversity receiver has been introduced in some studies to improve VLC-MIMO system performance by decorrelating the optical channels [185]–[188]. An angular diversity receiver consists of a set of narrow FoV detectors pointing in different directions [187]. Two designs of angle diversity receivers: pyramid receivers and hemispheric receivers are proposed in [185]. These proposed receivers outperformed the spatially separated photodiode array. In [186], the authors demonstrated the operation of a distinct topology, the generalized angular diversity receiver, which consists of a central detector surrounded by multiple adjustable inclined detectors. Additionally, several techniques have been studied to ameliorate the channel correlation problem and enhance the performance of VLC-MIMO systems. These techniques are based on those used in RF-MIMO systems, including Repetition Coding (RC), Spatial Multiplexing (SMP), and Spatial Modulation (SM) [189].

The primary advantage of the first method is its simplicity, as the same data stream is transmitted by all transmitters, thereby enhancing system robustness [188], [190], [191]. In [191], the authors analyzed the performance of RC and simple Orthogonal Space–Time Block Codes (OSTBCs), such as the Alamouti scheme. They concluded that a multiple-input single-output (MISO) system with RC outperforms OSTBCs because the signal power from the transmitters adds constructively at the VLC receiver. Consequently, they determined that OSTBCs are not necessary for VLC. Furthermore, the performance of RC in a VLC-MIMO system using angular diversity receivers under imperfect CSI is

investigated in [188]. The analytical results indicated that this system exhibits better error performance than a MISO VLC system, across different receiver locations and semi-half angles.

In contrast, SMP increases the spectral efficiency of the system by employing different signals at each transmitter [192], [193]. In [192], the authors introduced an adaptive bit and power loading algorithm for a DCO-OFDM VLC MIMO system, which selects between RC and SMP MIMO modes and applies bit- and power-loading techniques to enhance the data rate for a given target BER. An innovative superposed 64QAM constellation scheme for a 2×2 VLC-MIMO system utilizing the SMP approach is proposed in [193]. Experimental results demonstrated that this superposed constellation, combined with the SMP technique, achieves multiplexing gains in highly correlated VLC channels, outperforming the traditional superposed 64-QAM constellation.

Finally, only one transmitter is active during each time slot in SM. Each VLC transmitter is linked to a specific symbol in the constellation. Thus, when there's a need to transmit a particular symbol, only the corresponding transmitter is activated while others remain inactive. This simplifies the receiver's task of identifying which transmitter sent the received symbol. The key advantage of this approach is that it encodes information in two dimensions. Alongside the signal-encoded information, there's modulation in spatial dimensions, thereby enhancing the system's spectral efficiency. Moreover, it ensures that only one transmitter is active at any given time, preventing cross-channel interference and simplifying receiver complexity [67]. In [189], the authors conducted a comparison of three MIMO techniques using various 4×4 MIMO configurations, altering the positions of transmitters and receivers. The RC technique demonstrated the lowest spectral efficiency because it utilizes the same signal across all transmitters while offering easier system alignment. In contrast, SMP requires low channel correlation between transmitters and receivers but achieves the highest data rates. On the other hand, SM offers enhanced spectral efficiencies even under low SNR conditions and operates effectively in scenarios with high channel correlation.

2.12 MIMO in NOMA-VLC Systems

Most indoor environments use multiple LEDs to provide sufficient illumination, which motivates the implementation of MIMO in VLC systems. Employing MIMO techniques in VLC systems can increase spectral efficiency by overcoming the narrow modulation band-

width limitation of the LEDs [189], [194]. Moreover, tuning the field of views (FoVs) and transmission angles in VLC systems provides the opportunity for two additional degrees of freedom, leading to enhancements in the system's overall performance. Consequently, the integration of MIMO in NOMA-VLC systems introduces supplementary degrees of freedom, thereby boosting the performance of the system [195]. The block diagram of the 2×2 MIMO NOMA-based VLC system is shown in Figure 2.10.

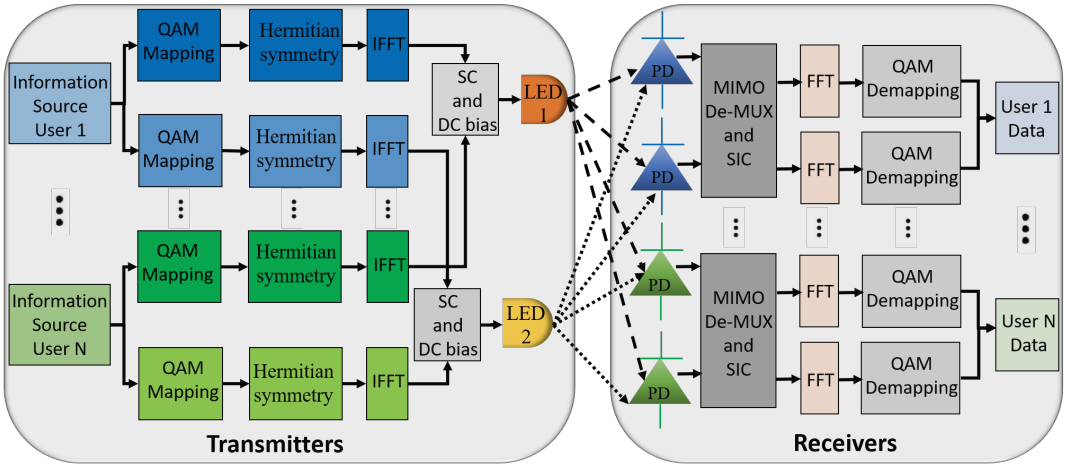

Figure 2.10 – Block diagram of 2×2 MIMO-based NOMA-VLC system with N users.

In [196], a VLC system based on MIMO-NOMA was experimentally validated using FPA which offers a low peak-to-average power ratio, a good balance between throughput and fairness, and a higher system capacity for a larger number of users. Several research studies have investigated the performance of incorporating NOMA in MIMO-VLC systems, attributing to the advantages mentioned earlier. An overview of NOMA-based MIMO-VLC systems is provided in Table 2.4.

Table 2.4 – An overview of MIMO-based NOMA-VLC systems.

System Model	Design Objective	Contribution	Ref.
2×2 MIMO with N users	BER	Evaluate the power allocation ratio for the best BER performance and propose minimum mean square error (MMSE) and intra symbol frequency averaging (ISFA) as efficient channel estimation methods to eliminate the inter-user interference effectively.	[196]
2×2 MIMO with N users	BER	Propose the offset quadrature amplitude modulation (OQAM)-OFDM based MIMO-NOMA and compare its performance with conventional OQAM based MIMO-OFDM	[197]
4×2 MIMO with N users	Achievable sum rate	Propose the low computational complexity normalized logarithmic gain ratio power allocation (NLGRPA) which outperforms NGDPA and GRPA methods	[163]
2×2 MIMO with N users	Achievable sum rate	Propose the low complexity NGDPA method and compare it with GRPA	[161]
2×2 MIMO with N users	Sum rate	Evaluate the percentage gain of sum rate for both (LOS) and (LOS + non-LOS) in a single reflection environment and calculate the delay spread using NGDPA and GRPA methods	[198]
M $\times$ L MIMO with N users	Spectral efficiency	Propose an algorithm for grouping the users into clusters based on the correlation among their channel gains and the proposed algorithm has better performance than zero forcing (ZF) and block diagonalization (BD) precoding schemes	[199]
2×2 MIMO with N users	Achievable capacity	Formulate an analytical model for system capacity and evaluate the performance of GRPA and NGDPA and compare them in terms of system coverage, user density, and user location	[200]

System Model	Design Objective	Contribution	Ref.
2×2 MIMO with N users	BER	Analyze MMSE equalizer with SIC and results show it outperforms the ZF equalizer with SIC	[201]

2.13 User Pairing in NOMA-VLC Systems

Certainly, NOMA presents superior outcomes for VLC systems compared to existing OMA strategies; however, the implementation of NOMA on all users jointly may not be feasible due to the escalating computational complexity of the SIC decoding process as the number of users rises. Furthermore, the additional signaling overhead associated with channel feedback management and error propagation may increase the deployment complexity of NOMA. Consequently, in order to address this issue, the concept of user pairing has emerged as an effective approach to reduce the decoding complexity of the SIC process [202]. User pairing involves dividing users into distinct pairs within a cell, with each pair being served using NOMA techniques [127]. Depending on performance requirements, user deployment scenarios, and implementation complexity, various user pairing schemes are utilized in NOMA-based VLC systems. Within all user pairing techniques, a distinction is made among weak users, located far from the transmitter and experience poor channel conditions, and strong users, located in close proximity to the transmitter and benefit from better channel conditions [160]. In the NOMA literature, there are different proposed user-pairing algorithms, such as:

1. Random user-pairing algorithm
2. Next-largest-difference user-pairing algorithm (NLUPA)
3. Divide and-NLUPA (D-NLUPA)
4. Distributed-NOMA (D-NOMA)
5. Uniform channel gain difference (UCGD)
6. User pairing that utilizes various algorithms such as the exhaustive search (ES) and genetic algorithms

These algorithms will be further detailed below.

2.13.1 Random user pairing

Random user pairing is perceived as one of the simplest and most convenient algorithms for user pairing. In this algorithm, the transmitter randomly selects users from a set of users and creates pairs. It is worth mentioning that the pairing in this case does not take into consideration the users' channel conditions and demonstrates suboptimal total rate performance [203]. Furthermore, the computational complexity of the random pairing algorithm is significantly reduced. The general concept of random user pairing is illustrated in Figure 2.11.

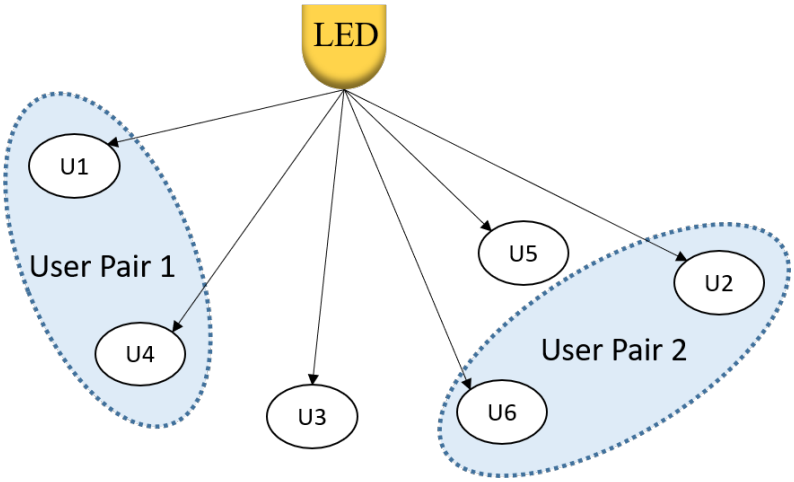

Figure 2.11 – Random user pairing.

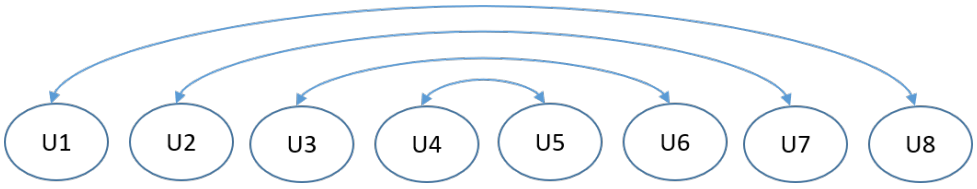

Figure 2.12 – NLUPA pairing.

2.13.2 Next-largest-difference-based user pairing algorithm

The enhancement in performance of NOMA over OMA becomes more significant when the difference in the channel gains between users, under consideration for pairing, increases [124]. Based on this observation, the authors in [124] have introduced a user pairing

algorithm known as next-largest-difference-based user pairing algorithm (NLUPA). In this algorithm, the user with the highest channel gain is paired with the user possessing the lowest channel gain, resulting in the highest capacity sum rate gain. Subsequently, the user with the next highest channel gain is paired with the corresponding user with the next lowest channel gain to achieve the subsequent highest capacity sum rate gain. This process continues until all pairs are established. The NLUPA pairing algorithm is illustrated in Figure 2.12.

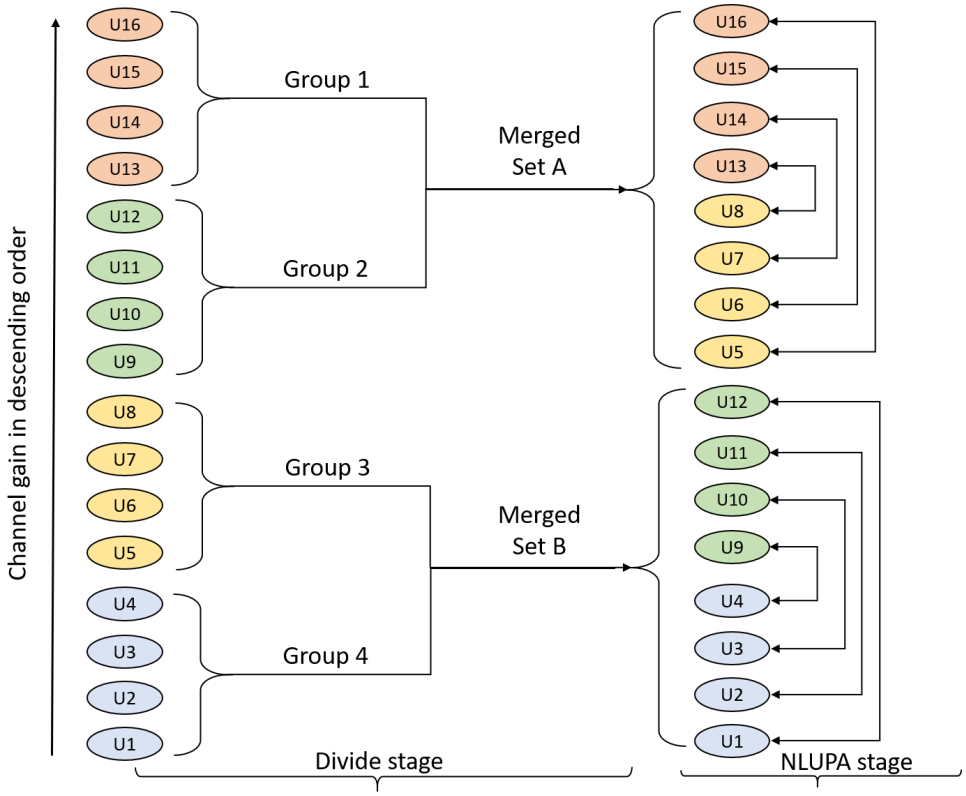

Figure 2.13 – D-NLUPA pairing.

2.13.3 Divide-and-NLUPA

The algorithm for user pairing that has been previously discussed is typically rooted in user grouping. To guarantee a minimal sum rate performance for each group, an enhanced NLUPA scheme known as divide-and-NLUPA (D-NLUPA) was introduced in [203]. In NLUPA, for N users, the initial pair experiences the highest gain as a result of a large difference in channel gains; however, the $N/2$-th pair's gain is not significant.

Consequently, there is a chance that certain user pairs may not witness a substantial increase in the sum rate. The distance between two users in a pair is proportional to the difference in their respective channel gains [204]. The 'divide' phase in D-NLUPA is implemented to establish a minimum range, thereby raising the minimum value of the distance accordingly. Through this 'divide' phase, user pairs with near-zero gains can be addressed, enabling each user pair to experience a minimum sum rate enhancement.

The user pairing algorithm example illustrated in Figure 2.13, for ($N = 16$) users, arranges all users based on their channel gains in ascending order and divides them into (N/g) groups, where ($g = 4$) denotes the number of users in each group. Specifically, the first and third groups are combined as set A, while the second and fourth groups are combined as set B. Subsequently, NLUPA is applied within set A and set B respectively for user pairing implementation. Consequently, each set possesses a minimum range value along with a corresponding minimum distance value. D-NLUPA ensures a minimum sum rate gain for each user pair by eliminating pairs with negligible gain.

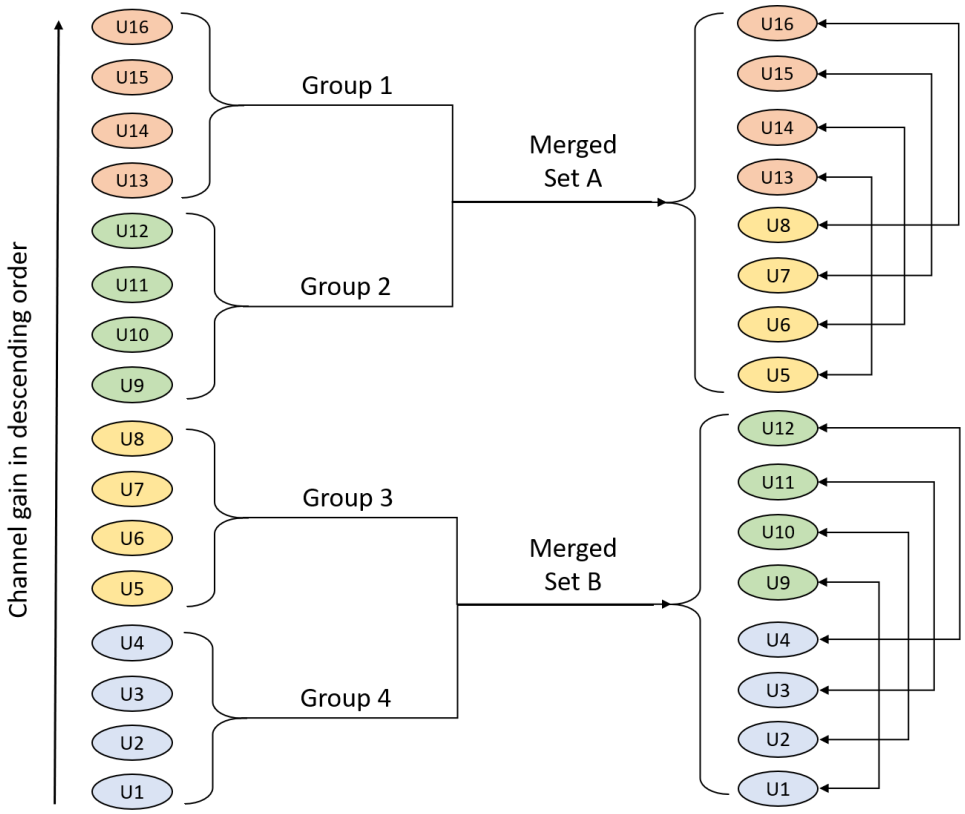

Figure 2.14 – D-NOMA pairing.

2.13.4 Distributed-NOMA

In spite of the division step in D-NLUPA, pairs with low gain differences still do not achieve maximum performance benefits, as the scheme cannot completely avoid zero channel gain differences. Consequently, a novel user pairing strategy, known as distributed-NOMA (D-NOMA), has been introduced in [205], representing a modified version of D-NLUPA. This particular strategy serves to enhance the overall performance throughput of pairs characterized by minimal differences in channel gain, while simultaneously ensuring favorable data rates among various pair groupings. The underlying assumption in this user pairing algorithm is that the number of strong users equals the number of weak users, thereby facilitating the pairing of all users. Consequently, this approach effectively mitigates performance deterioration among pairs with low differences in channel gain, ultimately leading to a controlled throughput advantageous to low gain users. Figure 2.14 illustrates the concept of D-NOMA pairing for four distinct user groups.

2.13.5 Uniform channel gain difference

In NOMA-based VLC systems, the relationship between channel gains of users and the powers allocated to them is inversely proportional, leading to substantial interference when the powers assigned to cell mid users in close proximity are similar. The drop in capacity for these cell mid pairs can be ascribed to two primary factors: increased noise affecting users with lower channel gains and imperfections in SIC affecting users with higher channel gains. The cause of these issues is the close correlation between channel gains and assigned powers. The uniform channel gain difference (UCGD) pairing is designed to serve users located in the middle of a cell by maintaining a consistent channel gain difference among paired users. By categorizing the channel gains of the cell's users into two distinct groups and pairing them accordingly, the UCGD approach ensures effective service for mid-cell users [206]. This user pairing algorithm involves sorting all users based on the median channel gain value, which then acts as a dividing point to create two groups: group I comprising users with lower channel gains than the median, and group II consisting of users with higher channel gains. Unlike traditional pairings between central and edge users, the UCGD scheme focuses on pairing mid-cell users with those in the central or edge areas of the cell, offering the benefits of NOMA's enhanced capacity gains while addressing issues related to successive interference cancellation (SIC) performance. The UCGD pairing algorithm is illustrated in Figure 2.15.

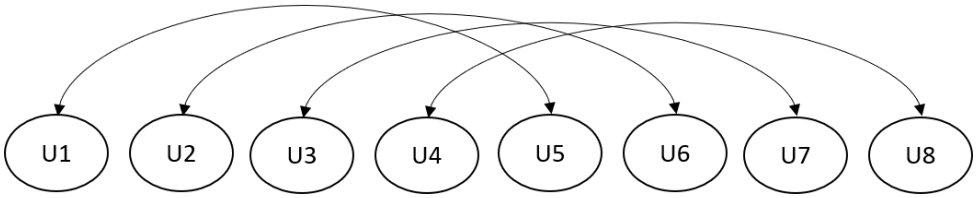

Figure 2.15 – UCGD pairing.

In contrast to NLUPA, the primary benefit of UCGD pairing lies in the enhancement of data rates for users with high channel gains. This occurs because users characterized by high channel gains are paired with middle users within the cell who need lower power levels, as opposed to users at the cell edge, who demand higher power resources. Consequently, users with high gains experience a relatively higher power allocation, leading to a boost in their capacity gains.

2.13.6 Hybrid user pairing

The hybrid user pairing algorithm, combining NLUPA and UCGD pairing, has been introduced in [207]. This algorithm is based on the principle of pairing distant users with nearby users through NLUPA. However, when a group of N users is close to the center of the cell and cannot be paired, $(N/2)$ users from each side are utilized for accommodating these users through UCGD pairing. The decision to transition from NLUPA to UCGD pairing is made when similar-gain users in the central area cannot be paired together. The hybrid pairing algorithm is illustrated in Figure 2.16, showcasing the pairing of two nearby users, U_4 and U_5. In this scenario, the immediate neighboring users, U_3 and U_6, come together to facilitate the pairing: U_3 is paired with U_5, and U_4 is paired with U_6, employing UCGD pairing, while the remaining users are paired using the straightforward NLUPA algorithm.

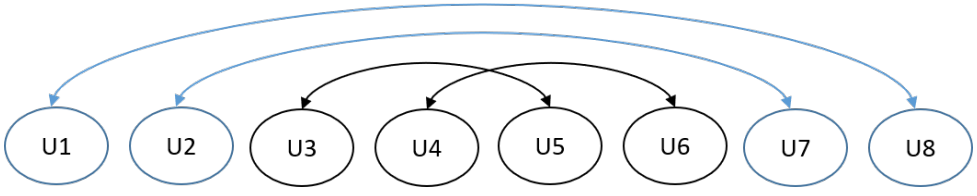

Figure 2.16 – Hybrid pairing.

2.13.7 User pairing optimization algorithms

In addition to the aforementioned schemes, various user pairing optimization algorithms are proposed to enhance the NOMA-VLC systems' performance. The exhaustive search (ES) method, which considers all possible combinations of user pairing, can be utilized to find an optimal solution. Nonetheless, the time complexity of ES grows exponentially with the increasing number of users [208]. To address this issue, novel user grouping algorithms have been introduced [209]–[211]. The authors of [209] introduced the bipartite matching-based user-pairing (BMUP) algorithm aimed at finding the optimal user grouping solution to minimize the outage probability in hybrid VLC/RF systems. In [210], an optimal user pairing algorithm was proposed to maximize system throughput, with a closed-form global optimal solution derived for general NOMA networks. However, these algorithms are constrained to scenarios with an even number of users, which limits their practicality. Therefore, a dynamic user grouping algorithm based on a genetic algorithm was proposed in [211], which not only addresses scenarios with an odd number of users but also enhances system throughput. Nevertheless, the genetic algorithm may encounter challenges in converging to a local optimal solution.

2.14 Summary

In this chapter, a review of the state of the art for visible light communication (VLC) systems has been discussed. We introduced VLC systems, highlighting their potential in providing high-speed wireless communication. Among various multiple access techniques we explored, non-orthogonal multiple access (NOMA) stands out due to its ability to enhance system capacity and user fairness. Furthermore, we discussed different power allocation techniques within NOMA-VLC systems, emphasizing both strategic design approaches and numerical search methods. Power allocation significantly impacts system performance, influencing metrics such as sum rate, fairness, and bit error rate (BER). In addition, we explored multiple input multiple output (MIMO) technology, which further enhances the performance of VLC systems. MIMO leverages multiple transmitting and receiving antennas to increase data rates and improve reliability. The combination of MIMO with NOMA can significantly boost spectral efficiency and user capacity in VLC systems. We also discussed various user pairing algorithms, which are crucial for improving NOMA-VLC performance.

These discussions underscore the importance of efficient power allocation and user

pairing strategies in leveraging the full potential of NOMA within VLC systems, ensuring optimal performance and resource utilization.

Chapter 3

Achievable Rate Performance of NOMA-MIMO-VLC Systems

3.1 Introduction

In this chapter, we evaluate the performance of multiple-input multiple-output (MIMO) communication systems applied with a non-orthogonal multiple access (NOMA)-based indoor visible light communication (VLC). We present two efficient user-pairing algorithms for NOMA in VLC, aiming to enhance achievable data rates effectively. Our investigation involves the application of three low-complexity power allocation techniques. Comparative analysis reveals performance enhancements when employing the presented schemes, especially when contrasted with NOMA without user pairing and orthogonal frequency division multiple access (OFDMA). Additionally, we explore the performance of both algorithms in scenarios with both even and odd numbers of users. Simulation results demonstrate the superiority of NOMA in comparison to OFDMA.

3.2 System and Channel Models

We model a multi-user VLC system based on NOMA-MIMO. In our study, we investigate a 2×2 MIMO downlink VLC indoor system featuring two light-emitting diode (LED) transmitters located on the room's ceiling, utilizing NOMA to serve N users. Each user is equipped with two photodiodes (PDs) oriented towards the ceiling, capable of utilizing the entire modulation bandwidth of the LEDs. Figure 3.1 shows the downlink 2×2 MIMO-VLC system which utilizes NOMA to serve N users.

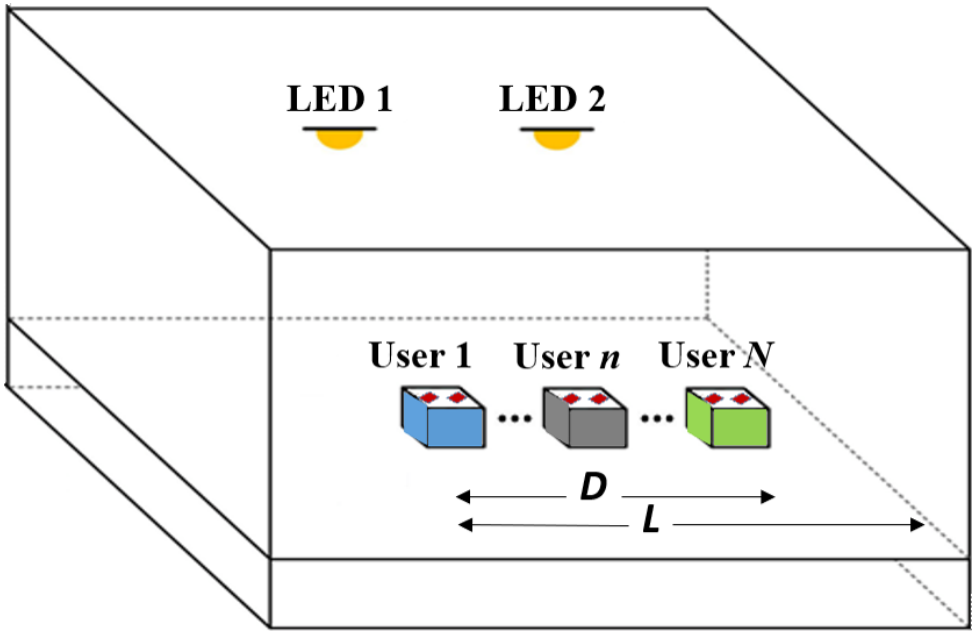

Figure 3.1 – The downlink 2 × 2 NOMA-MIMO-VLC system serving N users: D is the distance between user 1 and user N, L is the distance between user 1 and the room's edge.

The VLC channel model primarily focuses on the LOS component. Although the VLC channel includes a diffusive part, it is often considered negligible due to the significantly lower energy of the reflected signal compared to the LOS signal [212]. Figure 3.2 illustrates how a simple channel model of a single LED serves a user with a single PD. The direct current (DC) channel gain between the jth PD ($j = 1, 2$) of the nth user ($n = 1, \cdots, N$) and the ith LED ($i = 1, 2$) can be expressed as provided in [213]

$$h_{ji,n} = \begin{cases} \frac{A(m+1)}{2\pi d_{ji,n}^2} T_s(\psi_n) g(\psi_n) \cos^m(\phi_n) \cos(\psi_n), & 0 \leq \psi_n \leq \psi_c \\ 0, & \psi_n > \psi_c \end{cases} \tag{3.1}$$

where A represents the PD's detection area, $m = \frac{-ln(2)}{ln(\cos(\Phi_{1/2}))}$ denotes the order of Lambertian emission[1] and $\Phi_{1/2}$ stands for the LED's semi-angle at half power, $d_{ji,n}$ is the distance between the ith LED and the jth PD of the nth user. Field of view (FoV) is denoted by ψ_c, while the angle of incidence and the angle of irradiance are denoted by ψ_n and ϕ_n, respectively. $T_s(\psi_n)$ denotes the gain of the optical filter used at the receiver and $g(\psi_n)$ is the gain of the optical concentrator, which is given by [214]

1. The order of Lambertian emission defines the angular distribution of light emitted from a surface, where higher orders correspond to more focused, directional light beams.

$$g(\psi_n) = \begin{cases} \frac{n_c^2}{sin^2(\psi_c)}, & 0 \leq \psi_n \leq \psi_c \\ 0, & \psi_n > \psi_c \end{cases} \tag{3.2}$$

where n_c represents the corresponding refractive index of the optical concentrator. The noise produced at the PDs follows a Gaussian distribution of zero mean and has the following variance:

$$\sigma_{z_n}^2 = \sigma_{sh_n}^2 + \sigma_{th_n}^2 \tag{3.3}$$

where $\sigma_{sh_n}^2$ and $\sigma_{th_n}^2$ are the variances of the shot and thermal noises, respectively. The shot noise variance at the nth receiver is given by [215]

$$\sigma_{sh_n}^2 = 2qB(R_p P_{r_n} + I_{bg} I_2) \tag{3.4}$$

where $q = 1.6 * 10^{-19}$ Coulombs is the charge of an electron, R_p is photodetector responsivity, P_{r_n} is the received optical power for the nth user, B is the equivalent bandwidth, I_{bg} is the photocurrent due to background radiation and I_2 is the noise bandwidth factor. Thermal noise is generated within the transimpedance receiver circuit. If the noise effect from the gate leakage current is neglected, thermal variance is represented by [216]

$$\sigma_{th_n}^2 = 8\pi\kappa T_k C_{pd} A B^2 \left(\frac{1}{G_{ol}} I_2 + \frac{2\pi\Gamma}{g_m} C_{pd} A I_3 B \right) \tag{3.5}$$

which consists of feedback-resistor noise and FET channel noise, where $\kappa = 1.38 * 10^{-23}$ J/K is the Boltzmann's constant, T_k is the absolute temperature, G_{ol} is the open-loop voltage gain, C_{pd} is the fixed capacitance of the photodetector per unit area, Γ is the FET channel noise factor, g_m is the FET transconductance and $I_3 = 0.0868$ is a weighting function that depends on the input optical pulse shape [216].

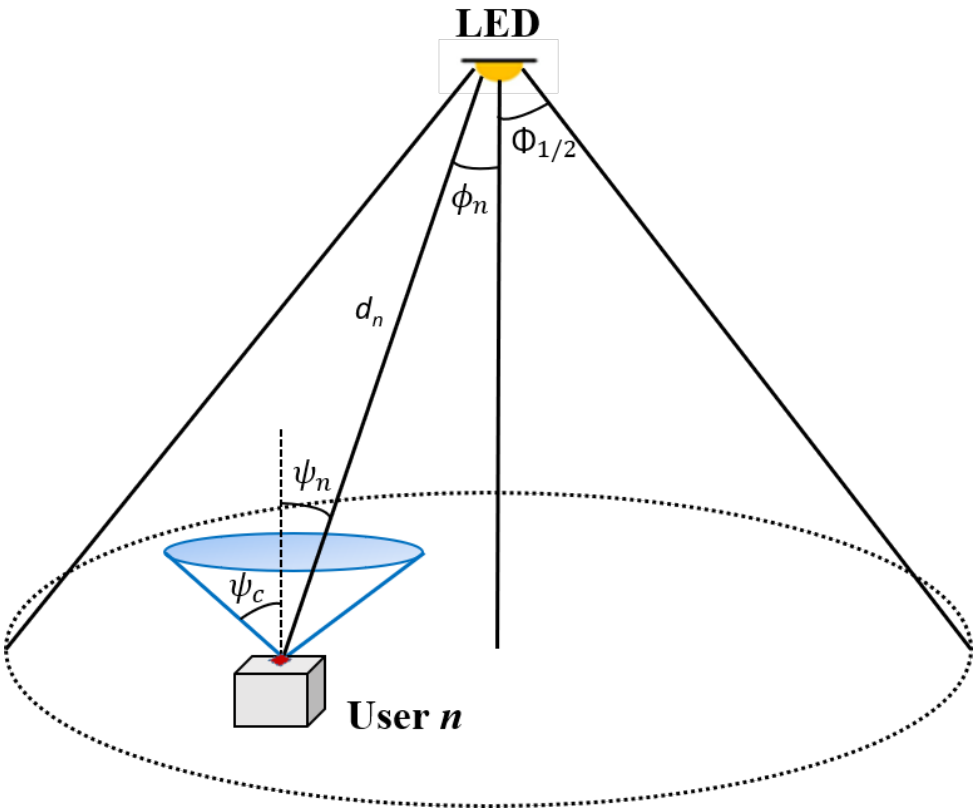

Figure 3.2 – VLC channel model: ϕ_n is the angle of irradiance, $\Phi_{1/2}$ is the LED's semi-angle at half power, d_n is the distance between the LED and the nth user, ψ_n is the angle of incidence, ψ_c is the field of view.

DC-biased optical OFDM (DCO-OFDM) modulation is employed as the transmitted signal must be real and positive. The 2×2 NOMA-MIMO-VLC system's schematic using DCO-OFDM is illustrated in Figure 3.3. The superimposed input signal to the ith LED, following modulation and power domain multiplexing, is expressed as

$$x_i = \sum_{n=1}^{N} \sqrt{p_{i,n}} s_{i,n} + I_{DC} \tag{3.6}$$

where $p_{i,n}$ is the electrical power allocated at the ith LED ($i = 1, 2$) for the nth user with overall electrical power $p_{elec} = \sum_{n=1}^{N} p_{i,n}$, signal $s_{i,n}$ is modulated in the ith LED for the nth user, and I_{DC} stands for the DC bias current provided for each LED. Without any loss of generality, we assume that $p_{elec} = 1$ and N users are ordered based on the sum of their

optical channel gains as follows

$$h_{1i,1} + h_{2i,1} > \cdots > h_{1i,n} + h_{2i,n} > \cdots > h_{1i,N} + h_{2i,N} \tag{3.7}$$

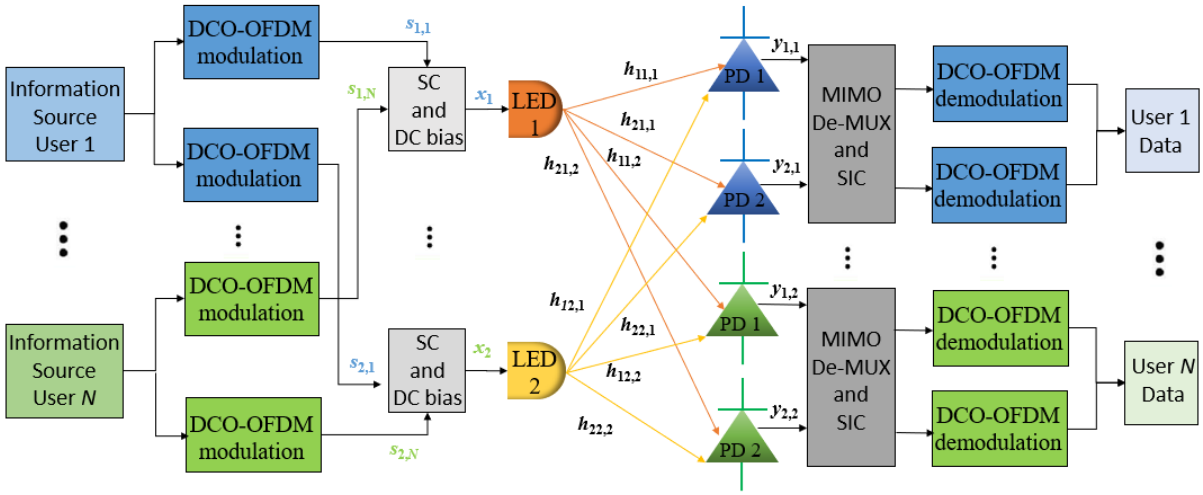

Figure 3.3 – Schematic of a 2 × 2 NOMA-MIMO-VLC system with N users.

The electrical signal vector received at the nth user is represented as

$$\mathbf{y}_n = R_p \zeta P_o \mathbf{H}_n \mathbf{x} + \mathbf{z}_n \tag{3.8}$$

where ζ is the modulation index, P_o is the LED's output optical power, $\mathbf{H}_n$ is the channel gain matrix relative to the nth user, $\mathbf{x} = [\, x_1 \quad x_2 \,]^T$ is the transmitted electrical signal vector where $[\cdot]^T$ is the transpose operation, $\mathbf{z}_n$ is an additive white Gaussian noise vector with zero mean and variance σ_z^2.

To successfully recover the transmitted data, zero-forcing (ZF) [2] MIMO receiver employing basic channel inversion is employed [162]. The normalized estimated electrical signal vector obtained by the ZF-based MIMO demultiplexing at the nth user is given by [217]

$$\widetilde{\mathbf{x}}_n = \frac{\mathbf{1}}{R_p \zeta P_o} \mathbf{H}_n^{-1} \mathbf{y}_n = \mathbf{x} + \frac{1}{R_p \zeta P_o} \mathbf{H}_n^{-1} \mathbf{z}_n \tag{3.9}$$

2. The ZF MIMO receiver, a linear detection technique, separates signals from multiple transmitters by inverting the channel matrix. It is chosen for its computational simplicity, making it more feasible for NOMA-MIMO-VLC systems compared to minimum mean squared error (MMSE) and maximum-likelihood (ML). Although ZF may enhance noise, it effectively eliminates interference, making it practical for scenarios where optimal bit error rate (BER) performance is not critical.

where H_n^{-1} is the inverse of H_n. To enable successive interference cancellation (SIC) at the receiver, the sequence for decoding users concerning the ith LED needs to be established [218]. The decoding order, in relation to the ith LED, is arranged as follows

$$O_{i,1} < \cdots < O_{i,n} < \cdots < O_{i,N} \tag{3.10}$$

When employing SIC at the nth user, message signals directed to users with weaker channel conditions are effectively eliminated. However, the message signal intended for users with stronger channel conditions remains present but is treated as noise in the system [219]. Consequently, the received signal-to-interference plus noise ratio (SINR) [3] received by the nth user from the ith LED can be described as [220]

$$SINR_{i,n} = \frac{(R_p \zeta P_o)^2 p_{i,n}}{(R_p \zeta P_o)^2 \sum_{l=1}^{n-1} p_{i,l} + \gamma_{i,n}^2} \tag{3.11}$$

where $\gamma_{i,n}$ is the ith element of vector $\boldsymbol{\gamma}_n = \mathbf{H}_n^{-1}\mathbf{z}_n$. Since the OFDM signal generally follows a Gaussian distribution, the combined interference and noise also exhibit a Gaussian distribution [221]. The achievable data rate for the nth user is given by [222]

$$R_{i,n} = \begin{cases} \frac{1}{2} B \, log_2 \left(1 + SINR_{i,n}\right), & n = 2, \ldots, N \\ \frac{1}{2} B \, log_2 \left(1 + \frac{(R_p \zeta P_o)^2 p_{i,n}}{\gamma_{i,n}^2}\right), & n = 1 \end{cases} \tag{3.12}$$

The scaling factor of 1/2 is due to the Hermitian symmetry. We assume that perfect SIC can be performed in the decoding as the nth user can successfully detect the message for the kth user ($n + 1 \leq k \leq N$).

3.3 Power Allocation Techniques and User-Pairing Algorithms

Efficient power allocation techniques ensure the optimal distribution of available power resources among users, thereby maximizing the system's performance. Moreover, user pairing where users are effectively grouped together is essential as it affects how well

3. The SINR is a metric used in wireless communications to quantify the quality of a signal in the presence of both interference from other signals and noise. It is defined as the ratio of the power of the desired signal to the sum of the power of interference signals and the power of noise.

NOMA can be realized. In this section, we discuss different efficient power allocation techniques and user-pairing algorithms that can improve the system's throughput and fairness.

3.3.1 Power allocation techniques

We depict various low-complexity power allocation methods recognizing their crucial role in enhancing NOMA performance by appropriately assigning power levels to users [223]. Our study primarily focuses on evaluating, in terms of achievable rates, the performance of NOMA-MIMO-VLC systems using prevalent low-complexity power allocation techniques fixed power allocation (FPA), gain ratio power allocation (GRPA), and normalized gain difference power allocation (NGDPA).

Fixed power allocation

The fixed power allocation (FPA) is a simple approach that allocates power levels to users based on their order of decoding, regardless of the actual values of their channel gain [167]. The electrical power assigned at the ith LED to users n and $n+1$ is represented by

$$p_{i,n} = \alpha_{i,n} p_{i,n+1} \tag{3.13}$$

where $\alpha_{i,n}$ is the power allocation factor $(0 < \alpha_{i,n} < 1)$.

Gain ratio power allocation

This allocation technique was introduced in [135] as an effective power allocation technique for NOMA-VLC systems. The power assigned in gain ratio power allocation (GRPA) depends on the channel gain ratio. However, the GRPA equation in [135] is modified to be suitable for 2×2 NOMA-MIMO-VLC systems with decoding order in Equation(3.10) where the electrical power assigned to users n and $n+1$ at the ith LED is given by

$$p_{i,n} = \left(\frac{h_{1i,n+1} + h_{2i,n+1}}{h_{1i,1} + h_{2i,1}} \right)^{n+1} p_{i,n+1} \tag{3.14}$$

Normalized gain difference power allocation

The normalized gain difference power allocation (NGDPA) was proposed for enhancing the achievable data rate of NOMA-MIMO-VLC systems [162]. Assigning power in

NGDPA depends on channel gain difference where the electrical power assigned at the ith LED to n and $n+1$ users is represented as [162]

$$p_{i,n} = \left(\frac{h_{1i,1} + h_{2i,1} - h_{1i,n+1} - h_{2i,n+1}}{h_{1i,1} + h_{2i,1}} \right)^{n} p_{i,n+1} \tag{3.15}$$

3.3.2 User-Pairing Algorithms

The user pairing concept has been proposed to group users into multiple pairs with the aim of maximizing the channel gain difference among users, thereby enhancing the performance of NOMA [224]. A hybrid NOMA and orthogonal multiple access (OMA) scheme can be employed to accommodate multiple user pairs effectively. To clarify, NOMA is used for the two users within each user pair, while OMA is applied for different user pairs [225]. Hereinafter, we explore two distinct user-pairing algorithms designed to efficiently group N users into $N/2$ pairs. Furthermore, we study the performance of both algorithms in even and odd numbers of user scenarios.

Even Number of Users

Both algorithms, uniform channel gain difference (UCGD) and next largest difference user pairing algorithm (NLUPA), adopt identical approaches for user grouping when the number of users is even. This process commences with the users being initially arranged in ascending order according to their individual channel gains. Subsequently, the users are categorized into two groups denoted as g_1 and g_2 which have users with high and low channel gains, respectively. Group g_1 encompasses the first half of sorted users, commencing from U_1 to $U_{N/2}$, while group g_2 includes the second half of users, commencing from $U_{(N/2)+1}$ to U_N. The UCGD algorithm aims to achieve an almost uniform channel gain difference between in-pair users of all pairs. To facilitate user pairing, one user is chosen from each group, and they are paired together [4]. Therefore, pairing using the UCGD algorithm can be defined as $\mho_{i,m} = \{g_{i,1}(m), g_{i,2}(m)\}$, where $\mho_{i,m}$ is the mth user pair $\mho_{i,m}$ for the ith LED. In this case, $g_{i,1}(m)$, $g_{i,2}(m)$ denote the mth user for the ith LED in groups g_1 and g_2, respectively, with $1 \leq m \leq N/2$. On the other hand, the user with the highest channel gain is paired with the user with the lowest channel gain

4. The optimal number of users within each pair depends on several factors, such as the power allocation techniques and user pairing algorithms. However, pairing two users is generally the most common approach, particularly for systems with low computational resources or real-time constraints, as it reduces SIC complexity and decoding latency [124], [206].

to achieve maximum channel gain difference within paired users in NLUPA. By following the same pattern of arranging and dividing users into two groups, user pairing can be accomplished in the following manner: $\mho_{i,m} = \{g_{i,1}(m), g_{i,2}((N/2) + 1 - m)\}$. However, the users with medium channel gains are paired with each other, which leads to lesser channel gain difference.

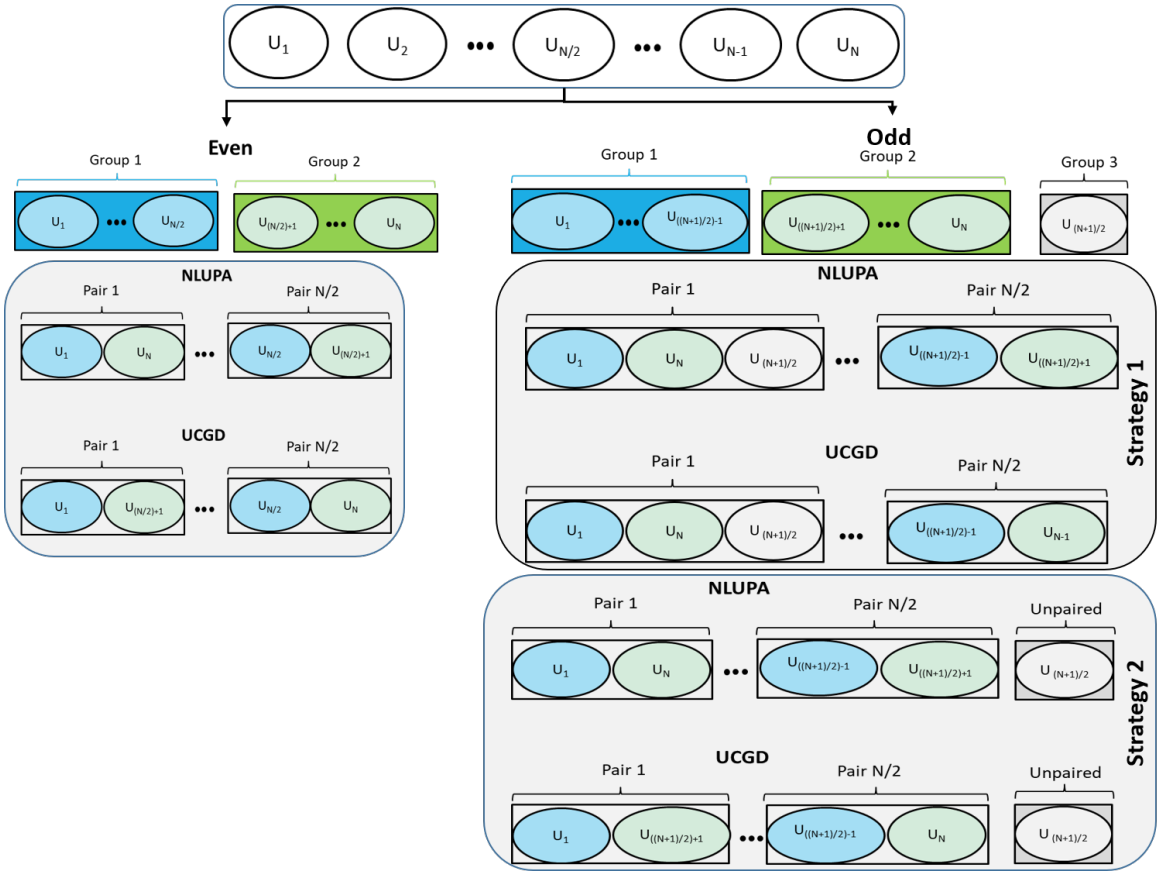

Figure 3.4 – Illustration of user grouping and pairing for even and odd number of users using NLUPA and UCGD.

Odd Number of Users

When the number of users is odd, N, after sorting the users in ascending order according to their channel gains, the users are categorized into three groups. The first group g_1 consists of users ranging from U_1 to $U_{((N+1)/2)-1}$, g_2 includes users from $U_{((N+1)/2)+1}$ to U_N, and g_3 contains $U_{((N+1)/2)}$, the middle user. Two strategies can be adopted for user pairing in the case of an odd number of users for both NLUPA and UCGD algorithms.

These strategies are illustrated using NLUPA as follows:

— First Strategy: Consider that all users have to be paired. The first pair consists of three users: $g_{i,1}(1)$, $g_{i,2}((N-1)/2)$ and $g_{i,3}(1)$, which correspond to the first user from group g_1 (nearest to the LED), the last user from group g_2 (farthest from the LED) and the middle user from group g_3, respectively.

— Second Strategy: Employs a different pairing approach in which the middle user is left unpaired, while the remaining users are paired in the same manner as NLUPA with an even number of users.

Figure 3.4 demonstrates the user grouping and pairing for even and odd numbers of users using NLUPA and UCGD. Moreover, an identical bandwidth allocation [5] is assessed for different user pairs, in all scenarios equal to $\frac{B}{N/2}$ for an even number of users and $\frac{B}{(N/2)+1}$ for an odd number of users.

3.4 Numerical Results and Discussions

This section investigates the performance of an indoor 2×2 NOMA-MIMO-VLC system employing three power allocation schemes and two user-pairing algorithms through numerical simulations. We chose not to employ any optimization technique in this study to investigate and maintain a low-computational-complexity system suitable for the practical implementation of NOMA-VLC MIMO. This objective guided our selection of power allocation schemes and user-pairing algorithms. The detailed simulation parameters of the system are shown in Table 3.1. We analyzed the achievable rate performance using Equation (3.12) based on the model depicted in Figure 3.1, where U_1 remains stationary and centered between both LEDs. The distance between U_1 and U_N is denoted by D, while the gap between U_1 and the room's edge is $L = 2$ m. We defined $Q = \frac{D}{L}$ as the normalized offset of U_N with respect to U_1, whereas $\frac{(n-1)D}{(N-1)L}$ is the normalized offset of U_n relative to U_1. In the obtained simulation results, we calculate the achievable rate performance for each Q value over a total of 500 iterations.

First, we studied the achievable data rate performance of two users. Furthermore, we conducted a performance comparison between OFDMA with a uniform power allocation and NOMA. Finally, to accommodate a greater number of users, we investigated the achievable rate performance of the system using NLUPA and UCGD user-pairing

5. Equal bandwidth allocation is a straightforward method that has proven effective and is widely used in most hybrid NOMA/OMA systems [103].

algorithms, comparing their performance for scenarios with both odd and even numbers of users. We chose five users for the odd-numbered scenarios and six users for the even-numbered scenarios as reasonable numbers to compare the performance of the presented techniques. However, it is important to note that our investigation was not limited to these scenarios, and any number of users can be explored for further analysis.

Table 3.1 – Simulation parameters [162].

Description	**Symbol**	**Value**
PD detection area	A	1 cm^2
Transmitter semi-angle	$\Phi_{1/2}$	60°
Modulation bandwidth	B	10 MHz
Output optical power	P_o	10 W
Responsivity	R_p	0.53 A/W
Optical filter gain	$T_s(\psi_n)$	0.9
Optical concentrator gain	$g(\psi_n)$	2.5
Modulation index	ζ	0.5
Distance between PDs of each user	d_{pd}	4 cm
Vertical spacing between the users and LEDs	d_{lu}	2.15 m
Spacing between the LEDs	d_l	1 m
FoV of PD	ψ_c	72°

3.4.1 Two-User Scenario

Initially, we demonstrate the achievable rate performance using the three power allocation techniques in two-user scenarios to elucidate the specific characteristics of each method. However, before comparing these techniques, we first analyze the impact of the value of $\alpha_{i,n}$ in Equation (3.13) on the achievable data rate performance, aiming to determine the value of $\alpha_{i,n}$ that attains best achievable rate for the FPA technique. The achievable data rate of each LED versus the normalized offset Q for a 2 × 2 NOMA-MIMO-VLC system serving 2 users, where the data rate that each LED can achieve is the aggregate of the achievable data rates for two users served by that LED is shown in Figure 3.5. Table 3.2 presents the user order of LED 1 and LED 2 at each Q for the two-user scenario. A higher order indicates more power is assigned to the user's signal.

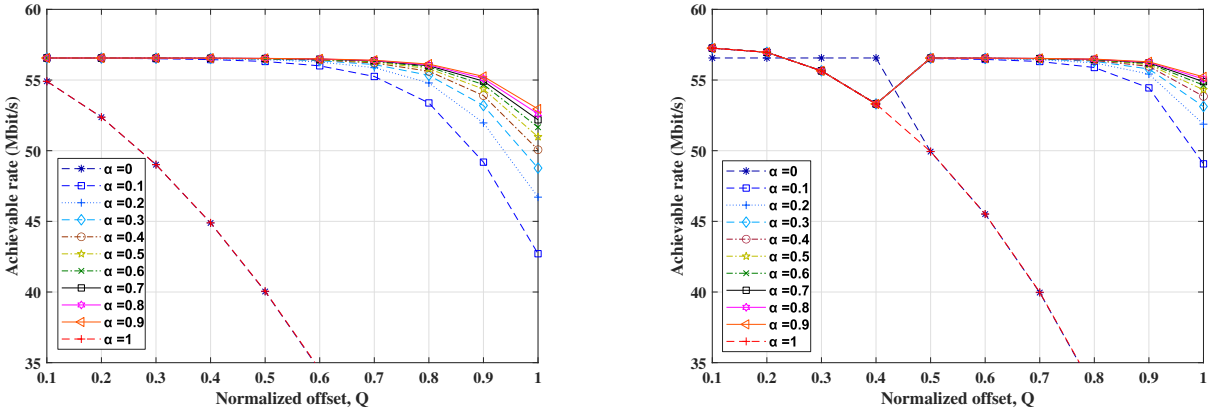

(a) (b)

Figure 3.5 – Achievable rate vs. normalized offset based NOMA using FPA with two users ($N = 2$): (**a**) LED 1, (**b**) LED 2.

Table 3.2 – User ordering of two-user scenario for both LEDs at different Q values: O_n is the user's order.

	LED 1		**LED 2**	
Q	O_1	O_2	O_1	O_2
0.1	U_1	U_2	U_2	U_1
0.2	U_1	U_2	U_2	U_1
0.3	U_1	U_2	U_2	U_1
0.4	U_1	U_2	U_2	U_1
0.5	U_1	U_2	U_2	U_1
0.6	U_1	U_2	U_1	U_2
0.7	U_1	U_2	U_1	U_2
0.8	U_1	U_2	U_1	U_2
0.9	U_1	U_2	U_1	U_2
1	U_1	U_2	U_1	U_2

For LED 1, U_1 is the near user and U_2 is the far user. The results indicate that the worst rate is achieved at $\alpha = 0$, where the entire power is allocated to U_2, and at $\alpha = 1$, where the power is equally distributed between both users which has a bad impact on the performance of NOMA. For other values of α, the achievable rate remains nearly constant at 56.6 Mbit/s in the range from $Q = 0.1$ to $Q = 0.5$, before it begins to decrease as the normalized offset increases. Similarly, for LED 2, the worst achievable rate performance

occurs at $\alpha = 0$ and $\alpha = 1$. However, the behavior of the achievable rate differs from that of LED 1 between $Q = 0.1$ and $Q = 0.5$, where U_1 is the far user and U_2 is the near user. From $Q = 0.6$ onwards, the user order reverses, and the behavior starts to resemble that of LED 1, with a higher achievable rate as U_2 is closer to LED 2 than LED 1. Despite the similarity of channel conditions for U_2 with respect to LED 2 at $Q = 0.1$ and 0.4 due to geometry, LED 2's achievable rate degrades due to the decreases of user 2's SINR as the Q increases from 0.1 to 0.4. It is noted that the best achievable data rate of both LEDs can be reached at $\alpha = 0.9$; where the data rate of LED 1 and LED 2 achieved at $Q = 1$ are 53.2 and 55.3 Mbit/s, respectively. We consider $\alpha = 0.9$ for FPA in the following results.

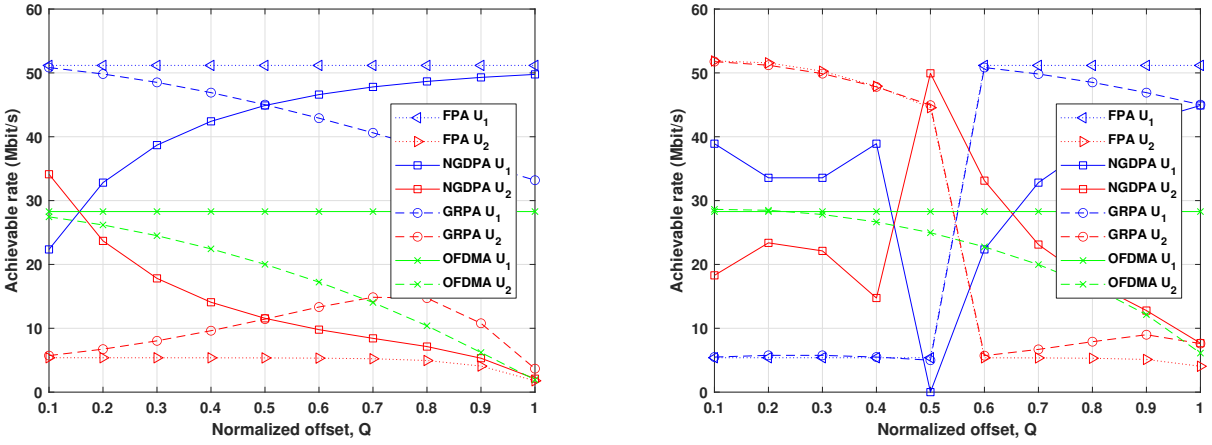

Figure 3.6 – Achievable rate vs. normalized offset-based NOMA and OFDMA with two users ($N = 2$) (**a**) LED 1, (**b**) LED 2.

Figure 3.6 illustrates the achievable rate for each user for both LEDs versus the normalized offset Q using OFDMA and NOMA with different power allocation techniques in the 2×2 NOMA-MIMO-VLC system, serving two users ($N = 2$). For LED 1, U_1 represents the nearby user, and U_2 is the far user, as depicted in Figure 3.1. In the case of FPA, U_1 achieves a consistently high data rate of 51.2 Mbit/s due to its high SINR according to Equation (3.12). However, U_2 achieves a constant data rate of 5.2 Mbit/s in the range from $Q = 0.1$ to $Q = 0.7$, which is due to significant interference from U_1. Then, as U_2 moves farther from the LED, the rate gradually decreases to 1.9 Mbit/s at $Q = 1$ due to the increasing noise, as depicted in Figure 3.6a.

On the other hand, the GRPA strategy aims to achieve fairness among users by initially

distributing power almost evenly between them. As U_2 moves farther away from the LED, more power is allocated to the distant user while reducing the power assigned to the nearby user. This explains why the data rate of U_1 decreases from 50.8 Mbit/s to 33.2 Mbit/s as Q increases. Simultaneously, the data rate of U_2 increases in the range from $Q = 0.1$ to $Q = 0.8$, but then decreases as the noise level increases.

Conversely, the NGDPA strategy is designed to improve the system's overall achievable rate. It begins by allocating more power to the far user and less power to the near user. As U_2 moves farther away from the LED, more power is gradually assigned to the near user, eventually reaching 49.8 Mbit/s at the edge of system coverage. Simultaneously, the power allocated to the far user decreases, resulting in a data rate of 2.1 Mbit/s at $Q = 1$. This dynamic allocation of power enhances the total achievable rate of the system. It is important to note that in the context of NOMA, the far user consistently obtains more power than the near user. The distinction between the aforementioned techniques lies in the specific amount of power allocated to each user, but the principle of favoring the far user with higher power remains consistent.

While in the OFDMA scenario, each user operates in a different frequency subband and the achievable rate of U_1 remains constant at 28.3 Mbit/s, as it has a fixed position. Meanwhile, the rate of U_2 decreases as the normalized offset Q increases, eventually reaching 1.9 Mbit/s at $Q = 1$.

For LED 2, the analysis differs because U_1 is considered the far user and U_2 is the near user in the range from $Q = 0.1$ to $Q = 0.5$, and vice versa in the range from $Q = 0.6$ to $Q = 1$ as shown in Figure 3.6b. This change in the roles of users affects the interference levels for each user and achievable data rates accordingly. In FPA, U_1 has a fixed low data rate of 5.4 Mbit/s due to the interference from U_2 in the range from $Q = 0.1$ to $Q = 0.5$. Then, the rate suddenly increases to 51.2 Mbit/s and remains fixed from $Q = 0.6$ to $Q = 1$. Meanwhile, U_2 starts with a rate of 51.8 Mbit/s, which gradually decreases due to increasing noise as U_2 moves farther from the LED. When the roles change, and U_2 becomes the far user, the rate drops to 5.4 Mbit/s at $Q = 0.6$ and continues to decrease till 4 Mbit/s at $Q = 1$.

The performance of GRPA is quite similar to that of FPA in the range from $Q = 0.1$ to $Q = 0.5$. However, from $Q = 0.6$ to $Q = 1$, as U_2 moves farther from the LED, the rate of U_1 decreases, while the rate of U_2 increases. This aligns with the concept of GRPA, which aims to enhance the performance of the far user.

In the NGDPA scheme, given that U_2 maintains the same channel gain at $Q = 0.1$

and $Q = 0.4$ and U_1 is stationary between both LEDs, the achievable rates are equal in these specified positions. However, there is a slight degradation in U_2's rate as its SINR decreases with increasing distance from the LED. The same scenario applies to the $Q = 0.2$ and $Q = 0.3$. At $Q = 0.5$, both users have identical channel gains. Following Equation (3.15), this implies that all the power is allocated to U_2, leaving U_1 with no power allocation. Consequently, U_1's rate becomes zero. Starting from Q = 0.6, the power allocation pattern shifts, with more power being assigned to the near user (U_1) and less power to the far user (U_2). This results in U_1 achieving 44.9 Mbit/s and U_2 achieving 7.7 Mbit/s at the end of system coverage.

It can be seen that the OFDMA performance for U_1 is consistent with what was discussed for LED 1, with no significant changes. However, there is an improvement in U_2's performance because it is always closer to LED 2 than to LED 1.

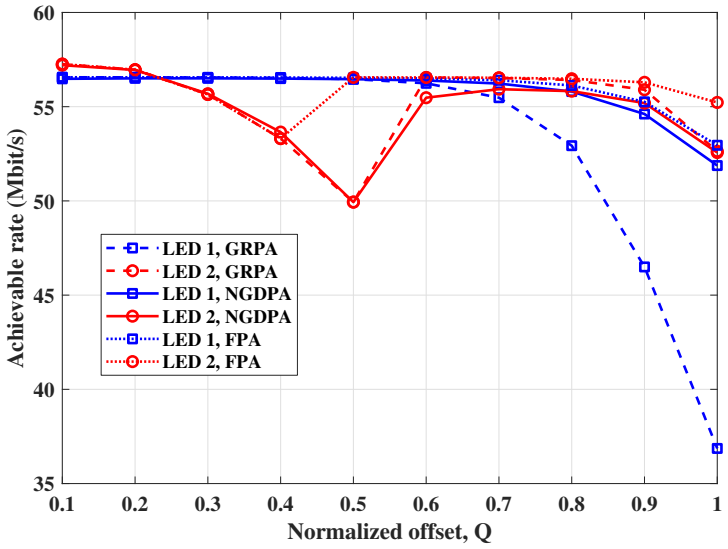

Figure 3.7 – Achievable rate vs. normalized offset based NOMA using NGDPA, GRPA and FPA with two users ($N = 2$).

To facilitate a clear comparison between the different power allocation techniques, we examine the achievable sum rate of both LEDs using NGDPA, GRPA, and FPA as shown in Figure 3.7. It is noted that the achievable sum rate of LED 1 for the three techniques is almost constant at 56.6 Mbit/s in the range $0.1 \leq Q \leq 0.6$; while the rate of LED 2 experiences variation as Q increases, reaching the lowest rate of almost 50 Mbit/s at $Q = 0.5$ for both NGDPA and GRPA. The reason behind this is the low performance of NOMA when both users are equidistant from LED 2, i.e., same channel conditions, which

renders the achievable rate to decrease due to distributing the same amount of power for users in GRPA according to Equation (3.14). Furthermore, in NGDPA, LED 2 assigns the entire power to user 2 according to Equation (3.15). It is noted that FPA does not suffer performance degradation at $Q = 0.5$ and achieves a rate of 56.6 Mbit/s as it relies on user ordering rather than the exact value of the channel gains. Moreover, the achievable rate of LED 1 decreases significantly with increasing Q using GRPA. It reaches a data rate of 37 Mbit/s at $Q = 1$ while the NGDPA and FPA experience a slight reduction and achieves rates of 51.9 Mbit/s and 53.2 Mbit/s at $Q = 1$, respectively. Furthermore, the achievable rate of LED 2 at $Q = 1$ using FPA outperforms NGDPA and GRPA which reaches 55.2 Mbit/s compared to their rates of 52.6 Mbit/s and 52.7 Mbit/s, respectively.

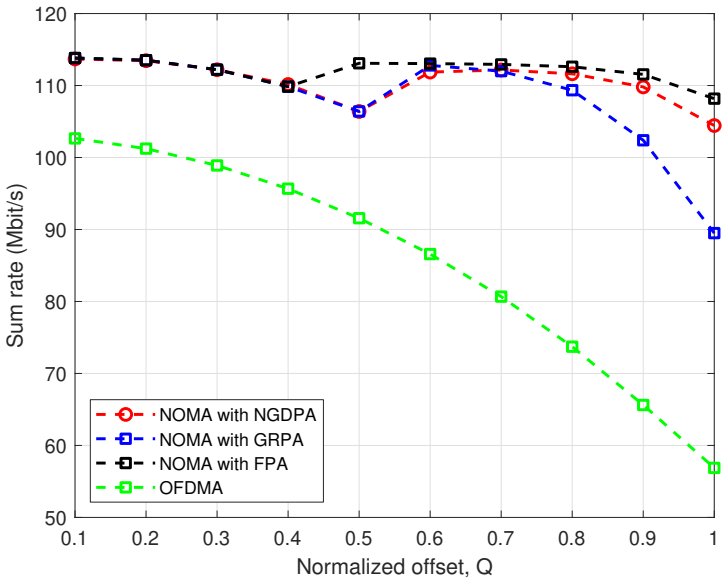

Figure 3.8 – Sum rate vs. normalized offset based NOMA using NGDPA, GRPA and FPA with two users ($N = 2$).

Figure 3.8 illustrates the sum rate for two users using OFDMA and NOMA with FPA, GRPA, and NGDPA. The sum rate is the aggregated achievable rate of the two users served by both LEDs. As we can see, OFDMA achieves the lowest sum rate at the system coverage edge compared to NOMA with different power allocation schemes. Moreover, FPA surpasses both NGDPA and GRPA at the system's edge, i.e., $Q = 1$, and when both users have the same channel gain at $Q = 0.5$.

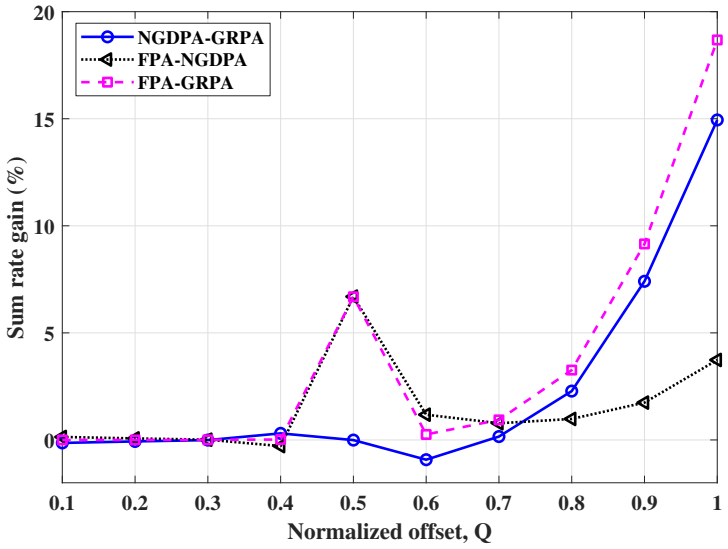

Figure 3.9 – Sum rate gain vs. normalized offset based NOMA using NGDPA, GRPA and FPA with two users ($N = 2$).

Figure 3.9 demonstrates the system's percentage difference in the sum rate performance using NGDPA, GRPA and FPA techniques. The results show that NGDPA outperforms GRPA in the range $Q > 0.7$ and achieves at the edge of the room a sum rate gain of 15.2%. However, FPA outperforms both NGDPA and GRPA by achieving a sum rate gain of 3.7% and 18.7%, respectively. Furthermore, FPA overcomes the performance reduction experienced by NGDPA and GRPA at $Q = 0.5$, as explained above, by achieving a sum rate gain of 6.7%.

It is worth noting that despite NGDPA achieving a better sum rate than GRPA when aggregating the rates of the users, as demonstrated in [162], in scenarios where both users have the same channel gain, NGDPA performs worse. Furthermore, when the users move far from the LED, NGDPA relies on increasing the power to the near user to achieve a high system sum rate. However, this increase in power allocation to the near user may not be necessary for decoding its data and comes at the expense of the far user. Furthermore, even a simpler technique, FPA, can achieve a better sum rate than NGDPA.

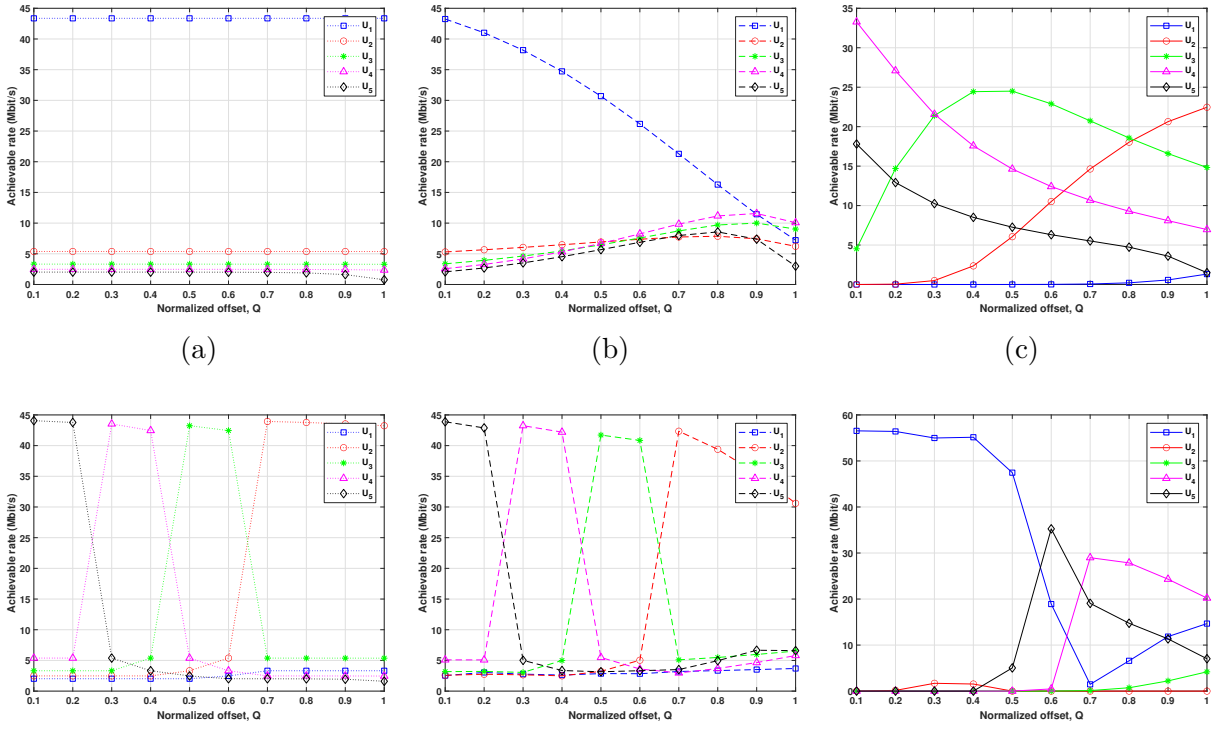

Figure 3.10 – Achievable rate vs. normalized offset-based NOMA with five users ($N = 5$) for LED 1 using (**a**) FPA, (**b**) GRPA, (**c**) NGDPA, and for LED 2 using (**d**) FPA, (**e**) GRPA, (**f**) NGDPA.

3.4.2 Five-User Scenario

We selected five users to represent the odd number user scenario, as it is the minimum odd number required to evaluate the two strategies of user pairing discussed in Subsection 3.3.2. We initially evaluate the achievable rates of five users utilizing NOMA with FPA, GRPA, and NGDPA without user pairing, as illustrated in Figure 3.10. Table 3.3 summarizes the user order of the five-user scenario without pairing for both LED 1 and LED 2 at each value of Q. It demonstrates the change in power distribution order at each Q and the corresponding interference experienced by each user. Each user treats those with a lower order as interference.

Table 3.3 – User ordering of five-user scenario for both LEDs at different Q values.

	LED 1					**LED 2**				
Q	O_1	O_2	O_3	O_4	O_5	O_1	O_2	O_3	O_4	O_5
0.1	U_1	U_2	U_3	U_4	U_5	U_5	U_4	U_3	U_2	U_1
0.2	U_1	U_2	U_3	U_4	U_5	U_5	U_4	U_3	U_2	U_1
0.3	U_1	U_2	U_3	U_4	U_5	U_4	U_5	U_3	U_2	U_1
0.4	U_1	U_2	U_3	U_4	U_5	U_4	U_3	U_5	U_2	U_1
0.5	U_1	U_2	U_3	U_4	U_5	U_3	U_4	U_2	U_5	U_1
0.6	U_1	U_2	U_3	U_4	U_5	U_3	U_2	U_4	U_1	U_5
0.7	U_1	U_2	U_3	U_4	U_5	U_2	U_3	U_4	U_1	U_5
0.8	U_1	U_2	U_3	U_4	U_5	U_2	U_3	U_4	U_1	U_5
0.9	U_1	U_2	U_3	U_4	U_5	U_2	U_3	U_4	U_1	U_5
1.0	U_1	U_2	U_3	U_4	U_5	U_2	U_3	U_4	U_1	U_5

In Figure 3.10a–c, the achievable rates of LED 1 are depicted, with U_1 to U_5 representing the order of users from the nearest to the farthest. In the case of FPA, despite U_1 having the lowest assigned power, it attains the highest rate of 43.4 Mbit/s due to the absence of interference from other users. The rates of the remaining users follow their order, with U_5 experiencing the lowest rate of 2 Mbit/s, showing degradation at the end of the coverage area due to elevated noise levels, as depicted in Figure 3.10a.

Meanwhile, the achievable rate of U_1 decreases, while the rates of the other users increase as they move farther from the LED. This is because GRPA assigns more power to the far users as Q increases, as shown in Figure 3.10b. Additionally, it is worth noting that the reduction in the achievable rate at $Q = 1$ is due to the increase in noise.

In contrast, NGDPA, at low Q values, allocates high power to far users U_4 and U_5 and very low power to near users U_1 and U_2. As Q increases, NGDPA reduces the power assigned to far users and increases the power assigned to near users. Consequently, the rate of far users decreases due to power reduction and increased interference from near users. The impact on U_1 is relatively slight, given its initial low power, while U_2 achieves a higher rate with increasing Q. The rate of U_3, the middle user, increases at low Q and then decreases as interference, particularly from U_2, rises.

In Figure 3.10d–f, the achievable rates of LED 2 are illustrated, featuring a distinct order of users based on the value of Q. The same concept employed for LED 1 in FPA is also applied for LED 2, where the achievable rates of users follow their order, with

the highest rate for the nearest user and the lowest for the farthest. Furthermore, the performance of GRPA closely aligns with FPA, particularly at low Q values. However, GRPA aims to improve the performance of the far users as Q increases. This behavior is evident starting from $Q = 0.7$ onward, where the rate of U_5 (farthest user) increases, while U_2's (nearest user) rate decreases after reaching its peak.

On the other hand, NGDPA allocates high power to the farthest users at low Q and high power to the nearest users at high Q. For instance, at low Q values, U_1 (farthest user) receives very high power, while other users are allocated very low power, resulting in low interference and consequently high data rates. As the user order changes, the data rate of U_1 decreases to zero at $Q = 0.7$, then rises as U_1 becomes the middle user. It is noteworthy that the utilization of NGDPA may lead certain users to achieve a zero data rate, as it concentrates most of the power on one or a few users, leaving others with insufficient power.

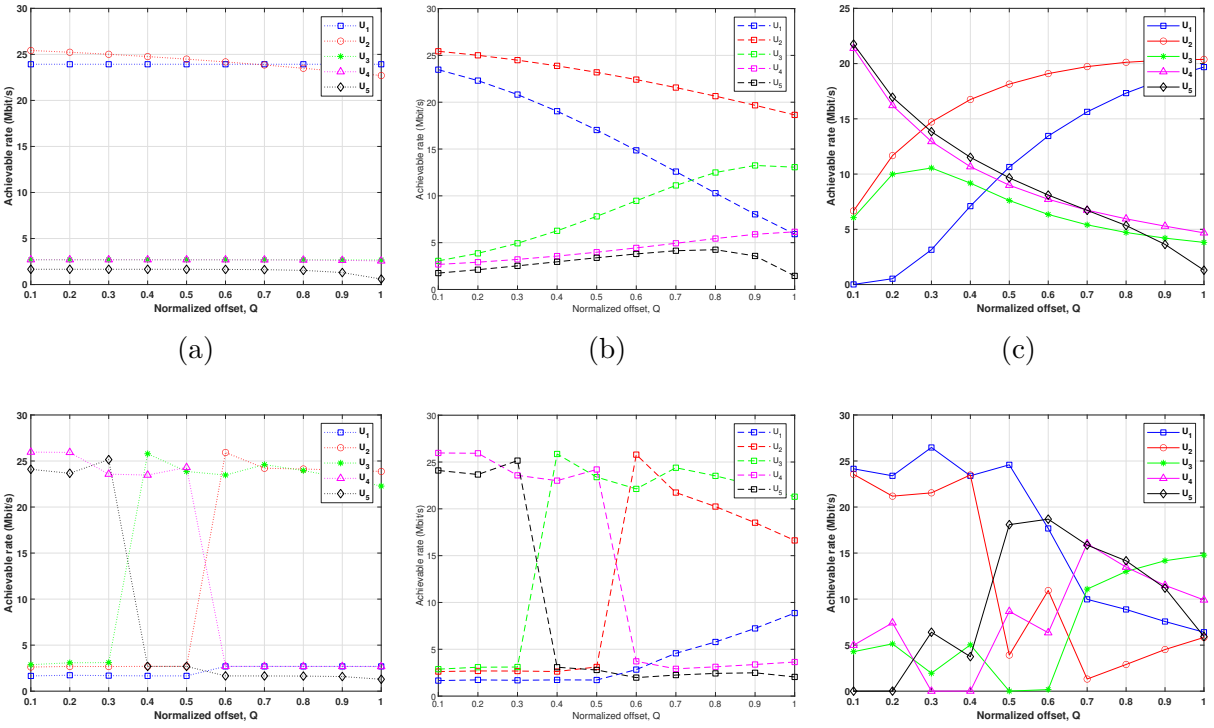

Figure 3.11 – Achievable rate vs. normalized offset-based NOMA with five users ($N = 5$) with Strategy 1 NLUPA/UCGD user pairing of LED 1 using (**a**) FPA, (**b**) GRPA, (**c**) NGDPA, and of LED 2 using (**d**) FPA, (**e**) GRPA, (**f**) NGDPA.

Table 3.4 – User ordering of five-user scenario with Strategy 1 NLUPA/UCGD user pairing for both LEDs at different Q values.

	LED 1					**LED 2**				
	Group 1			Group 2		Group 1			Group 2	
Q	O_1	O_2	O_3	O_1	O_2	O_1	O_2	O_3	O_1	O_2
0.1	U_1	U_3	U_5	U_2	U_4	U_5	U_3	U_1	U_4	U_2
0.2	U_1	U_3	U_5	U_2	U_4	U_5	U_3	U_1	U_4	U_2
0.3	U_1	U_3	U_5	U_2	U_4	U_4	U_3	U_1	U_5	U_2
0.4	U_1	U_3	U_5	U_2	U_4	U_4	U_5	U_1	U_3	U_2
0.5	U_1	U_3	U_5	U_2	U_4	U_3	U_2	U_1	U_4	U_5
0.6	U_1	U_3	U_5	U_2	U_4	U_3	U_4	U_5	U_2	U_1
0.7	U_1	U_3	U_5	U_2	U_4	U_2	U_1	U_5	U_3	U_4
0.8	U_1	U_3	U_5	U_2	U_4	U_2	U_1	U_5	U_3	U_4
0.9	U_1	U_3	U_5	U_2	U_4	U_2	U_1	U_5	U_3	U_4
1.0	U_1	U_3	U_5	U_2	U_4	U_2	U_1	U_5	U_3	U_4

In the following analysis, we assess the achievable rates of five users employing NOMA with FPA, GRPA, and NGDPA coupled with NLUPA and UCGD using Strategy 1 user-pairing algorithm, as depicted in Figure 3.11. Remarkably, for the five-user scenario only, NLUPA and UCGD exhibit identical performance as they share the same pairing strategy. The division of users into two groups proves advantageous, enabling more effective power allocation among users in comparison to the without pairing scenario. For instance, the performance of U_2 (nearest user in g_2) for LED 1 demonstrates significant data rate improvement across all three power allocation techniques, as more power is allocated to its signal and there is no interference from U_1, unlike in the without pairing scenario. Although more power is assigned to U_1 compared to the without pairing scenario, the reduction in bandwidth has a greater effect, resulting in a decrease in the achievable rate across all three power allocation techniques. Moreover, as more power is allocated to the signals of U_3, U_4, and U_5 with reduced interference compared to the without pairing scenario, their performance exhibits a noticeable enhancement in achievable rate. The degree of enhancement varies depending on the power allocation technique, with FPA yielding slight improvements and GRPA and NGDPA providing more substantial enhancement. Furthermore, in NGDPA, the occurrences of users achieving zero data rate at various Q values are substantially reduced for both LEDs compared to the without pairing scenario. Table 3.4 summarizes the user order of the five-user scenario with Strategy 1 NLUPA/UCGD user pairing for both LED 1 and LED 2 at each value of Q. The

variations in achievable rates for LED 2 across all users are attributed to the distinct user order at each value of Q. The power allocation and interference levels change according to the user order, as illustrated in Table 3.4.

Figure 3.12 shows the achievable rate performance of five users using NOMA with FPA, GRPA, and NGDPA associated with the NLUPA Strategy 2 user-pairing algorithm. Notably, the performance of the unpaired user (U_3 in LED 1) experiences a significant enhancement as it does not share power with other users compared to the NLUPA/UCGD Strategy 1 user-pairing, as shown in Figure 3.12a-c. Similarly, the unpaired user in LED 2 also shows performance improvement; however, in this case, the unpaired user varies depending on the user order at each Q value. It is worth mentioning that this strategy resolves the NGDPA issue seen in the without pairing and Strategy 1 scenarios, as none of the users experience zero data rate at any Q value for either LED as shown in Figure 3.12c and f. Table 3.5 summarizes the user order of the five-user scenario with Strategy 2 NLUPA user pairing for both LED 1 and LED 2 at each value of Q.

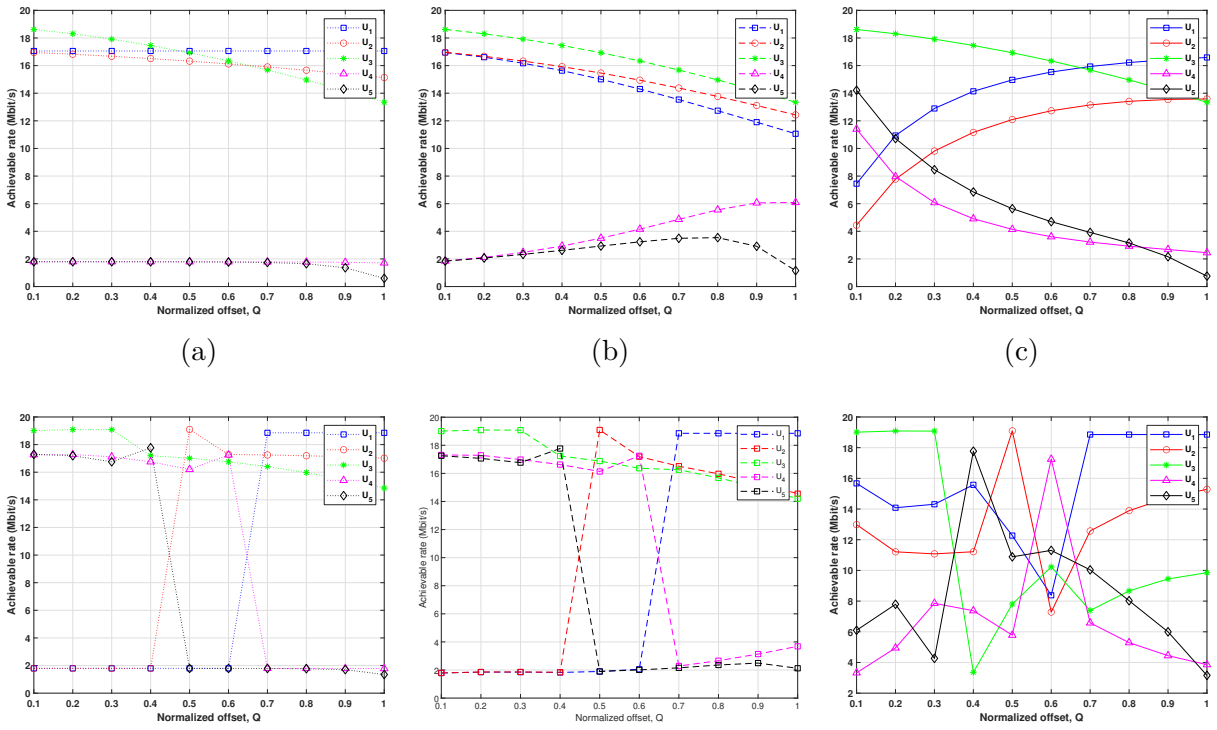

(a) (b) (c)

(d) (e) (f)

Figure 3.12 – Achievable rate vs. normalized offset-based NOMA with five users ($N = 5$) with Strategy 2 NLUPA user pairing of LED 1 using (**a**) FPA, (**b**) GRPA, (**c**) NGDPA, and of LED 2 using (**d**) FPA, (**e**) GRPA, (**f**) NGDPA.

Table 3.5 – User ordering of five-user scenario with Strategy 2 NLUPA user pairing for both LEDs at different Q values.

	LED 1					**LED 2**				
	Group 1		Group 2	Group 3		Group 1		Group 2	Group 3	
Q	O_1	O_2	O_1	O_1	O_2	O_1	O_2	O_1	O_1	O_2
0.1	U_1	U_5	U_3	U_2	U_4	U_5	U_1	U_3	U_4	U_2
0.2	U_1	U_5	U_3	U_2	U_4	U_5	U_1	U_3	U_4	U_2
0.3	U_1	U_5	U_3	U_2	U_4	U_4	U_1	U_3	U_5	U_2
0.4	U_1	U_5	U_3	U_2	U_4	U_4	U_1	U_5	U_3	U_2
0.5	U_1	U_5	U_3	U_2	U_4	U_3	U_1	U_2	U_4	U_5
0.6	U_1	U_5	U_3	U_2	U_4	U_3	U_5	U_4	U_2	U_1
0.7	U_1	U_5	U_3	U_2	U_4	U_2	U_5	U_1	U_3	U_4
0.8	U_1	U_5	U_3	U_2	U_4	U_2	U_5	U_1	U_3	U_4
0.9	U_1	U_5	U_3	U_2	U_4	U_2	U_5	U_1	U_3	U_4
1.0	U_1	U_5	U_3	U_2	U_4	U_2	U_5	U_1	U_3	U_4

Figure 3.13 depicts the achievable rate performance of five users using NOMA with FPA, GRPA, and NGDPA associated with UCGD strategy 2 user-pairing algorithm. The performance of FPA aligns with NLUPA Strategy 2 in both LEDs, exhibiting consistent results even as the pairs change, i.e., g_1 (U_1 and U_4) instead of (U_1 and U_5), but with identical power distribution, as shown in Figure 3.13a and d. In contrast, GRPA's performance in both LEDs shows slight variations in this strategy compared to the NLUPA Strategy 2, as changes in the paired users lead to adjustments in the power assigned to each user, as depicted in Figure 3.13b and e. This occurs because GRPA's power distribution depends on the channel gain value. Similarly, NGDPA's performance in this strategy follows the same trend, showing differences compared to NLUPA Strategy 2, as shown in Figure3.13c and f. Table 3.6 summarizes the user order of the five-user scenario with Strategy 2 UCGD user pairing for both LED 1 and LED 2 at each value of Q.

It is noteworthy that for both NLUPA and UCGD, Strategy 2 involves fewer applications of SIC compared to Strategy 1. Specifically, Strategy 2 applies SIC $\frac{N-1}{2}$ times, while Strategy 1 applies it $(\frac{N+1}{2})+1$ times. On the other hand, both NLUPA and UCGD apply SIC $\frac{N}{2}$ times for an even number of users.

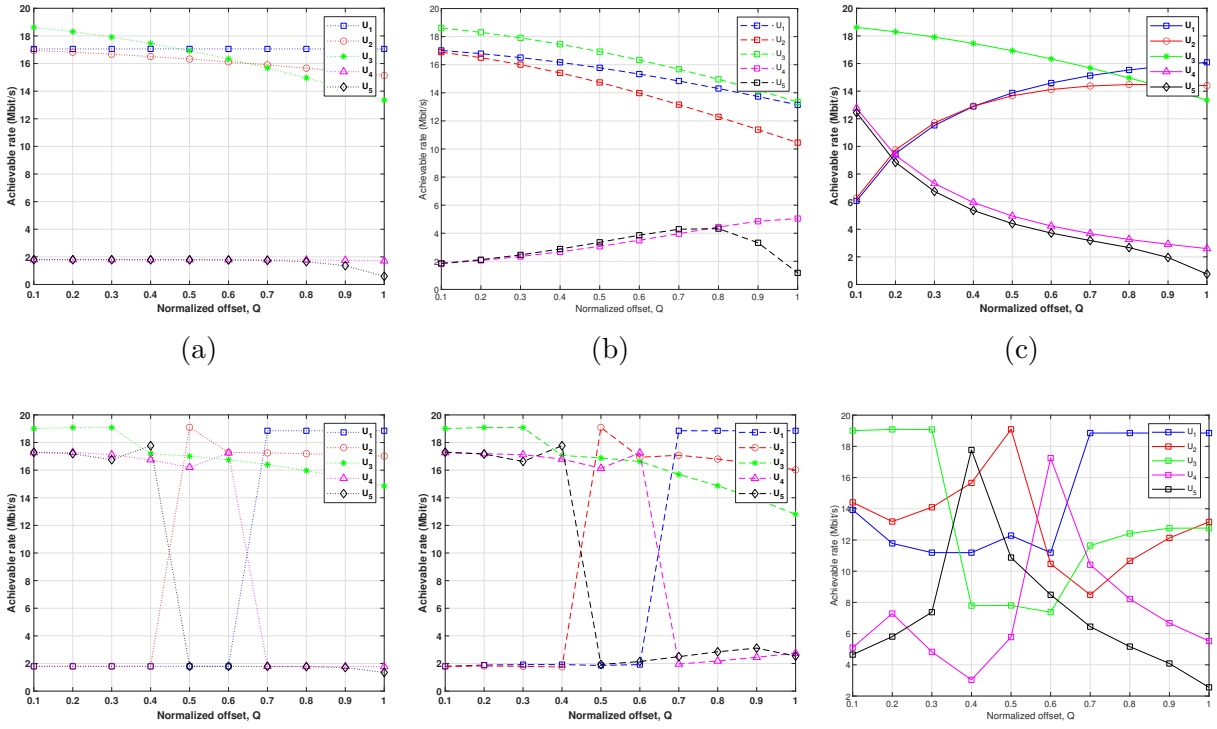

(a) (b) (c)

(d) (e) (f)

Figure 3.13 – Achievable rate vs. normalized offset-based NOMA with five users ($N = 5$) with Strategy 2 UCGD user pairing of LED 1 using (**a**) FPA, (**b**) GRPA, (**c**) NGDPA, and of LED 2 using (**d**) FPA, (**e**) GRPA, (**f**) NGDPA.

Table 3.6 – User ordering of five-user scenario with Strategy 2 UCGD user pairing for both LEDs at different Q values.

	LED 1					**LED 2**				
	Group 1		Group 2	Group 3		Group 1		Group 2	Group 3	
Q	O_1	O_2	O_1	O_1	O_2	O_1	O_2	O_1	O_1	O_2
0.1	U_1	U_4	U_3	U_2	U_5	U_5	U_2	U_3	U_4	U_1
0.2	U_1	U_4	U_3	U_2	U_5	U_5	U_2	U_3	U_4	U_1
0.3	U_1	U_4	U_3	U_2	U_5	U_4	U_2	U_3	U_5	U_1
0.4	U_1	U_4	U_3	U_2	U_5	U_4	U_2	U_5	U_3	U_1
0.5	U_1	U_4	U_3	U_2	U_5	U_3	U_5	U_2	U_4	U_1
0.6	U_1	U_4	U_3	U_2	U_5	U_3	U_1	U_4	U_2	U_5
0.7	U_1	U_4	U_3	U_2	U_5	U_2	U_4	U_1	U_3	U_5
0.8	U_1	U_4	U_3	U_2	U_5	U_2	U_4	U_1	U_3	U_5
0.9	U_1	U_4	U_3	U_2	U_5	U_2	U_4	U_1	U_3	U_5
1.0	U_1	U_4	U_3	U_2	U_5	U_2	U_4	U_1	U_3	U_5

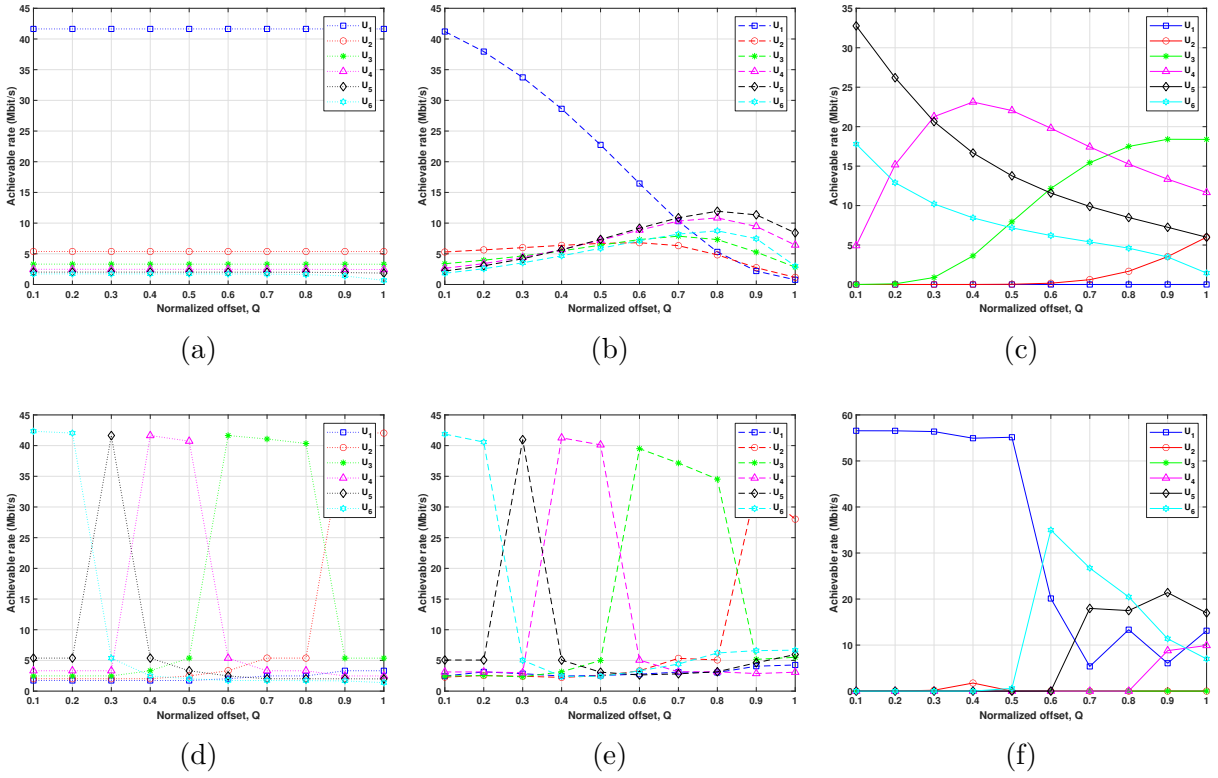

Figure 3.14 – Achievable rate vs. normalized offset-based NOMA with six users ($N = 6$) for LED 1 using (**a**) FPA, (**b**) GRPA, (**c**) NGDPA, and for LED 2 using (**d**) FPA, (**e**) GRPA, (**f**) NGDPA.

3.4.3 Six-User Scenario

In this subsection, we present the system's performance with six users, providing an example of an even number of users. We evaluate the achievable rates of six users utilizing NOMA with FPA, GRPA, and NGDPA without user pairing, as illustrated in Figure 3.14.

The pattern remains consistent with the five-user scenario, where FPA yields data rates in descending order based on the users' ordering from near to far. However, with GRPA, as Q increases, the achievable rate of the near user decreases, while that of the far users increases. In contrast, NGDPA increases the achievable rate for the near users as Q increases and decreases it for the far users. Moreover, increasing the number of users increases instances of users reaching zero data rate with NGDPA, as observed when comparing the scenarios with five and six users. The user order of the six-user scenario without pairing, for both LED 1 and LED 2 at each value of Q, is summarized in Table 3.7.

Table 3.7 – User ordering of six-user scenario for both LEDs at different Q values.

	LED 1						**LED 2**					
Q	O_1	O_2	O_3	O_4	O_5	O_6	O_1	O_2	O_3	O_4	O_5	O_6
0.1	U_1	U_2	U_3	U_4	U_5	U_6	U_6	U_5	U_4	U_3	U_2	U_1
0.2	U_1	U_2	U_3	U_4	U_5	U_6	U_6	U_5	U_4	U_3	U_2	U_1
0.3	U_1	U_2	U_3	U_4	U_5	U_6	U_5	U_6	U_4	U_3	U_2	U_1
0.4	U_1	U_2	U_3	U_4	U_5	U_6	U_4	U_5	U_3	U_6	U_2	U_1
0.5	U_1	U_2	U_3	U_4	U_5	U_6	U_4	U_3	U_5	U_2	U_6	U_1
0.6	U_1	U_2	U_3	U_4	U_5	U_6	U_3	U_4	U_2	U_5	U_1	U_6
0.7	U_1	U_2	U_3	U_4	U_5	U_6	U_3	U_2	U_4	U_1	U_5	U_6
0.8	U_1	U_2	U_3	U_4	U_5	U_6	U_3	U_2	U_4	U_1	U_5	U_6
0.9	U_1	U_2	U_3	U_4	U_5	U_6	U_2	U_3	U_1	U_4	U_5	U_6
1.0	U_1	U_2	U_3	U_4	U_5	U_6	U_2	U_3	U_1	U_4	U_5	U_6

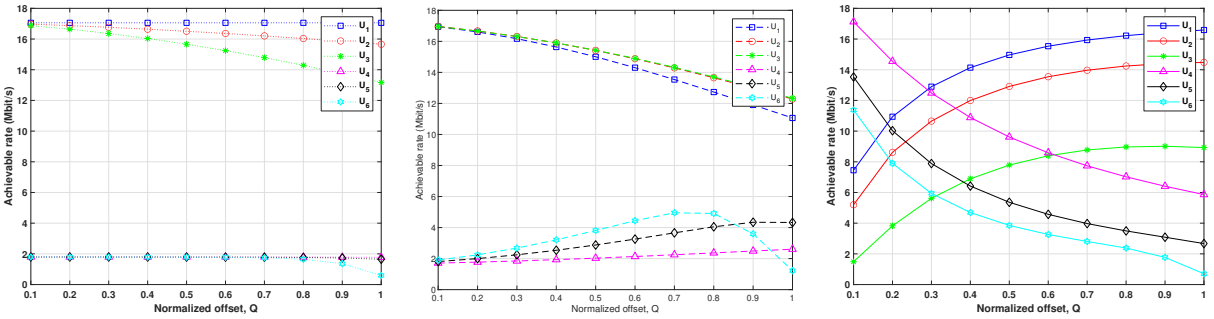

(a) (b) (c)

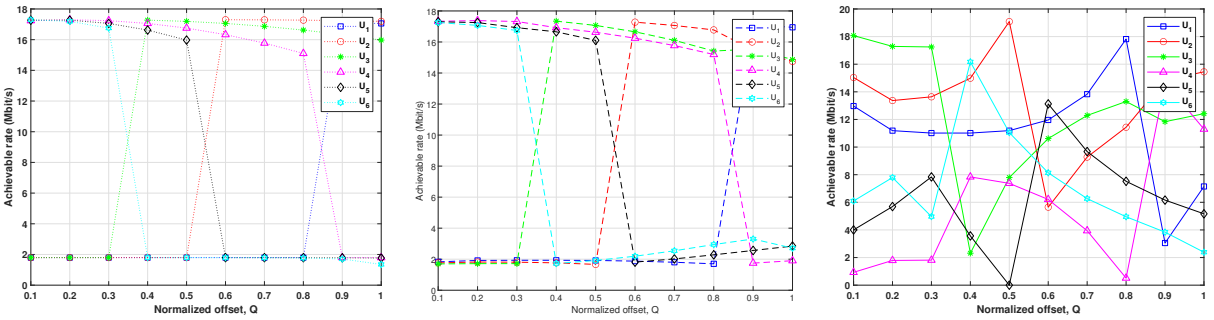

(d) (e) (f)

Figure 3.15 – Achievable rate vs. normalized offset-based NOMA with six users ($N = 6$) with NLUPA user-pairing of LED 1 using (**a**) FPA, (**b**) GRPA, (**c**) NGDPA, and of LED 2 using (**d**) FPA, (**e**) GRPA, (**f**) NGDPA.

Table 3.8 – User ordering of six-user scenario with NLUPA for both LEDs at different Q values.

	LED 1						**LED 2**					
	Group 1		Group 2		Group 3		Group 1		Group 2		Group 3	
Q	O_1	O_2	O_1	O_2	O_1	O_2	O_1	O_2	O_1	O_2	O_1	O_2
0.1	U_1	U_6	U_2	U_5	U_3	U_4	U_6	U_1	U_5	U_2	U_4	U_3
0.2	U_1	U_6	U_2	U_5	U_3	U_4	U_6	U_1	U_5	U_2	U_4	U_3
0.3	U_1	U_6	U_2	U_5	U_3	U_4	U_5	U_1	U_6	U_2	U_4	U_3
0.4	U_1	U_6	U_2	U_5	U_3	U_4	U_4	U_1	U_5	U_2	U_3	U_6
0.5	U_1	U_6	U_2	U_5	U_3	U_4	U_4	U_1	U_3	U_6	U_5	U_2
0.6	U_1	U_6	U_2	U_5	U_3	U_4	U_3	U_6	U_4	U_1	U_2	U_5
0.7	U_1	U_6	U_2	U_5	U_3	U_4	U_3	U_6	U_2	U_5	U_4	U_1
0.8	U_1	U_6	U_2	U_5	U_3	U_4	U_3	U_6	U_2	U_5	U_4	U_1
0.9	U_1	U_6	U_2	U_5	U_3	U_4	U_2	U_6	U_3	U_5	U_1	U_4
1.0	U_1	U_6	U_2	U_5	U_3	U_4	U_2	U_6	U_3	U_5	U_1	U_4

In contrast to the case of an odd number of users, all users are paired, eliminating the need for Strategy 1 and Strategy 2 classification. Figure 3.15 demonstrates the beneficial impact of considering NLUPA user pairing, where pairing the users enhances the achievable rate performance of most users, especially in the NGDPA technique, compared to the without pairing scenario. Although NLUPA reduces the occurrences of users experiencing zero data rates with NGDPA, it can still happen, as demonstrated by U_5 at $Q = 0.5$, as shown in Figure 3.15f. The user order of the six-user scenario with NLUPA user pairing, for both LED 1 and LED 2 at each value of Q, is summarized in Table 3.8.

Figure 3.16 shows the achievable performance rates of six users using NOMA with FPA, GRPA, and NGDPA combined with the UCGD user-pairing algorithm. It is worth mentioning that UCGD improves the achievable rate performance, as no user experiences a zero data rate, unlike with NLUPA in the NGDPA technique, as shown in Figure 3.16f. The user order of the six-user scenario with UCGD user pairing, for both LED 1 and LED 2 at each value of Q, is summarized in Table 3.9.

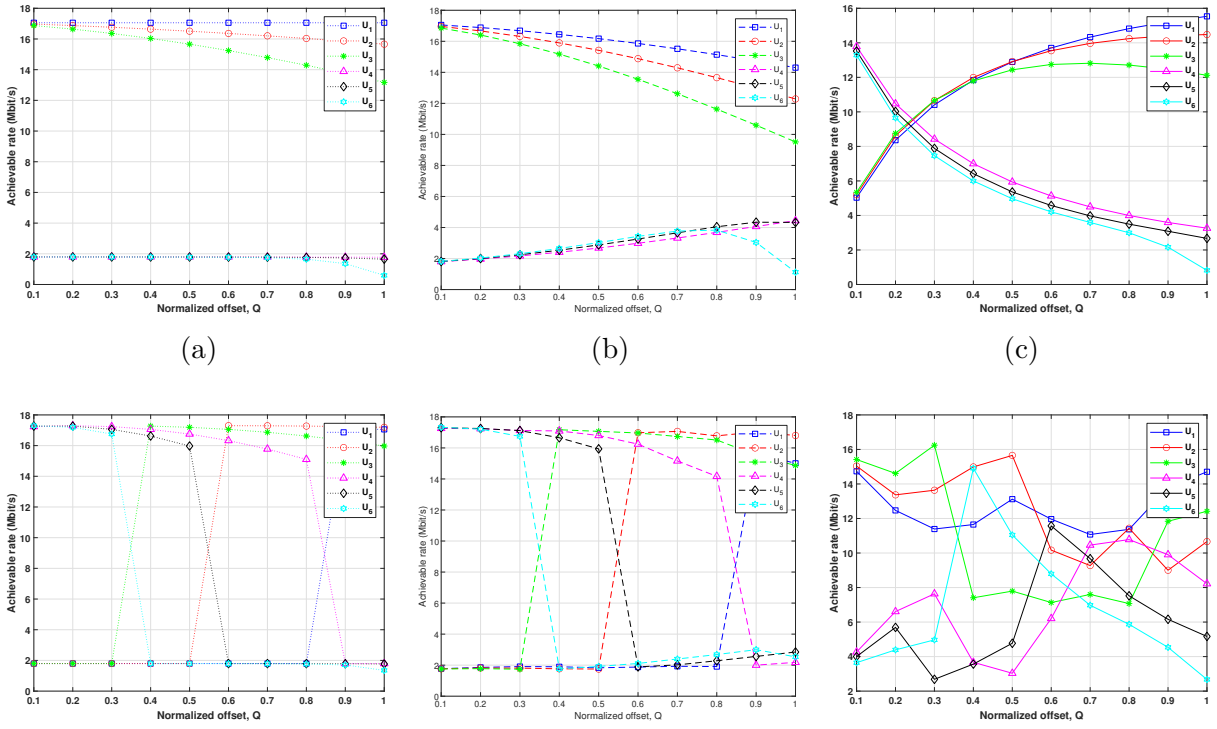

Figure 3.16 – Achievable rate vs. normalized offset-based NOMA with six users ($N = 6$) with UCGD user-pairing of LED 1 using (**a**) FPA, (**b**) GRPA, (**c**) NGDPA, and of LED 2 using (**d**) FPA, (**e**) GRPA, (**f**) NGDPA.

Table 3.9 – User ordering of six-user scenario with UCGD user pairing for both LEDs at different Q values.

	LED 1						**LED 2**					
	Group 1		Group 2		Group 3		Group 1		Group 2		Group 3	
Q	O_1	O_2	O_1	O_2	O_1	O_2	O_1	O_2	O_1	O_2	O_1	O_2
0.1	U_1	U_4	U_2	U_5	U_3	U_6	U_6	U_3	U_5	U_2	U_4	U_1
0.2	U_1	U_4	U_2	U_5	U_3	U_6	U_6	U_3	U_5	U_2	U_4	U_1
0.3	U_1	U_4	U_2	U_5	U_3	U_6	U_5	U_3	U_6	U_2	U_4	U_1
0.4	U_1	U_4	U_2	U_5	U_3	U_6	U_4	U_6	U_5	U_2	U_3	U_1
0.5	U_1	U_4	U_2	U_5	U_3	U_6	U_4	U_2	U_3	U_6	U_5	U_1
0.6	U_1	U_4	U_2	U_5	U_3	U_6	U_3	U_5	U_4	U_1	U_2	U_6
0.7	U_1	U_4	U_2	U_5	U_3	U_6	U_3	U_1	U_2	U_5	U_4	U_6
0.8	U_1	U_4	U_2	U_5	U_3	U_6	U_3	U_1	U_2	U_5	U_4	U_6
0.9	U_1	U_4	U_2	U_5	U_3	U_6	U_2	U_4	U_3	U_5	U_1	U_6
1.0	U_1	U_4	U_2	U_5	U_3	U_6	U_2	U_4	U_3	U_5	U_1	U_6

3.4.4 Performance Comparison

For the purpose of a clear comparison between the different power allocation techniques with and without the suggested user-pairing algorithms, we compare the sum rate performance for both five and six users scenarios. The sum rate is the aggregated achievable rate of the users served by both LEDs.

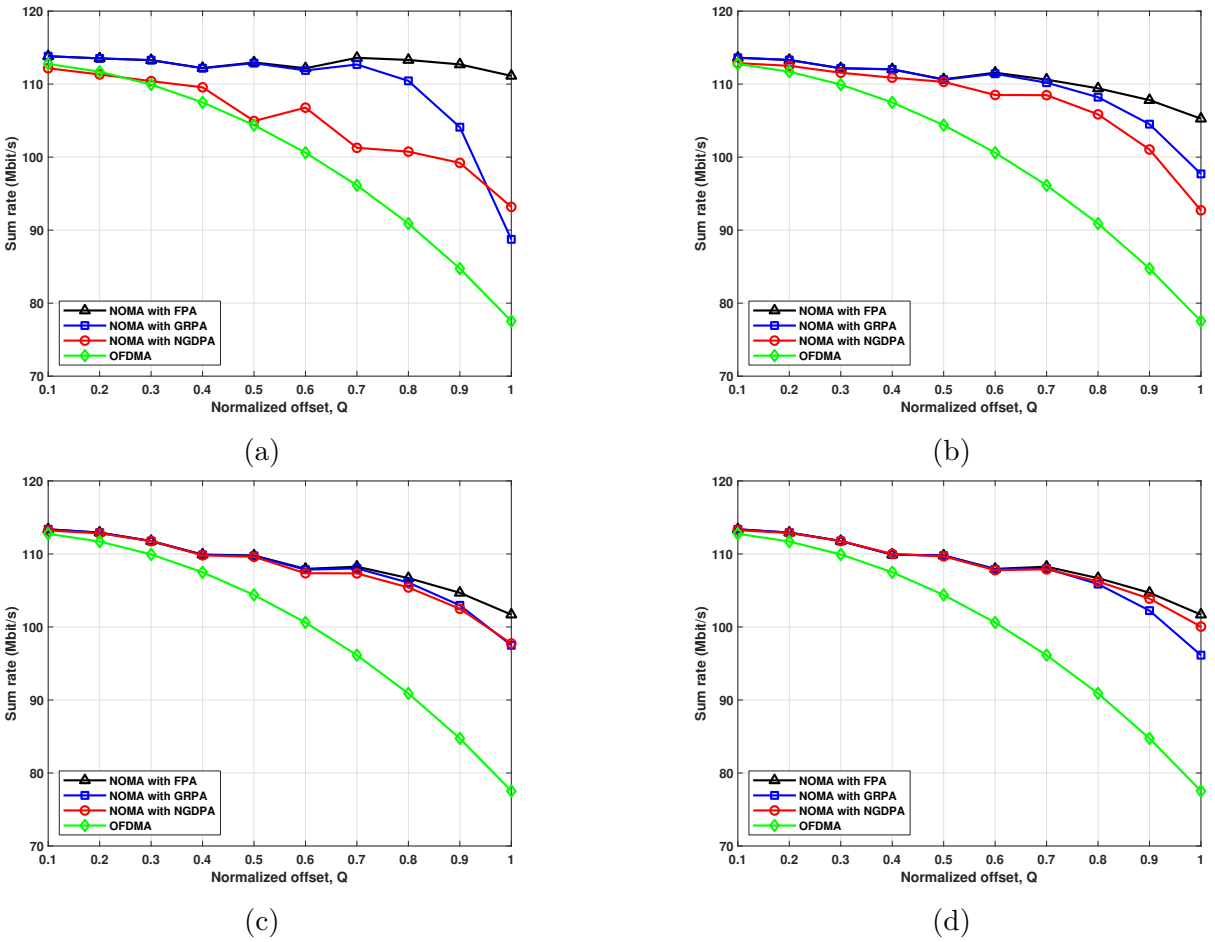

Figure 3.17 – Sum rate vs. normalized offset-based OFDMA and NOMA with five users ($N = 5$) (**a**) without grouping, (**b**) NLUPA/UCGD Strategy 1, (**c**) NLUPA Strategy 2, (**d**) UCGD Strategy 2.

Figure 3.17 illustrates the sum rate for five users using OFDMA and NOMA with FPA, GRPA, and NGDPA with and without user-pairing NLUPA and UCGD algorithms. As we can see in Figure 3.17, OFDMA consistently achieves the lowest sum rate at the system coverage edge compared to NOMA with different power allocation schemes. It is

crucial to explore the suitable user-pairing algorithm for each power allocation scheme. In the five-user scenario, GRPA achieves a better sum rate using NLUPA Strategy 2, with a marginal difference with NLUPA/UCGD Strategy 1, while NGDPA witnesses significant improvement using UCGD Strategy 2. On the other hand, FPA without grouping demonstrates the best sum rate performance, primarily contributed by the near user, while grouping allows other users to achieve better rates.

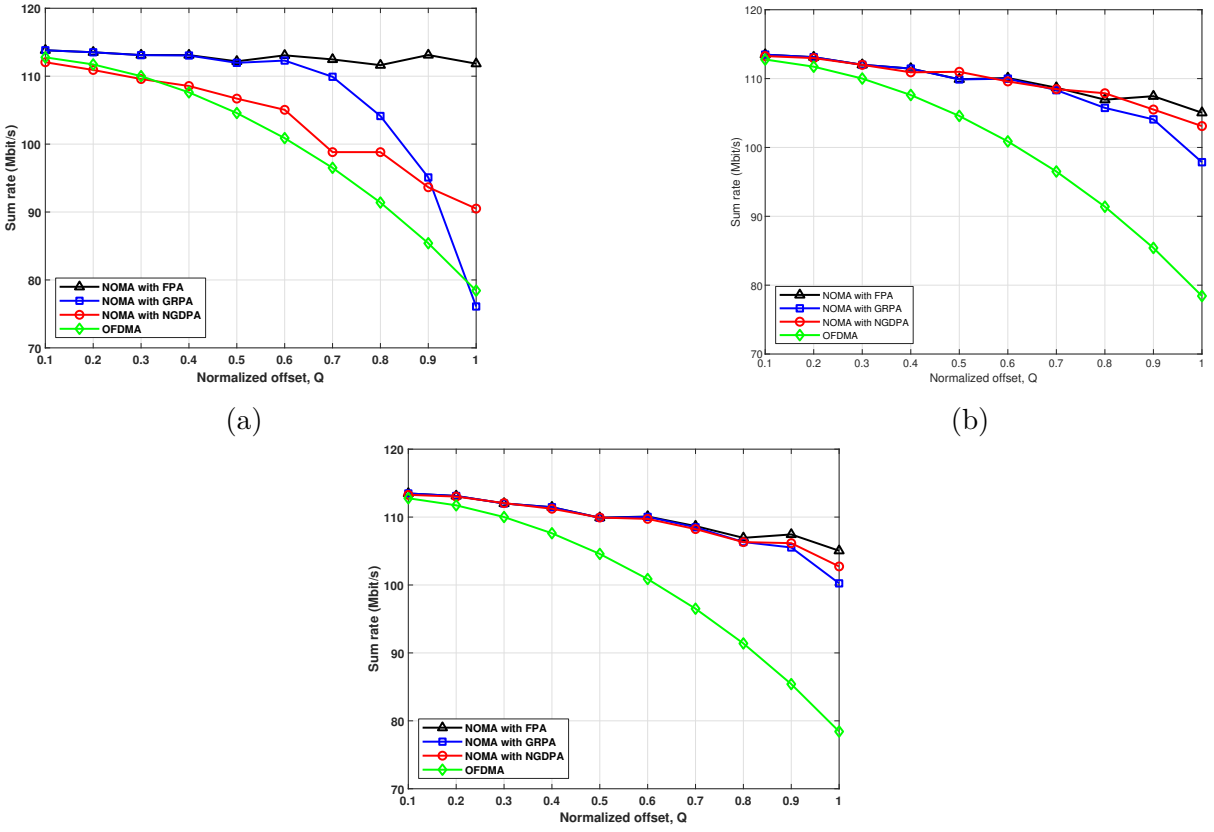

Figure 3.18 – Sum rate vs. normalized offset-based OFDMA and NOMA with six users ($N = 6$) (**a**) without grouping, (**b**) NLUPA, (**c**) UCGD.

The sum rate for six users using OFDMA and NOMA with FPA, GRPA, and NGDPA with and without user-pairing NLUPA and UCGD algorithms is shown in Figure 3.18. OFDMA consistently reaches the lowest sum rate at the system coverage edge, as the five-user scenario, compared to NOMA with various power allocation schemes, except for GRPA in the six-user scenario without grouping. Additionally, in the six-user scenario, GRPA achieves its best sum rate using UCGD, while NGDPA shows substantial im-

provement using NLUPA. In contrast, FPA, as the five-user scenario, performs optimally without grouping. It is essential to note that while FPA demonstrates the highest sum rate on the system level, it does not necessarily imply the optimal distribution of power among users based on their individual requirements.

3.5 Summary

In this chapter, we explored the performance of two efficient user-pairing algorithms, NLUPA and UCGD, in conjunction with three low-complexity power allocation techniques (FPA, GRPA and NGDPA) in indoor 2×2 MIMO-NOMA VLC systems. The investigation covered achievable rate performance in scenarios with both odd and even numbers of users. We evaluated the value of the power allocation coefficient that attains the best achievable rate for the FPA technique. The numerical results showed a significant improvement in the achievable rate performance of GRPA with user pairing. Moreover, utilizing user pairing with NGDPA notably reduced instances of users reaching a zero data rate. Furthermore, the findings indicate that NOMA outperforms OFDMA in terms of sum rate. Although FPA achieved the best performance without user grouping, it does not necessarily indicate the optimal distribution of power among users based on their individual requirements.

Chapter 4

Bit Error Rate Performance of NOMA-MIMO-VLC Systems

4.1 Introduction

This chapter delves into the bit error rate (BER) analysis of multiple-input multiple-output (MIMO)- non-orthogonal multiple access (NOMA)-based visible light communication (VLC) systems, focusing on the impact of various power allocation techniques, user pairing strategies, and diversity combining methods on system performance. Through detailed analysis, comparisons are made between the diversity combining techniques: selection combining (SC), equal gain combining (EGC), and maximum ratio combining (MRC) to assess their influence on the BER in different configurations. Moreover, we derived an analytical expression for BER under the assumption of perfect channel state information (CSI) and validated the results through simulations. Overall, this chapter offers a comprehensive examination of the factors affecting BER in MIMO-NOMA-VLC systems and demonstrates how performance can be enhanced through various approaches.

4.2 System Model

We adopt a system model for a multi-user NOMA-MIMO-VLC system. Hereinafter, we explore a $J \times I$ downlink VLC indoor system based NOMA-MIMO considering on-off keying (OOK) [1] modulation. Illustrated in Figure 4.1, this setup showcases the downlink MIMO-VLC system, leveraging NOMA to accommodate N users. Each user is equipped with J photodiodes (PDs) and and has access to the entire modulation bandwidth of the light-emitting diode (LED). The channel gain modeling primarily considers the LOS, with

1. On-off keying (OOK) is a digital modulation scheme where a binary "1" is represented by the presence of a signal, and a binary "0" by its absence. It is commonly used in optical communication systems due to its simplicity and low power consumption.

multipath delays deemed negligible, as defined in Equation 3.1. The multi-user NOMA-MIMO-VLC downlink system is demonstrated in Figure 4.2. The N users are ordered based on the sum of their optical channel gains, as expressed in Equation 3.7. After the modulation and power domain multiplexing, the input signal to the ith LED is expressed as

$$x_i = \sum_{n=1}^{N} \sqrt{p_{i,n}} s_{i,n} + I_{DC} \tag{4.1}$$

where $p_{i,n}$ is the electrical power allocated at the ith LED for the nth user, signal $s_{i,n}$ is modulated in the ith LED for the nth user, and I_{DC} is the DC bias current provided for each LED.

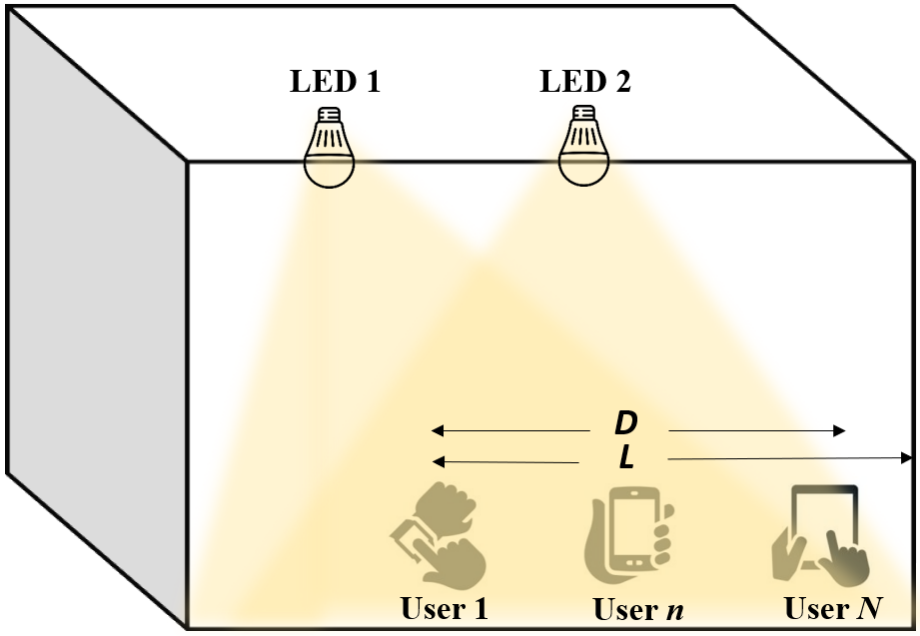

Figure 4.1 – Illustration of a downlink NOMA-MIMO-VLC system accommodating N users.

Repetition coding (RC) is employed at the transmitter to acquire transmit diversity benefit. The transmission of signals occurs simultaneously from all LEDs in RC [191]. Hence, the transmitted signals from the LEDs are represented as $s_{1,n} = s_{2,n} = \ldots = s_{I,n}$. The transmitted optical power from the LEDs is constructively combined at the receiver.

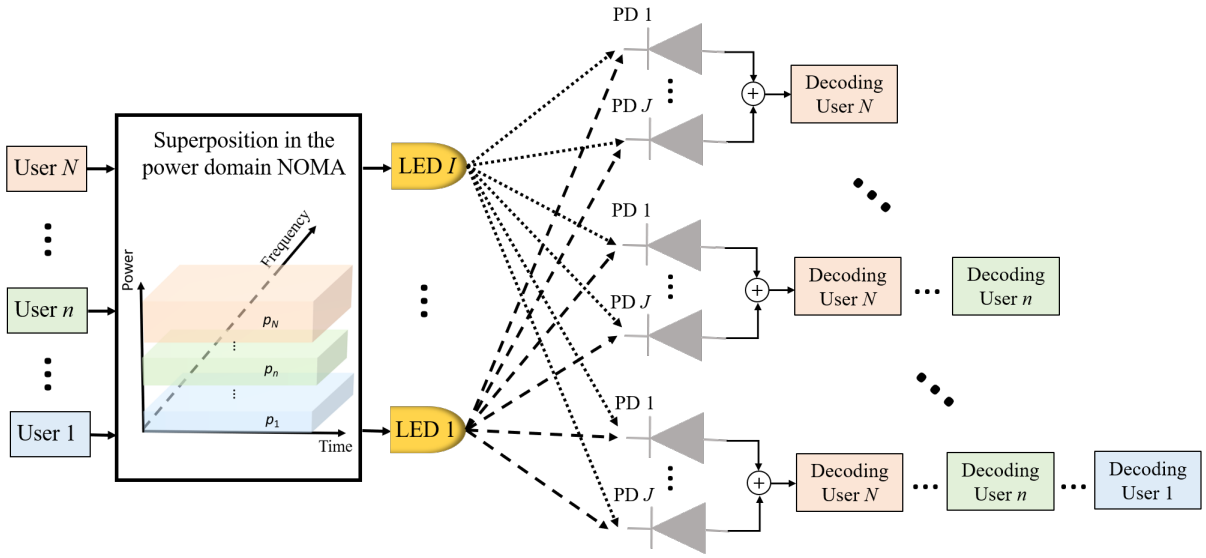

Figure 4.2 – Multi-user NOMA-MIMO-VLC downlink system.

4.3 Diversity Combining Techniques

At the receiver, we employ various diversity combining techniques to leverage receiver diversity, thereby improving the reliability of the received data.

4.3.1 Selection combining

Observing multiple signal paths, the receiver in selection combining (SC) selects the PD with the highest received signal-to-noise ratio (SNR). Suppose that the jth PD at the nth user is selected after SC then the SC output can be expressed as [226]

$$y_n = R_p \zeta P_o \sum_{i=1}^{I} h_{i,n} x_i + z_n \tag{4.2}$$

where R_p denotes the responsivity of the PD, ζ is the modulation index, P_o represents the LED's output optical power, and z_n is additive white Gaussian noise with zero mean and variance σ_n^2, comprising thermal and shot noises, as detailed in Chapter 3 section 3.2.

4.3.2 Equal gain combining

Prior to combining the received optical signal at each PD, equal gain combining (EGC) co-phases and allocates equal weights to each one. The EGC output signal at nth user can be expressed as [227]

$$y_n = R_p \zeta P_o \sum_{j=1}^{J} \sum_{i=1}^{I} h_{ji,n} x_i + z_{j,n} \tag{4.3}$$

4.3.3 Maximum ratio combining

After co-phasing the received signals in maximum ratio combining (MRC), weights are allocated to each signal and added. The weights are determined based on the knowledge of channel gain of the respective PD's at nth user to maximize the output SNR. Consequently, the output of the MRC combiner at nth user is represented as [227]

$$y_n = R_p \zeta P_o \sum_{j=1}^{J} \sum_{i=1}^{I} h_{ji,n} w_{j,n} x_i + z_{j,n} \tag{4.4}$$

where $w_{j,n} = h_{ji,n}$ is the allocated weight at jth PD at the nth user.

4.4 BER Analytical Expression

In this section, we derive an analytic expression for the BER of MIMO-NOMA-VLC systems utilizing OOK under perfect CSI. For simplicity, the equivalent channel gain at the nth user terminal is defined as $h_{i,n}$ for SC, $h_{i,n} = \sum_{j=1}^{J} h_{ji,n}$ for EGC and $h_{i,n} = \sum_{j=1}^{J} h_{ji,n} w_{j,n} = \sum_{j=1}^{J} h_{ji,n}^2$ for MRC. At the nth receiver, the decoder, using a maximum-likelihood (ML) detector, decodes and subtracts the signals intended for all users U_k, where $(n+1 \leq k \leq N)$. Additionally, each detection stage accounts for interference from the signals of all users with higher decoding order i.e., $\sum_{i=1}^{I} \sum_{m=1}^{k-1} p_{i,m} s_m$. Consequently, the detection threshold of the ML detector must account for the interference terms present in the received signal. With OOK modulation considered, the interference

generated by $s_1, \ldots, s_{k-1}$ is represented as

$$\sum_{t=1}^{2^{n-1}} \sum_{m=1}^{k-1} p_m T_{tm}, \tag{4.5}$$

where the matrix T comprises the elements

$$\begin{aligned} \mathbf{T} &= \begin{bmatrix} T_{1\,1} & T_{1\,2} & \ldots & T_{1\,k-2} & T_{1\,k-1} \\ T_{2\,1} & T_{2\,2} & \ldots & T_{2\,k-2} & T_{2\,k-1} \\ T_{3\,1} & T_{3\,2} & \ldots & T_{3\,k-2} & T_{3\,k-1} \\ \vdots & \vdots & \vdots & \vdots & \vdots \\ T_{2^{n-1}\,1} & T_{2^{n-1}\,2} & \cdots & T_{2^{n-1}\,k-2} & T_{2^{n-1}\,k-1} \end{bmatrix} \\ &= \begin{bmatrix} 0 & 0 & \ldots & 0 & 0 \\ 0 & 0 & \ldots & 0 & 1 \\ 0 & 0 & \ldots & 1 & 0 \\ \vdots & \vdots & \vdots & \vdots & \vdots \\ 1 & 1 & \ldots & 1 & 1 \end{bmatrix}. \end{aligned} \tag{4.6}$$

This matrix reflects the potential interference combinations depending on the transmitted OOK vectors. Hereinafter, the Gaussian distribution with a probability density function (PDF) having mean μ and variance σ^2, is denoted as $\mathcal{N}(\mu, \sigma^2)$. Therefore, the PDF of the received signal s_k at the nth user, under the interference $p_m T_{tm}$, which follows a Gaussian distribution, is represented as

$$\begin{cases} f_{Y_n|S_k}\left(y_n \mid s_k = 0\right) = \mathcal{N}_{y_n}\left(R_p \zeta P_o h_{i,n} p_{i,m} T_{tm}, \sigma_n^2\right) \\ f_{Y_n|S_k}\left(y_n \mid s_k = 1\right) = \mathcal{N}_{y_n}\left(R_p \zeta P_o h_{i,n}\left(p_{i,k} + p_{i,m} T_{tm}\right), \sigma_n^2\right) \end{cases} \tag{4.7}$$

The threshold of the ML detector at U_n for detecting the kth user's signal can be defined as the mid-point between the minimum and maximum possible received signal values, which is given by

$$\rho_{n_k} = \frac{R_p \zeta P_o \sum_{i=1}^{I} h_{i,n}(p_{i,k} + \sum_{m=1}^{k-1} p_{im})}{2} \tag{4.8}$$

The error probability at nth user for detecting the signal s_k depends on the state of s_k. Particularly, when $s_k = 0$, the conditional probability of error can be expressed as

$$P_{e_{n\to k|s_k=0}} = \int_{\rho_{n_k}}^{\infty} \mathcal{N}_{y_n}(R_p\zeta P_o \sum_{i=1}^{I} h_{i,n} \sum_{m=1}^{k-1} p_{i,m}s_m, \sigma_n)\mathrm{d}y_n \tag{4.9}$$

This expression can be rewritten using Q-function as

$$P_{e_{n\to k|s_k=0}} = Q\left(\frac{R_p\zeta P_o}{\sigma_n}\sum_{i=1}^{I} h_{i,n}\left(\frac{p_{i,k}+\sum_{m=1}^{k-1} p_{i,m}}{2} - \sum_{m=1}^{k-1} p_{i,m}s_m\right)\right) \tag{4.10}$$

and

$$Q(x) \triangleq \frac{1}{\sqrt{2\pi}}\int_{x}^{\infty} e^{-\frac{y^2}{2}}\mathrm{d}y \tag{4.11}$$

where $Q(\cdot)$ is the Gaussian Q-function. Conversely, when $s_k = 1$ is transmitted, the conditional probability of error can be represented as

$$P_{e_{n\to k|s_k=1}} = \int_{-\infty}^{\rho_{n_k}} \mathcal{N}_{y_n}(R_p\zeta P_o \sum_{i=1}^{I} h_{i,n}(p_{i,k} + \sum_{m=1}^{k-1} p_{i,m}s_m), \sigma_n)\mathrm{d}y_n \tag{4.12}$$

This expression can be rewritten using Q-function as

$$P_{e_{n\to k|s_k=1}} = 1 - Q\left(\frac{R_p\zeta P_o}{\sigma_n}\sum_{i=1}^{I} h_{i,n}\left(-\frac{p_{i,k}+\sum_{m=1}^{k-1} p_{i,m}}{2} - \sum_{m=1}^{k-1} p_{i,m}s_m\right)\right) \tag{4.13}$$

Using the identity $Q(-x) \triangleq 1 - Q(x)$, the expression can be rewritten as

$$P_{e_{n\to k|s_k=1}} = Q\left(\frac{R_p\zeta P_o}{\sigma_n}\sum_{i=1}^{I} h_{i,n}\left(\frac{p_{i,k}+\sum_{m=1}^{k-1} p_{i,m}}{2} + \sum_{m=1}^{k-1} p_{i,m}s_m\right)\right) \tag{4.14}$$

Hence, the expression for the error probability can be represented as

$$P_{e_{n\to k}} = \frac{1}{2^k}\left[\sum_{t=1}^{2^{n-1}} Q\left(\frac{R_p\zeta P_o}{\sigma_n}\sum_{i=1}^{I} h_{i,n}\left(\frac{p_{i,k}+\sum_{m=1}^{k-1} p_{i,m}}{2} - \sum_{m=1}^{k-1} p_{i,m}T_{tm}\right)\right)\right. \\ \left. + \sum_{t=1}^{2^{n-1}} Q\left(\frac{R_p\zeta P_o}{\sigma_n}\sum_{i=1}^{I} h_{i,n}\left(\frac{p_{i,k}+\sum_{m=1}^{k-1} p_{i,m}}{2} + \sum_{m=1}^{k-1} p_{i,m}T_{tm}\right)\right)\right] \tag{4.15}$$

The decoding process for the farthest user does not require successive interference cancellation (SIC) involvement, Therefore the error probability for this user can be determined by substituting $n = k = N$ in Equation 4.15. For all other users, SIC must be implemented during decoding. Consequently, the output signal at the nth user, where $n \neq N$, is represented as

$$\widehat{y}_n = y_n - R_p\zeta P_o \sum_{i=1}^{I}\sum_{v=n+1}^{N} h_{i,n}p_{i,v}\widehat{s}_v \tag{4.16}$$

where $\widehat{s}_v$ represents the decoded symbol corresponding to the vth user $(n+1 < v < N)$. The error probability for the nth user is expressed as

$$P_{e_n} = \sum_{l=1}^{2^{N-n}} P\left(e_n^l \mid e_{n+1}^l, e_{n+2}^l, \ldots, e_N^l\right) \tag{4.17}$$

where l represents all potential error combinations at the nth user, including errors in self-decoding as well as those arising during the implementation of SIC from the $(n+1)$th to the Nth user. Moreover, e_n^l is a Bernoulli random variable that takes on two possible values to represent either an error or a correct outcome in self-decoding. A self-decoding error at the nth user occurs when $\widehat{s}_n \neq s_n$ which is represented as $e_n^l = 1$. Conversely, the self-decoding is correct when $\widehat{s}_n = s_n$ which is indicated by $e_n^l = 0$. To further solve Equation 4.17, two decoding scenarios can be considered: perfect SIC and imperfect SIC.

4.4.1 Perfect SIC

Perfect SIC decoding occurs when $\widehat{s}_v = s_v$ where $(n+1 \leq v \leq N)$. In this scenario, the error probability for the nth user can be expressed by substituting $l = 1$ into

Equation 4.17 as

$$P_{e_{n_{per}}} = P\left(e_n^1 = 1\right) \prod_{v=n+1}^{N} P\left(e_v^1 = 0\right) = P_{e_{n\to k|n=k}} \prod_{v=n+1}^{N} \left(1 - P_{e_{n_v}}\right) \tag{4.18}$$

where $P_{e_{n\to k|n=k}}$ represents the error probability associated with self-decoding, $n = k$, at the terminal of the nth user and $P_{e_{n_v}}$ denotes the error probability of the vth user, as decoded at the terminal of the nth user.

Further analysis of Equation 4.18 can be achieved by substituting the corresponding values from Equation 4.15.

4.4.2 Imperfect SIC

For the scenario of imperfect SIC , when $\widehat{s}_v \neq s_v$ for $(n+1 \leq v \leq N)$, the error probability at the nth user is determined by substituting $2 \leq l \leq 2^{N-n}$ into Equation 4.17 as

$$P_{e_{n_{im}}} = \sum_{l=2}^{2^{N-n}} P\left(e_n^l \mid e_{n+1}^l, e_{n+2}^l, \ldots, e_N^l\right) \tag{4.19}$$

where $P\left(e_n^l \mid e_{n+1}^l, e_{n+2}^l, \ldots, e_N^l\right)$ represents the error probability for the lth error combination at the nth user, which is expressed as

$$\begin{aligned} P\left(e_n^l \mid e_{n+1}^l, e_{n+2}^l, \ldots, e_N^l\right) = \sum_{c=0}^{2^k-1} & P\left(\widehat{y}_n \neq s_n \mid s_1^c, s_2^c, \ldots, s_n^c, \widehat{s^c}_{n+1}, \ldots, \widehat{s^c}_N\right) \\ & \times P\left(\widehat{s^c}_{n+1} \neq s_{n+1} \mid s_1^c, s_2^c, \ldots, s_n^c, s_{n+1}^c, \ldots, \widehat{s^c}_N\right) \\ & \times P\left(\widehat{s^c}_n \neq s_n \mid s_1^c, s_2^c, \ldots, s_n^c, s_{n+1}^c, \ldots, s_N^c\right) \\ & \times P\left(s_1^c\right) P\left(s_2^c\right) \cdots P\left(s_n^c\right) \cdots P\left(s_N^c\right) \end{aligned} \tag{4.20}$$

where c denotes all the possible symbol combinations. The overall error probability for the nth user can be derived by utilizing Equations 4.17, 4.18, and 4.20 as

$$P_{e_n} = P_{e_{n_{per}}} + P_{e_{n_{im}}} \tag{4.21}$$

4.5 Numerical Results and Discussions

We investigate the performance of an indoor 2×2 NOMA-MIMO-VLC system employing three power allocation schemes and three diversity combining techniques. The derived BER analytical expressions are utilized to analyze the considered setups, with simulations conducted to verify the accuracy of the presented results. In the obtained simulation results, we calculate the BER for each transmit SNR value over a total of 500 iterations. We study the BER performance according to the model described in Figure 4.1, where user 1 remains stationary and positioned equidistant between both LEDs. The distance between user 1 and user N is denoted by D; whereas, the gap between user 1 and the room edge is $L = 2$ m. The output optical power and the spacing between the LEDs are 1 W and 0.5 m, respectively. The normalized offsets of user N relative to user 1 and user n relative to user 1 are represented by $Q = \frac{D}{L}$ and $\frac{(n-1)D}{(N-1)L}$, respectively. Table 3.1 provides the detailed configuration and simulation parameters for the system.

4.5.1 Two-User Scenario

First, we investigate the impact of the power allocation factor in the FPA scheme for both LEDs, as described in Equation 3.13, on the system's BER performance. It is worth mentioning that as the value of channel gain is in the order of 10^{-5}, the corresponding transmit SNR results exhibit an offset of about 100 dB with respect to the received SNR [130], [228].

The BER versus power allocation factor α for FPA is depicted at a transmit SNR of 125 dB for a 2×2 NOMA-MIMO-VLC system utilizing SC, EGC and MRC, serving 2 users, in Figure 4.3. Here, user 2 is positioned at the room edge, i.e., $Q = 1$. The results indicate that the BER of U_2 increases as the power allocation coefficient α rises across all diversity combining techniques, due to the decreasing amount of power allocated to U_2. Moreover, as α increases from 0.1 to 0.5, the BER of U_1 decreases. This inverse BER behavior between U_1 and U_2 results from the corresponding increase and decrease in allocated power as α rises. However, when the power allocated to U_1 increases in the range beyond $\alpha > 0.5$, the BER of U_1 begins to rise due to the reduction in power allocated to U_2, which leads to an increase in errors during the SIC process of decoding U_2's signal at U_1. Notably, the best average BER performance for all considered diversity techniques is achieved at $\alpha = 0.3$. Additionally, MRC exhibits better performance compared to EGC

and SC for both users in terms of BER across all α values. It is important to highlight that our analysis is applicable to any number of users.

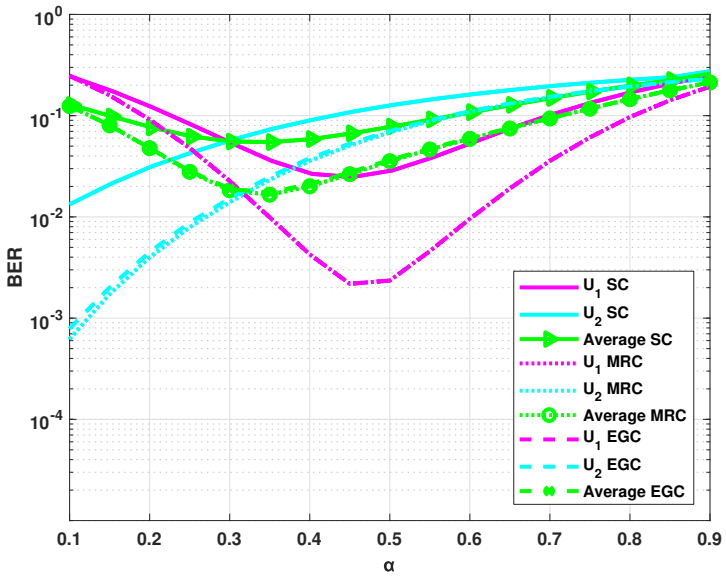

Figure 4.3 – BER vs. power allocation factor (α) of FPA.

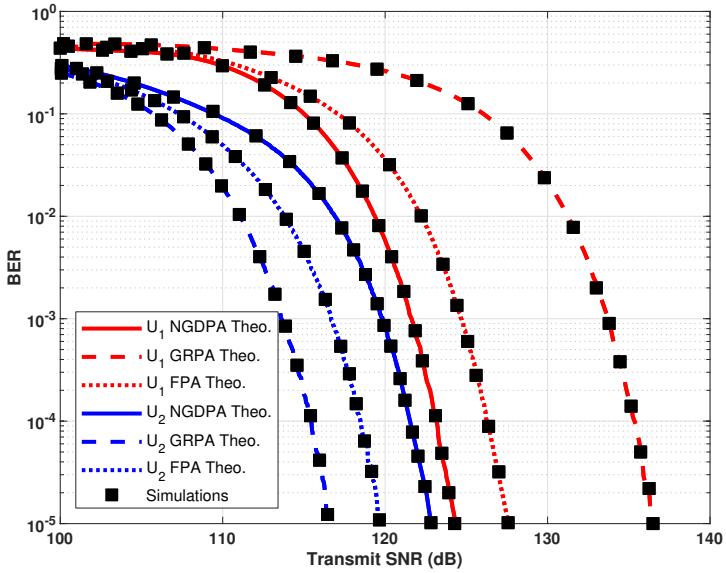

Figure 4.4 – BER vs. transmit SNR utilizing SC with NGDPA, GRPA and FPA with two users ($N = 2$).

We evaluate the BER performance of SC, EGC and MRC employing NGDPA, GRPA and FPA. We consider $\alpha = 0.3$ for FPA in the following results. Figure 4.4 illustrates

the BER performance of SC utilizing NGDPA, GRPA and FPA techniques. The derived analytical results are demonstrated to be in excellent agreement with the corresponding simulation results. It is noted that the BER performance of U_2 using GRPA outperforms NGDPA and FPA due to GRPA assigning 91% of the total power to the data of U_2, achieving a BER of 10^{-5} at 116.7 dB, compared to 67% and 77% using NGDPA and FPA, respectively. On the other hand, the BER of U_1 using GRPA demonstrates the poorest performance, reaching a BER of 10^{-5} at 136.2 dB, as it allocates only 9% of the total power to U_1 data, compared to 33% and 23% using NGDPA and FPA, respectively.

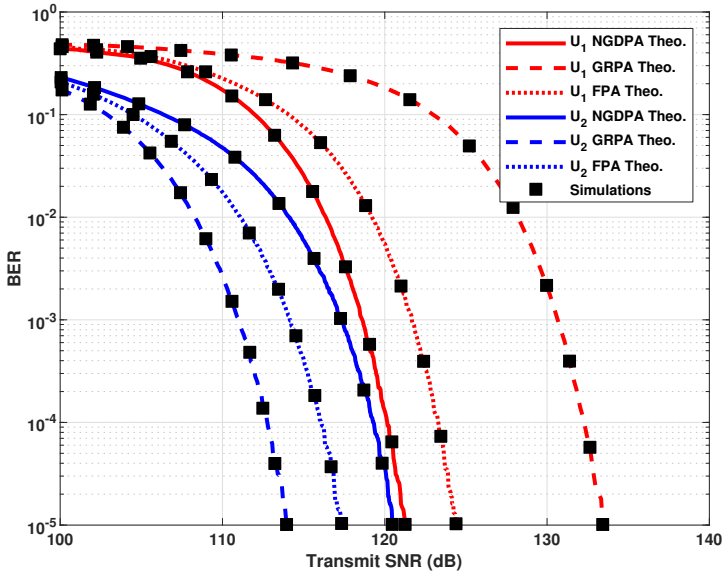

Figure 4.5 – BER vs. transmit SNR utilizing EGC with NGDPA, GRPA and FPA with two users ($N = 2$).

The BER versus transmit SNR for EGC employing NGDPA, GRPA and FPA techniques is presented in Figure 4.5. The BER arrangement in EGC for both users mirrors that of SC, as the power distribution for each user remains unchanged across all three diversity combining techniques. It is noted that U_2 using EGC demonstrates superior BER performance compared to U_2 using SC with GRPA reaching 10^{-5} at 113.8 dB. Furthermore, it is worth mentioning that EGC achieves approximately a 3 dB lower SNR value at a BER of 10^{-5} compared to SC, for both users and across all three power allocation techniques.

Figure 4.6 demonstrates the BER versus SNR for MRC employing NGDPA, GRPA and FPA schemes. The findings indicate that MRC achieves a marginally improved performance of approximately 0.4 dB lower SNR value at BER of 10^{-5} compared to EGC across all three power allocation techniques. However, for U_2 using NGDPA, it achieves a more substantial improvement, with a 1.1 dB lower SNR value at a BER of 10^{-5} compared to EGC.

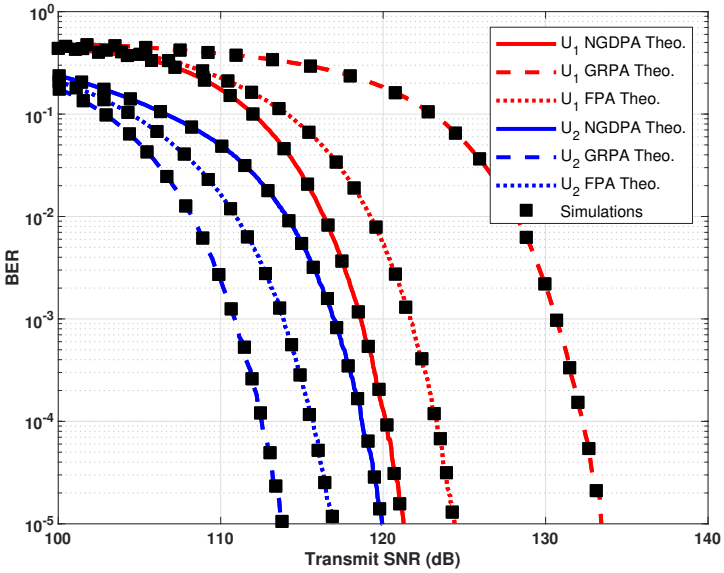

Figure 4.6 – BER vs. transmit SNR utilizing MRC with NGDPA, GRPA and FPA with two users ($N = 2$).

4.5.2 Three-User Scenario

To apply user pairing techniques to our system, we selected scenarios with three and four users to represent cases with odd and even numbers of users. These were chosen because they are the minimum numbers required to implement user pairing and provide a clear comparison between the different user pairing techniques and the without-pairing scenario applying the three diversity combining techniques.

In this subsection, we present the system's performance with three users, providing an example of an odd number of users. Figure 4.7 demonstrates the BER performance of SC, EGC and MRC employing NGDPA, GRPA and FPA techniques. For all the power allocation techniques across the three diversity combining techniques, U_3 is the farthest user, has the highest power, and can decode its data directly. U_2 must apply SIC to decode the data of U_3 before decoding its own data, while U_1 has to apply SIC twice

to decode its own data. The power distribution for each power allocation technique is presented in Table 4.1.

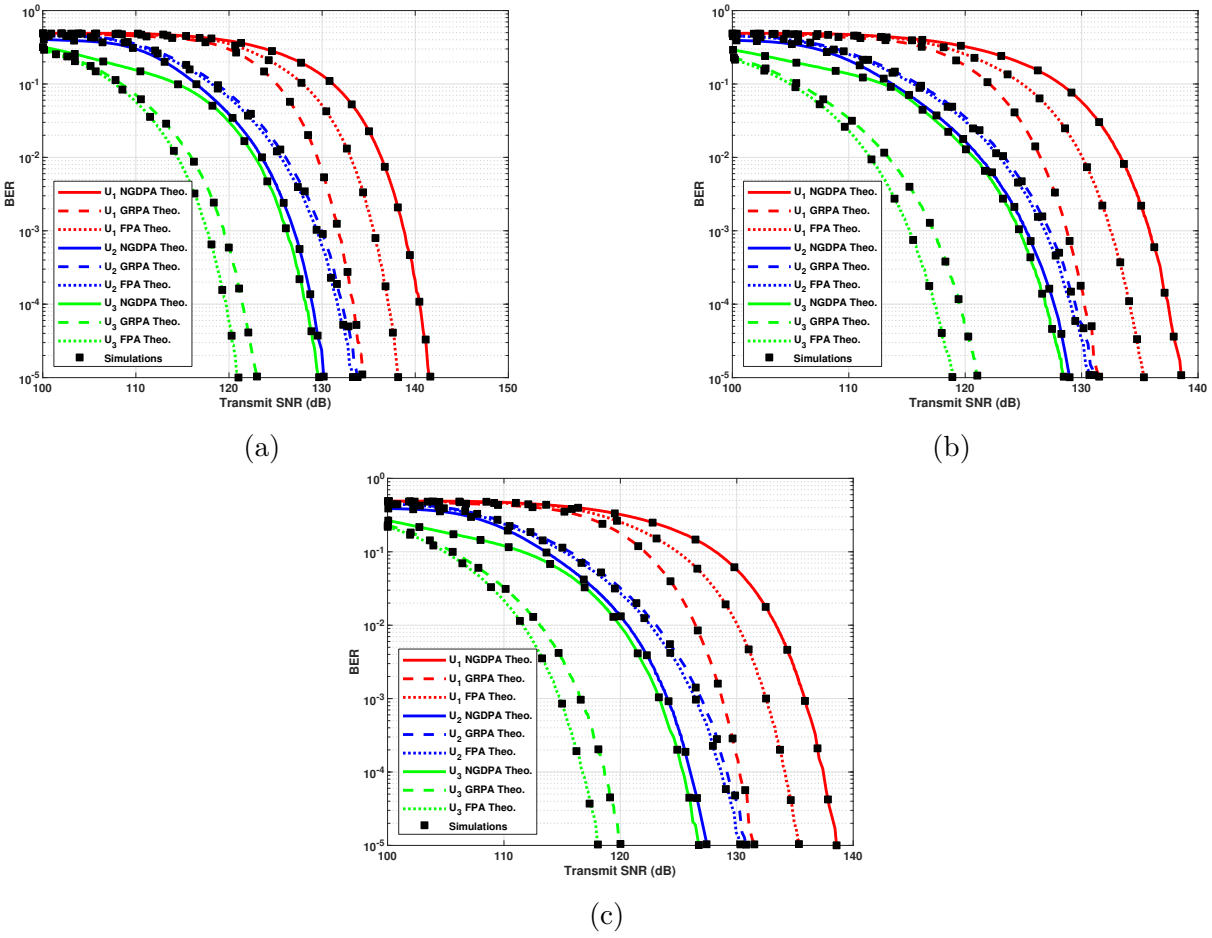

Figure 4.7 – BER vs. transmit SNR employing NGDPA, GRPA and FPA with three users ($N = 3$) using (**a**) SC, (**b**) EGC, (**c**) MRC.

Table 4.1 – The power distribution in three-user scenario: p_n is the power assigned to the nth user.

Power allocation	p_1	p_2	p_3
NGDPA	4.2%	39.3%	56.5%
GRPA	10.6%	20.4%	69%
FPA	6.5%	21.6%	71.9%

It can be noted that FPA achieves the best BER performance for U_3, reaching a BER of 10^{-5} at 120.8 dB, compared to 122.7 dB and 129.6 dB using GRPA and NGDPA, respectively, as shown in Figure 4.7a. NGDPA provides the best BER performance for U_2, with 39.3% of the total power allocated to its signal, showing performance close to that of U_3 starting from a SNR of 120 dB. This is attributed to the larger power allocated to U_2 and the relatively high power allocated to U_3, which improves the SIC performance at U_2. Notably, employing EGC can improve BER performance to varying degrees depending on the user and the power allocation technique used, in comparison to SC, as illustrated in Figure 4.7b. On average, EGC achieves about 2.2 dB lower SNR at a BER of 10^{-5} across all three power allocation techniques for the three users. Furthermore, the findings indicate that MRC achieves an improved performance of approximately 0.9 dB lower SNR on average at BER of 10^{-5} compared to EGC across all three power allocation techniques, as shown in 4.7c. Table 4.2 summarizes the SNR values at a BER of 10^{-5} for SC, EGC, and MRC employing NGDPA, GRPA, and FPA techniques in a three-user scenario.

Table 4.2 – Summary of SNR values at a BER of 10^{-5} for SC, EGC, and MRC employing NGDPA, GRPA, and FPA techniques in a three-user scenario.

SC			
Power allocation	U_1	U_2	U_3
NGDPA	141.5 dB	130.4 dB	129.6 dB
GRPA	134.4 dB	133.8 dB	122.7 dB
FPA	138.2 dB	133.3 dB	120.8 dB
EGC			
NGDPA	138.5 dB	129 dB	128.4 dB
GRPA	131.5 dB	131.1 dB	120.8 dB
FPA	135.6 dB	130.6 dB	118.5 dB
MRC			
NGDPA	138.5 dB	127.4 dB	126.7 dB
GRPA	131.2 dB	130.8 dB	119.8 dB
FPA	135.1 dB	130.3 dB	117.9 dB

In the following analysis, we evaluate the BER of three users employing NOMA with FPA, GRPA, and NGDPA in conjunction with the user pairing algorithm, as depicted in Figure 4.8. Notably, in the three-user scenario, NLUPA and UCGD demonstrate identical

performance since U_2 remains unpaired in both strategies. The power distribution for each power allocation technique is detailed in Table 4.3.

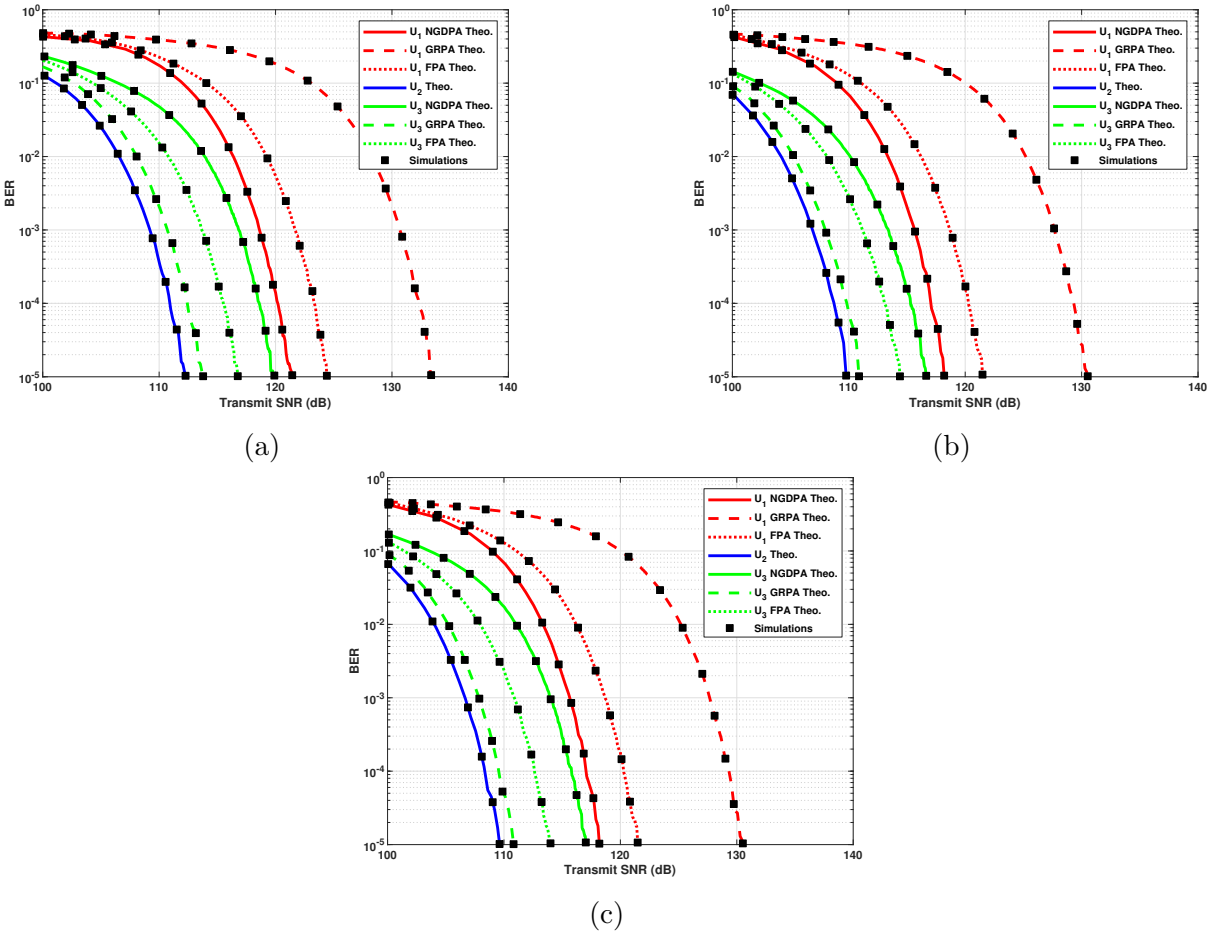

Figure 4.8 – BER vs. transmit SNR employing NGDPA, GRPA and FPA with three users ($N = 3$) applying user pairing using (**a**) SC, (**b**) EGC, (**c**) MRC.

It is observed that U_2 experiences a significant enhancement in performance across the three diversity combining techniques, as it does not share power with other users. Additionally, the BER performance of U_1 and U_3 shows improvement for all the power allocation techniques across the three diversity combining techniques compared to the scenario without pairing. EGC, in particular, enhances BER performance to varying degrees depending on the user and the power allocation technique used, with an average improvement of 2.8 dB at a BER of 10^{-5} compared to SC, as illustrated in Figure 4.8b. Moreover, the results indicate that MRC achieves approximately 0.5 dB lower SNR on

average at a BER of 10^{-5} compared to EGC across all three power allocation techniques, as shown in 4.8c. Table 4.4 provides a summary of the SNR values at a BER of 10^{-5} for SC, EGC, and MRC utilizing NGDPA, GRPA, and FPA techniques in a three-user scenario with user pairing.

Table 4.3 – The power distribution in three-user scenario with user pairing.

Power allocation	p_1	p_3
NGDPA	32.6%	67.4%
GRPA	8.7%	91.3%
FPA	23.1%	76.9%

Table 4.4 – Summary of SNR values at a BER of 10^{-5} for SC, EGC, and MRC employing NGDPA, GRPA, and FPA techniques in a three-user scenario with user pairing.

SC			
Power allocation	U_1	U_3	U_2
NGDPA	121.4 dB	119.7 dB	112.3 dB
GRPA	133.4 dB	113.8 dB	
FPA	124.4 dB	116.7 dB	
EGC			
NGDPA	118.2 dB	116.6 dB	109.8 dB
GRPA	130.5 dB	110.9 dB	
FPA	121.5 dB	114.4 dB	
MRC			
NGDPA	117.6 dB	116.1 dB	109.3 dB
GRPA	130.1 dB	110.4 dB	
FPA	121.1 dB	113.9 dB	

4.5.3 Four-User Scenario

In this subsection, we present the BER performance of the system with four users as an example of an even number of users. Initially, we evaluate the BER of SC, EGC and MRC with four users utilizing NOMA with FPA, GRPA, and NGDPA without user pairing, as depicted in Figure 4.9. The power distribution for each power allocation technique is detailed in Table 4.5.

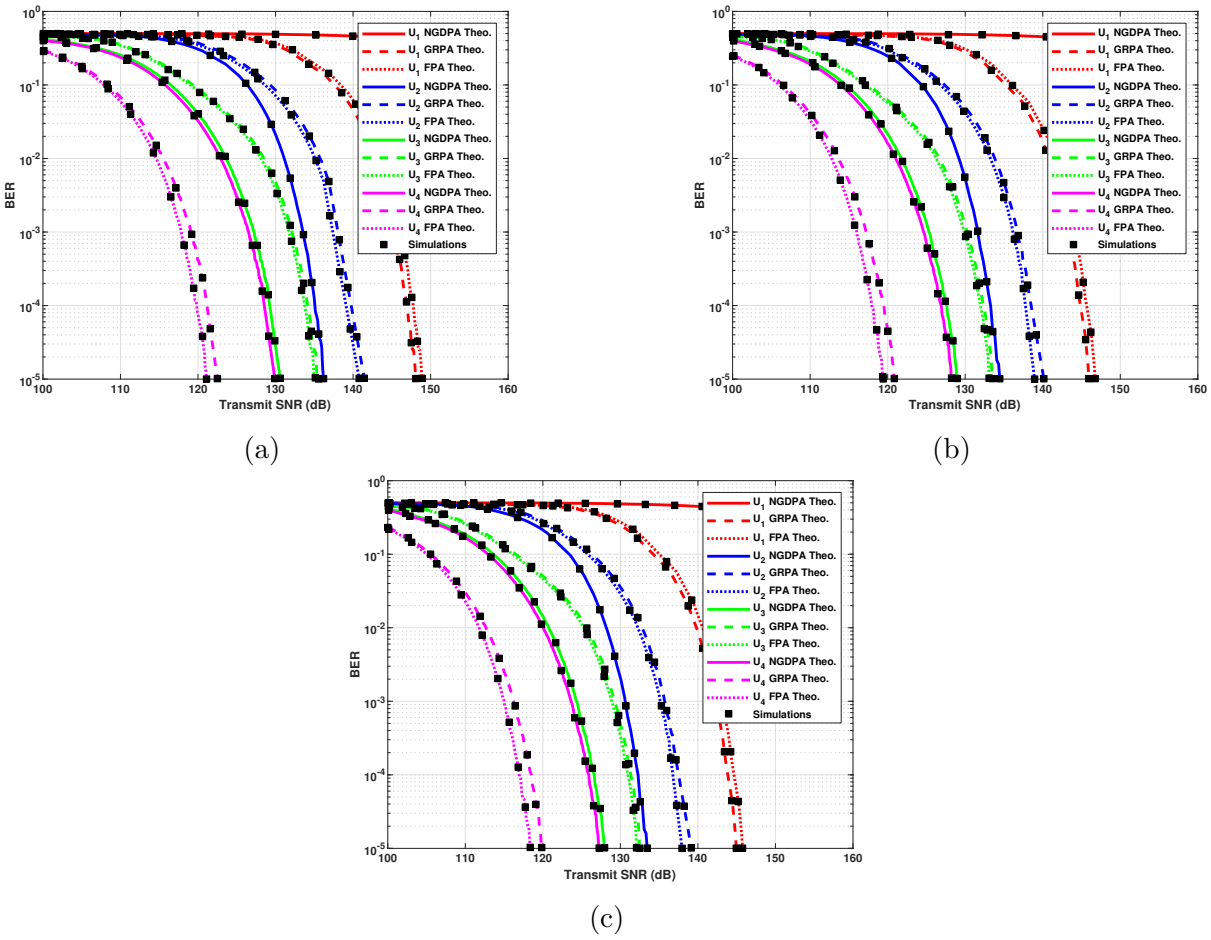

Figure 4.9 – BER vs. transmit SNR employing NGDPA, GRPA and FPA with four users ($N = 4$) using (**a**) SC, (**b**) EGC, (**c**) MRC.

It is observed that U_1 has a constant BER of approximately 0.5, meaning it is unable to decode its data across the three diversity combining techniques when NGDPA is employed, due to the low power allocation of only 0.15% of the overall power. Moreover, It can be noted that utilizing EGC enhances BER performance to varying degrees, contingent upon the user and the power allocation technique, compared to SC, as shown in Figure 4.9b. On average, EGC attains approximately 1.75 dB lower SNR at a BER of 10^{-5} compared to SC across all three power allocation techniques for the four users. Additionally, MRC demonstrates an improvement of around 1 dB lower SNR on average at BER of 10^{-5} compared to EGC across all three power allocation techniques, as illustrated in Figure 4.9c. The SNR values at a BER of 10^{-5} for SC, EGC, and MRC employing NGDPA, GRPA, and FPA techniques in a four-user scenario are summarized in Table 4.6.

Table 4.5 – The power distribution in four-user scenario.

Power allocation	p_1	p_2	p_3	p_4
NGDPA	0.15%	8.35%	37.4%	54.1%
GRPA	4.8%	6.5%	20.1%	68.6%
FPA	1.9%	6.4%	21.1%	70.6%

Table 4.6 – Summary of SNR values at a BER of 10^{-5} for SC, EGC, and MRC employing NGDPA, GRPA, and FPA techniques in a four-user scenario.

SC				
Power allocation	U_1	U_2	U_3	U_4
NGDPA	-	136.2 dB	130.6 dB	129.9 dB
GRPA	148 dB	141.4 dB	135.5 dB	122.5 dB
FPA	148.9 dB	140.8 dB	134.9 dB	121.1 dB
EGC				
NGDPA	-	134.5 dB	129.1 dB	128.3 dB
GRPA	146 dB	140.2 dB	133.4 dB	120.8 dB
FPA	146.6 dB	139 dB	133.1 dB	119.5 dB
MRC				
NGDPA	-	133.5 dB	128 dB	127.2 dB
GRPA	144.9 dB	139.1 dB	132.5 dB	119.8 dB
FPA	145.7 dB	137.9 dB	132.1 dB	118.4 dB

In the following analysis, the BER performance of SC, EGC and MRC employing NGDPA, GRPA and FPA in conjunction with NLUPA is presented, as shown in Figure 4.10. Unlike the three-user scenario, all users are paired in this case. The detailed power distribution for each technique is presented in Table 4.7. It is worth mentioning that U_1 experiences a significant improvement in performance across the three diversity combining techniques, as it is able to decode its own data. Furthermore, the BER performance of U_2, U_3 and U_4 shows considerable improvement for all power allocation techniques and diversity combining methods, with an average enhancement of approximately 12.5 dB at a BER of 10^{-5} compared to the scenario without pairing. It is observed that EGC improves BER performance with an average improvement of 2.4 dB at a BER of 10^{-5} compared to SC, as depicted in Figure 4.10b. Moreover, MRC results indicate an average

SNR reduction of approximately 0.5 dB at a BER of 10^{-5} compared to EGC across all three power allocation techniques, as illustrated in Figure 4.10c. Table 4.8 presents the SNR values at a BER of 10^{-5} for SC, EGC, and MRC employing NGDPA, GRPA, and FPA techniques in a four-user scenario with NLUPA.

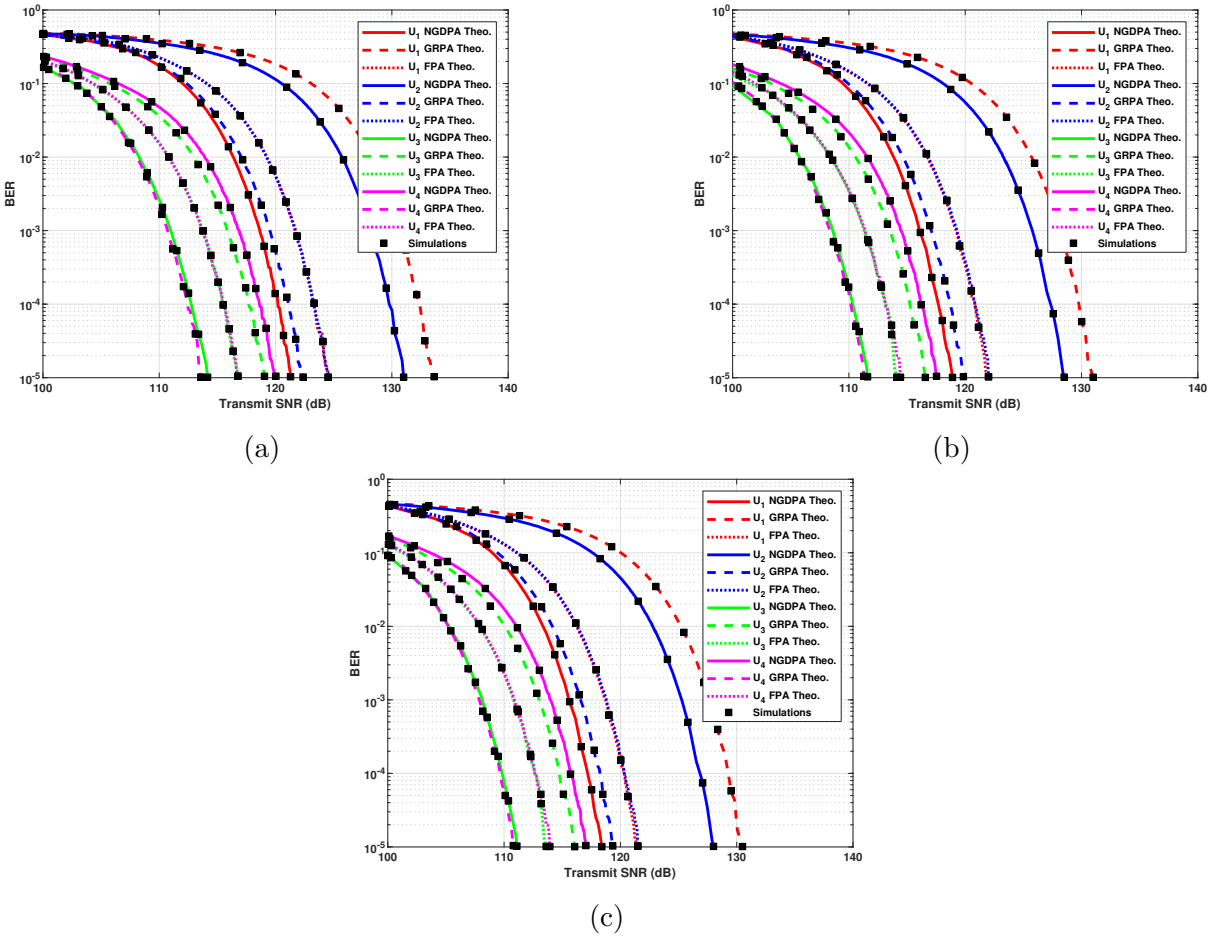

Figure 4.10 – BER vs. transmit SNR employing NGDPA, GRPA and FPA with four users ($N = 4$) applying NLUPA using (**a**) SC, (**b**) EGC, (**c**) MRC.

Table 4.7 – The power distribution in four-user scenario with NLUPA.

Power allocation	p_1	p_4	p_2	p_3
NGDPA	33%	67%	11.8%	88.2%
GRPA	9%	91%	28.8%	71.2%
FPA	23.1%	76.9%	23.1%	76.9%

Table 4.8 – Summary of SNR values at a BER of 10^{-5} for SC, EGC, and MRC employing NGDPA, GRPA, and FPA techniques in a four-user scenario with NLUPA.

SC				
Power allocation	U_1	U_4	U_2	U_3
NGDPA	121.3 dB	120 dB	131 dB	114.2 dB
GRPA	133.6 dB	113.6 dB	122.4 dB	119.1 dB
FPA	124.5 dB	116.8 dB	124.5 dB	116.8 dB
EGC				
NGDPA	119 dB	117.5 dB	128.6 dB	111.7 dB
GRPA	131 dB	111.4 dB	119.8 dB	116.5 dB
FPA	122 dB	114.2 dB	122 dB	114.2 dB
MRC				
NGDPA	118.4 dB	117 dB	128 dB	111.1 dB
GRPA	130.5 dB	110.8 dB	119.3 dB	116 dB
FPA	121.5 dB	113.8 dB	121.5 dB	113.6 dB

Figure 4.11 demonstrates the BER performance of SC, EGC and MRC employing NGDPA, GRPA and FPA in conjunction with UCGD. The power distribution for each power allocation technique is presented in Table 4.9. It is worth mentioning that the BER performance shows improvement for all power allocation techniques and diversity combining methods, with an average enhancement of approximately 1 dB at a BER of 10^{-5} compared to the scenario with NLUPA. Additionally, it is observed that EGC enhances BER performance by an average of 2.5 dB at a BER of 10^{-5} compared to SC, while MRC achieves an additional SNR reduction of approximately 0.6 dB at a BER of 10^{-5} compared to EGC across all three power allocation techniques, as depicted in Figures 4.11b and 4.11c. Table 4.10 summarizes the SNR values at a BER of 10^{-5} for SC, EGC, and MRC employing NGDPA, GRPA, and FPA techniques in a four-user scenario with UCGD.

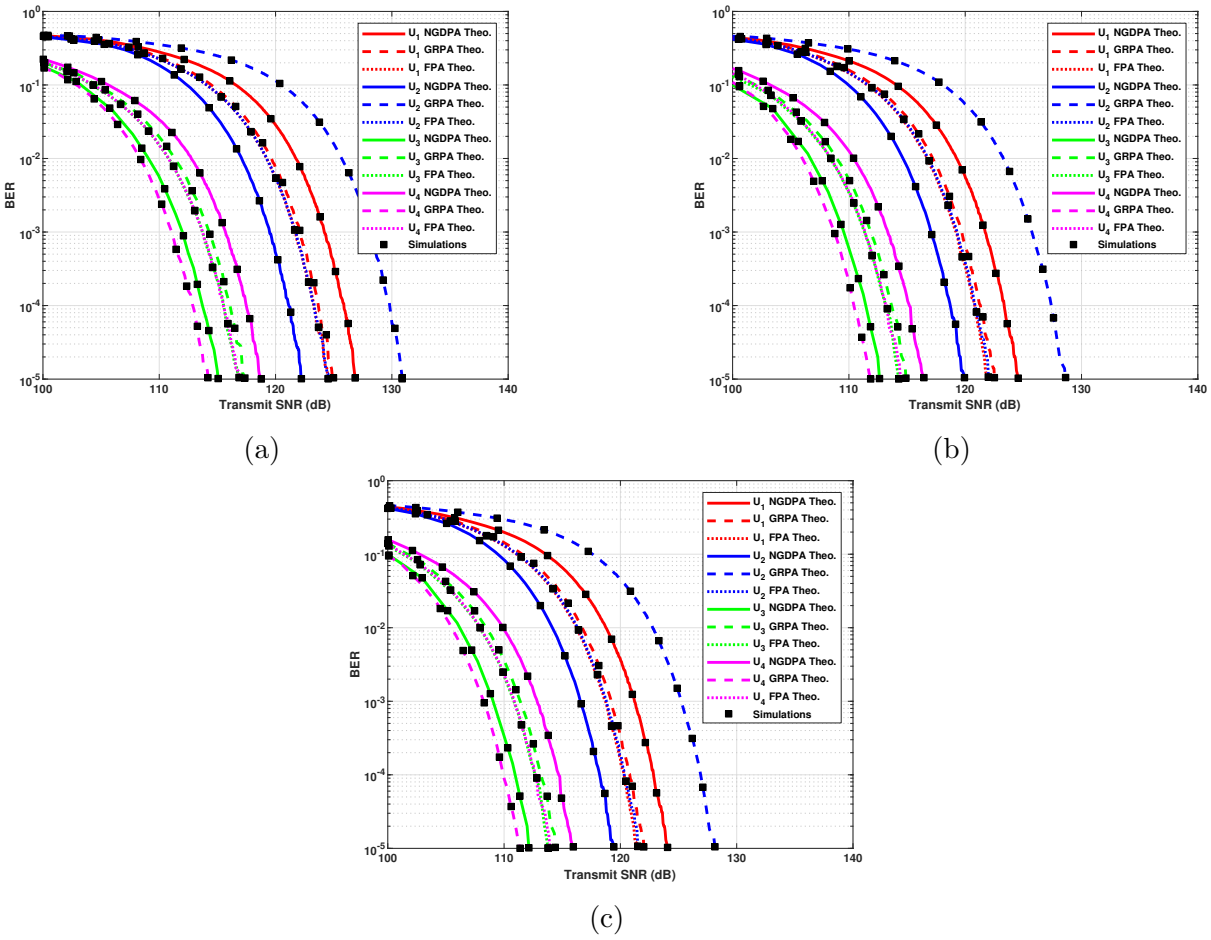

Figure 4.11 – BER vs. transmit SNR employing NGDPA, GRPA and FPA with four users ($N = 4$) applying UCGD using (**a**) SC, (**b**) EGC, (**c**) MRC.

Table 4.9 – The power distribution in four-user scenario with UCGD.

Power allocation	p_1	p_3	p_2	p_4
NGDPA	17.6%	82.4%	29.4%	70.6%
GRPA	22.8%	77.2%	11.2%	88.8%
FPA	23.1%	76.9%	23.1%	76.9%

Table 4.10 – Summary of SNR values at a BER of 10^{-5} for SC, EGC, and MRC employing NGDPA, GRPA, and FPA techniques in a four-user scenario with UCGD.

SC				
Power allocation	U_1	U_3	U_2	U_4
NGDPA	126.8 dB	115.1 dB	122.2 dB	118.8 dB
GRPA	124.9 dB	117.4 dB	130.9 dB	114.2 dB
FPA	124.5 dB	116.9 dB	124.5 dB	116.9 dB
EGC				
NGDPA	124.5 dB	112.7 dB	119.9 dB	116.5 dB
GRPA	122.4 dB	114.8 dB	128.7 dB	111.8 dB
FPA	122 dB	114.3 dB	122 dB	114.3 dB
MRC				
NGDPA	124 dB	112.1 dB	119.4 dB	115.9 dB
GRPA	122 dB	114.4 dB	128.1 dB	111.3 dB
FPA	121.5 dB	113.8 dB	121.5 dB	113.8 dB

4.6 Summary

In this chapter, we explored the BER performance of three low-complexity power allocation techniques in conjunction with two efficient user-pairing algorithms in indoor 2×2 MIMO-NOMA VLC systems. The system performance is compared utilizing three diversity combining techniques to enhance the reliability of the received signal. we derived an analytical expression for the BER for MIMO-NOMA-VLC and the accuracy of the derived analytical results was confirmed through comparisons with the corresponding simulation outcomes. The results indicate that the BER performance of the system utilizing user pairing algorithms significantly improves compared to scenarios without pairing in both three and four-user setups. Furthermore, in the four-user scenario, UCGD demonstrates an average enhancement of about 1 dB at a BER of 10^{-5} compared to NLUPA across all power allocation techniques and diversity combining methods.

Chapter 5

Conclusions and Future Work

5.1 Conclusions

Visible Light Communication (VLC) offers several advantages, making it a promising technology for future wireless communication systems. Its use of the unlicensed visible light spectrum provides abundant bandwidth, helping to alleviate the congestion in radio frequency (RF) communication systems. Additionally, VLC ensures high energy efficiency by leveraging existing lighting infrastructure, particularly light-emitting diodes (LEDs), to provide both illumination and communication. Its inherent security benefits, stemming from the fact that visible light cannot penetrate walls, make it ideal for environments where confidentiality is crucial. Moreover, the absence of electromagnetic interference makes VLC suitable for sensitive environments such as hospitals and aircraft.

However, VLC faces several challenges. The primary disadvantage is its dependency on line-of-sight (LOS) transmission, where physical obstructions can degrade signal quality. The coverage area is limited by the relatively small illumination footprint of LEDs, requiring dense deployment for continuous connectivity. Furthermore, the main challenge lies in the limited modulation bandwidth of LEDs.

To address these challenges, advanced techniques such as power domain non-orthogonal multiple access (NOMA), multiple-input multiple-output (MIMO), and user pairing algorithms were investigated in this thesis.

NOMA improves spectral efficiency by allowing multiple users to share the same time and frequency resources, while MIMO enhances spatial diversity by simultaneously utilizing multiple LED transmitters and photodiode (PD) receivers. User pairing algorithms help manage the complexity of NOMA's successive interference cancellation (SIC) process, enhancing resource allocation among users with varying channel conditions. These techniques, when combined, offer robust solutions to the limitations of VLC, enabling better utilization of its bandwidth and improving overall system performance.

In this study, we applied NOMA to a MIMO-based VLC system, utilizing three low-

complexity power allocation techniques: Fixed Power Allocation (FPA), Gain Ratio Power Allocation (GRPA), and Normalized Gain Difference Power Allocation (NGDPA). The achievable rate performance was evaluated for 2 × 2 MIMO-NOMA-VLC systems with different efficient user pairing algorithms, such as: next largest user pairing algorithm (NLUPA) and uniform channel gain difference (UCGD) algorithm. The study also explored the achievable rate performance in scenarios with both odd and even numbers of users. Furthermore, comparative analyses revealed significant performance enhancements with the presented schemes, especially when contrasted with NOMA without user pairing and orthogonal frequency division multiple access (OFDMA).

Moreover, we evaluated the bit error rate (BER) performance of the three power allocation techniques in conjunction with the two user pairing algorithms in indoor 2 × 2 MIMO-NOMA VLC systems utilizing three diversity combining techniques to enhance the reliability of the received signal. A detailed analysis was conducted to compare the diversity combining techniques: selection combining (SC), equal gain combining (EGC), and maximum ratio combining (MRC), assessing their impact on the BER under different configurations. An analytical expression for the BER in MIMO-NOMA-VLC systems was derived, and its accuracy was validated by comparing it with simulation results. Our analysis of different diversity combining techniques revealed that MRC consistently achieved the best BER performance across all power allocation schemes. EGC also demonstrated significant improvements over SC, particularly when paired with efficient power allocation techniques and user pairing algorithms. Our results demonstrate that the improvement in BER performance varies significantly, ranging from approximately 0.4 dB to 20 dB, depending on the power allocation technique and diversity combining method employed, as well as whether user pairing is implemented and which user pairing algorithm is used.

5.2 Recommendations for Future Work

The results of this dissertation suggest several intriguing paths that can be explored in future work.

1. Practical implementation of the system: A crucial aspect of future work is the practical implementation of the presented MIMO-NOMA-VLC system. Conducting real experiments to validate the theoretical models and optimize system parameters under practical constraints such as hardware imperfections, deployment complexity, and scalability would provide valuable insights for real deployment.

2. Effect of user mobility: In dynamic indoor environments, user mobility is a critical factor that affects the performance of MIMO-NOMA-VLC systems. Future work should analyze the impact of mobility on system performance and investigate the system's limitations, particularly regarding the maximum number of users it can handle in terms of achievable rate and BER.
3. Study of imperfect CSI: The current analysis assumes perfect channel state information (CSI). Future studies should focus on the effects of imperfect CSI on the performance of MIMO-NOMA-VLC systems, especially in practical settings where errors in channel estimation can degrade system performance.
4. Power allocation and user pairing optimization: Although the low-complexity power allocation techniques and user pairing algorithms applied in this thesis have demonstrated significant performance gains, more advanced methods, including deep learning techniques, could further enhance the system's efficiency.
5. VLC-RF/IR systems for bidirectional communication: Exploring hybrid VLC and RF or infrared (IR) systems for bidirectional communication presents a promising area of investigation. This approach enables bidirectional transmission by utilizing visible light for downlink communication and RF or IR for the uplink.
6. Enhancing modulation techniques: Future research could focus on developing higher-order modulation techniques to increase data rates and address bandwidth limitations in VLC systems, ultimately improving spectral efficiency.

List of Publications

International Journal Papers

1. **H. S. Ibrahim**, M. Abaza, A. Mansour, and A. Alfalou, "Performance Analysis of Power Allocation and User-Pairing Techniques for MIMO-NOMA in VLC Systems," *Photonics*, vol. 11, p. 206, 2024.
2. **H. S. Ibrahim**, M. Abaza, A. Mansour, and A. Alfalou, "A Survey of NOMA for VLC Systems: Research Challenges and Future Trends," *Sensors*, vol. 22, no. 4, p. 1395, Feb. 2022.

Conference Papers

1. **H. S. Ibrahim**, M. Abaza, A. Mansour, and A. Alfalou, "Diversity Combining and Power Allocation Techniques for NOMA-MIMO-VLC Systems," *Procedia Computer Science*, vol. 246, pp. 4683-4691, 2024.
2. M. A. Benbouzid, **H. S. Ibrahim**, N. Belghachem, and A. Mansour, "PD-NOMA Technique for Outdoor FSO-OCDMA Under Various Atmospheric Conditions," in *8th International Conference on Image and Signal Processing and their Applications (ISPA)*, Biskra, Algeria, 2024, pp. 1-6.
3. **H. S. Ibrahim**, M. Abaza, A. Mansour, and A. Alfalou, "Power Allocation Techniques for Non-orthogonal Multiple Access Based MIMO Visible Light Communication Systems," in *8th International Conference on Signal and Image Processing (ICSIP)*, Wuxi, China, 2023, pp. 930-934.

BIBLIOGRAPHY

[1] G. J. Holzmann and B. Pehrson, *The Early History of Data Networks*. Los Alamitos, Calif: IEEE Computer Society Press, 1995.

[2] L. U. Khan, « Visible light communication: Applications, architecture, standardization and research challenges », *Digital Communications and Networks*, vol. 3, no. 2, pp. 78–88, May 2017.

[3] S. Manohar and D. Razansky, « Photoacoustics: a historical review », *Advances in Optics and Photonics*, vol. 8, no. 4, pp. 586–617, Dec. 2016.

[4] S. Kaur, P. Singh, V. Tripathi, and R. Kaur, « Recent trends in wireless and optical fiber communication », *Global Transitions Proceedings*, International Conference on Intelligent Engineering Approach(ICIEA-2022), vol. 3, no. 1, pp. 343–348, Jun. 2022.

[5] J. Cho, J. H. Park, J. K. Kim, and E. F. Schubert, « White light-emitting diodes: History, progress, and future », *Laser & Photonics Reviews*, vol. 11, no. 2, p. 1 600 147, 2017.

[6] A. Nardelli, E. Deuschle, L. D. de Azevedo, J. L. N. Pessoa, and E. Ghisi, « Assessment of Light Emitting Diodes technology for general lighting: A critical review », *Renewable and Sustainable Energy Reviews*, vol. 75, pp. 368–379, Aug. 2017.

[7] S. Kumar, P. Tiwari, and M. Zymbler, « Internet of Things is a revolutionary approach for future technology enhancement: a review », *Journal of Big Data*, vol. 6, no. 1, p. 111, 2019.

[8] K. David and H. Berndt, « 6G Vision and Requirements: Is There Any Need for Beyond 5G? », *IEEE Vehicular Technology Magazine*, vol. 13, no. 3, pp. 72–80, Sep. 2018.

[9] Y. Tanaka, S. Haruyama, and M. Nakagawa, « Wireless optical transmissions with white colored LED for wireless home links », *in International Symposium on Personal Indoor and Mobile Radio Communications (PIMRC)*, vol. 2, London, UK, Sep. 2000, pp. 1325–1329.

[10] Y. Tanaka, T. Komine, S. Haruyama, and M. Nakagawa, « Indoor visible light data transmission system utilizing white LED lights », *IEICE Transactions on Communications*, vol. E86-B, no. 8, pp. 2440–2454, Aug. 2003.

[11] S. Kumar and P. Singh, « A Comprehensive Survey of Visible Light Communication: Potential and Challenges », *Wireless Personal Communications*, vol. 109, no. 2, pp. 1357–1375, Nov. 2019.

[12] S. Gupta, D. Roy, S. Bose, V. Dixit, and A. Kumar, « Illuminating the future: A comprehensive review of visible light communication applications », *Optics & Laser Technology*, vol. 177, p. 111 182, May 2024.

[13] S. Vappangi and V. V. Mani, « A survey on the integration of visible light communication with power line communication: Conception, applications and research challenges », *Optik*, vol. 266, p. 169 582, Sep. 2022.

[14] R. L. Priol, M. Hélard, S. Haese, and S. Roy, « MIMO Techniques in a Visible Light Communication (VLC) Link with Imager », *in Interregional NEWCAS Conference (NEWCAS)*, Quebec City, Canada, Jun. 2022, pp. 270–274.

[15] M. A. S. Sejan, M. H. Rahman, M. A. Aziz, D.-S. Kim, Y.-H. You, and H.-K. Song, « A Comprehensive Survey on MIMO Visible Light Communication: Current Research, Machine Learning and Future Trends », *Sensors*, vol. 23, no. 2, p. 739, 2023.

[16] S. A. H. Mohsan, M. Sadiq, Y. Li, A. V. Shvetsov, S. V. Shvetsova, and M. Shafiq, « NOMA-Based VLC Systems: A Comprehensive Review », *Sensors*, vol. 23, no. 6, p. 2960, 2023.

[17] H. Marshoud, S. Muhaidat, P. C. Sofotasios, S. Hussain, M. A. Imran, and B. S. Sharif, « Optical Non-Orthogonal Multiple Access for Visible Light Communication », *IEEE Wireless Communications*, vol. 25, no. 2, pp. 82–88, 2018.

[18] Z. Ghassemlooy, L. N. Alves, S. Zvanovec, and M. A. Khalighi, Eds., *Visible Light Communications: Theory and Applications*. Boca Raton: CRC Press, Dec. 2016.

[19] Y. Qian, « Beyond 5G Wireless Communication Technologies », *IEEE Wireless Communications*, vol. 29, no. 1, pp. 2–3, 2022.

[20] E. Zhang and N. Masoud, « Increasing GPS Localization Accuracy With Reinforcement Learning », *IEEE Transactions on Intelligent Transportation Systems*, vol. 22, no. 5, pp. 2615–2626, 2021.

[21] A. Feldmann et al., « The Lockdown Effect: Implications of the COVID-19 Pandemic on Internet Traffic », *in Proceedings of the ACM Internet Measurement Conference*, New York, USA, Oct. 2020, pp. 1–18.

[22] M. Candela, V. Luconi, and A. Vecchio, « Impact of the COVID-19 pandemic on the Internet latency: A large-scale study », *Computer Networks*, vol. 182, p. 107 495, 2020.

[23] M. Agiwal, A. Roy, and N. Saxena, « Next Generation 5G Wireless Networks: A Comprehensive Survey », *IEEE Communications Surveys Tutorials*, vol. 18, no. 3, pp. 1617–1655, 2016.

[24] A. Mansour, R. Mesleh, and M. Abaza, « New challenges in wireless and free space optical communications », *Optics and Lasers in Engineering*, vol. 89, pp. 95–108, Feb. 2017.

[25] R. K. Upadhyay, « Wireless Technology and its Applications: A Review Study », *International Journal of Computer Applications*,

[26] A. Dogra, R. K. Jha, and S. Jain, « A Survey on Beyond 5G Network With the Advent of 6G: Architecture and Emerging Technologies », *IEEE Access*, vol. 9, pp. 67 512–67 547, 2021.

[27] C. A. Gutierrez, O. Caicedo, and D. U. Campos-Delgado, « 5G and Beyond: Past, Present and Future of the Mobile Communications », *IEEE Latin America Transactions*, vol. 19, no. 10, pp. 1702–1736, 2021.

[28] R. F. Miranda, C. H. Barriquello, V. A. Reguera, *et al.*, « A Review of Cognitive Hybrid Radio Frequency/Visible Light Communication Systems for Wireless Sensor Networks », *Sensors*, vol. 23, no. 18, p. 7815, 2023.

[29] M. Z. Chowdhury, M. K. Hasan, M. Shahjalal, M. T. Hossan, and Y. M. Jang, « Optical Wireless Hybrid Networks: Trends, Opportunities, Challenges, and Research Directions », *IEEE Communications Surveys & Tutorials*, vol. 22, no. 2, pp. 930–966, Jan. 2020.

[30] D. Borah, A. Boucouvalas, C. Davis, S. Hranilovic, and K. Yiannopoulos, « A review of communication-oriented optical wireless systems », *EURASIP Journal on Wireless Communications and Networking*, vol. 2012, no. 1, p. 91, 2012.

[31] S. Kirthiga and M. Jayakumar, « Performance Studies and Review of Millimeter Wave MIMO Beamforming at 60 GHz », *Procedia Technology*, SMART GRID TECHNOLOGIES, vol. 21, pp. 658–666, Jan. 2015.

[32] G. Chittimoju and U. D. Yalavarthi, « A Comprehensive Review on Millimeter Waves Applications and Antennas », *Journal of Physics: Conference Series*, vol. 1804, no. 1, pp. 1–7, 2021.

[33] C. Seker, M. T. Guneser, and T. Ozturk, « A Review of Millimeter Wave Communication for 5G », *in 2nd International Symposium on Multidisciplinary Studies and Innovative Technologies (ISMSIT)*, Ankara, Turkey, Oct. 2018, pp. 1–5.

[34] R. K. Saha, « A Hybrid Interweave–Underlay Countrywide Millimeter-Wave Spectrum Access and Reuse Technique for CR Indoor Small Cells in 5G/6G Era », *Sensors*, vol. 20, no. 14, 2020.

[35] I. Union, « Traffic estimates for the years 2020 to 2030. Rep. ITU 2015,2370. Available online:https://www.itu.int/dms_pub/ itu-r/opb/rep/R-REP-M.2370-2015-PDF-E.pdf »,

[36] S. Chen, Y.-C. Liang, S. Sun, S. Kang, W. Cheng, and M. Peng, « Vision, Requirements, and Technology Trend of 6G: How to Tackle the Challenges of System Coverage, Capacity, User Data-Rate and Movement Speed », *IEEE Wireless Communications*, vol. 27, no. 2, pp. 218–228, Apr. 2020.

[37] Y. Xing, O. Kanhere, S. Ju, and T. S. Rappaport, « Indoor Wireless Channel Properties at Millimeter Wave and Sub-Terahertz Frequencies », *in IEEE Global Communications Conference (GLOBECOM)*, Hawaii, USA, Dec. 2019, pp. 1–6. arXiv: 1908.09765.

[38] A. Al-Saman, M. Mohamed, M. Cheffena, and A. Moldsvor, « Wideband Channel Characterization for 6G Networks in Industrial Environments », *Sensors*, vol. 21, no. 6, p. 2015, 2021.

[39] M. Z. Chowdhury, M. Shahjalal, S. Ahmed, and Y. M. Jang, « 6G Wireless Communication Systems: Applications, Requirements, Technologies, Challenges, and Research Directions », *IEEE Open Journal of the Communications Society*, vol. 1, pp. 957–975, Jul. 2020.

[40] L. Bariah, L. Mohjazi, S. Muhaidat, P. Sofotasios, G. Karabulut Kurt, and O. Dobre, « A Prospective Look: Key Enabling Technologies, Applications and Open Research Topics in 6G Networks », *IEEE Access*, vol. 8, pp. 174 792–174 820, Aug. 2020.

[41] N. Balani, P. Kalamdar, D. Pillay, K. Ladekar, K. Vishwakarma, and N. Pachpor, « Review on Optical Wireless Communication Technologies », *International Journal of All Research Education and Scientific Methods (IJARESM)*, vol. 9, no. 5, pp. 1174–1177, 2021.

[42] D. Garg and A. Nain, « Next generation optical wireless communication: a comprehensive review », *Journal of Optical Communications*, vol. 44, no. s1, s1535–s1550, Feb. 2023.

[43] M. Abaza, R. Mesleh, A. Mansour, and A. Alfalou, « MIMO techniques for high data rate free space optical communication system in log-normal channel », *in The International Conference on Technological Advances in Electrical, Electronics and Computer Engineering (TAEECE)*, Konya, Turkey, 2013-05-09/2013-05-11, pp. 1–5.

[44] M. Abaza, R. Mesleh, A. Mansour, and H. Aggoune, « Performance analysis of MISO multi-hop FSO links over log-normal channels with fog and beam divergence attenuations », *Optics Communications*, vol. 334, pp. 247–252, Jan. 2015.

[45] M. Uysal and H. Nouri, « Optical wireless communications — An emerging technology », *in International Conference on Transparent Optical Networks (ICTON)*, Graz, Austria, 2014-07-06/2014-07-10, pp. 1–7.

[46] K. Mihkel, « A systematic Review of Wireless Infrared Communication », M.S. Thesis, Dept. of Computer Science, University of Tartu, Estonia, 2020.

[47] C. Singh, J. John, Y. N. Singh, and K. K. Tripathi, « A Review of Indoor Optical Wireless Systems », *IETE Technical Review*, vol. 19, no. 1-2, pp. 3–17, Jan. 2002.

[48] X. Zhang, Y. Liu, Y. Wang, and J. Bai, « Performance analysis and optimization for non-uniformly deployed mmWave cellular network », *EURASIP Journal on Wireless Communications and Networking*, vol. 2019, no. 1, p. 49, 2019.

[49] P. Tiwari, V. Gahlaut, M. Kaushik, P. Rani, A. Shastri, and B. Singh, « Advancing 5G Connectivity: A Comprehensive Review of MIMO Antennas for 5G Applications », *International Journal of Antennas and Propagation*, vol. 2023, no. 1, pp. 1–19, Aug. 2023.

[50] O. Alsulami, A. T. Hussein, M. T. Alresheedi, and J. M. H. Elmirghani, « Optical Wireless Communication Systems, A Survey », *arXiv preprint arXiv:1812.11544*, Dec. 2018. arXiv: 1812.11544.

[51] A. Jahid, M. H. Alsharif, and T. J. Hall, « A Contemporary Survey on Free Space Optical Communication: Potential, Technical Challenges, Recent Advances and Research Direction », vol. 200, p. 103 311, Apr. 2022. arXiv: 2012.00155 [cs, eess, math].

[52] A. Malik and P. Singh, « Free Space Optics: Current Applications and Future Challenges », *International Journal of Optics*, vol. 2015, pp. 1–7, Nov. 2015.

[53] K. K. Soumya and J. Zacharias, « FSO Challenges and Solutions at 5G Networks - A Review », *in International Conference on Control, Communication and Computing (ICCC)*, Thiruvananthapuram, India, May 2023, pp. 1–5.

[54] M. Z. Chowdhury, M. T. Hossan, A. Islam, and Y. M. Jang, « A Comparative Survey of Optical Wireless Technologies: Architectures and Applications », *IEEE Access*, vol. 6, pp. 9819–9840, 2018.

[55] A. Refaai, M. Abaza, M. S. El-Mahallawy, and M. H. Aly, « Performance analysis of multiple NLOS UV communication cooperative relays over turbulent channels », *Optics Express*, vol. 26, no. 16, pp. 19 972–19 985, Aug. 2018.

[56] R. Yuan and M. Jianshe, « Review of ultraviolet non-line-of-sight communication », *China Communications*, vol. 13, pp. 63–75, Jun. 2016.

[57] L. Guo, Y. Guo, J. Wang, and T. Wei, « Ultraviolet communication technique and its application », *Journal of Semiconductors*, vol. 42, no. 15, p. 081 801, 2021.

[58] R. Yuan, X. Chu, T. Shan, and M. Peng, *Monte-Carlo Integration Based Multiple-Scattering Channel Modeling for Ultraviolet Communications in Turbulent Atmosphere*, Jun. 2024.

[59] A. A. B. Raj, P. Krishnan, U. Darusalam, *et al.*, « A Review–Unguided Optical Communications: Developments, Technology Evolution, and Challenges », *Electronics*, vol. 12, no. 8, p. 1922, 2023.

[60] G. Schirripa Spagnolo, L. Cozzella, and F. Leccese, « Underwater Optical Wireless Communications: Overview », *Sensors*, vol. 20, no. 8, p. 2261, 2020.

[61] K. Sun, W. Cui, and C. Chen, « Review of Underwater Sensing Technologies and Applications », *Sensors*, vol. 21, no. 23, p. 7849, 2021.

[62] N. Saeed, A. Celik, T. Y. Al-Naffouri, and M.-S. Alouini, « Underwater optical wireless communications, networking, and localization: A survey », *Ad Hoc Networks*, vol. 94, p. 101 935, 2019.

[63] *.Ke*, A. Nirmalathas, C. Lim, *et al.*, « Short-Range Optical Wireless Communications for Indoor and Interconnects Applications », *ZTE Communications*, vol. 14, pp. 13–22, 2016.

[64] K. Wang, « Remote-Powered Infrared Indoor Optical Wireless Communication Systems », *IEEE Photonics Technology Letters*, vol. 34, no. 9, pp. 455–458, May 2022.

[65] J. Kahn and J. Barry, « Wireless infrared communications », *Proceedings of the IEEE*, vol. 85, no. 2, pp. 265–298, Feb. 1997.

[66] V. Jungnickel, V. Pohl, S. Nonnig, and C. von Helmolt, « A physical model of the wireless infrared communication channel », *IEEE Journal on Selected Areas in Communications*, vol. 20, no. 3, pp. 631–640, Apr. 2002.

[67] P. Loureiro, F. Guiomar, and P. Monteiro, « Visible Light Communications: A Survey on Recent High-Capacity Demonstrations and Digital Modulation Techniques », *Photonics*, vol. 10, no. 9, p. 993, 2023.

[68] A. R. Ndjiongue, T. M. N. Ngatched, O. A. Dobre, and A. G. Armada, « VLC-Based Networking: Feasibility and Challenges », *IEEE Network*, vol. 34, no. 4, pp. 158–165, Jul. 2020.

[69] S. Al-Ahmadi, O. Maraqa, M. Uysal, and S. M. Sait, « Multi-User Visible Light Communications: State-of-the-Art and Future Directions », *IEEE Access*, vol. 6, pp. 70 555–70 571, 2018.

[70] L. Bravo Alvarez, S. Montejo-Sánchez, L. Rodríguez-López, C. Azurdia-Meza, and G. Saavedra, « A Review of Hybrid VLC/RF Networks: Features, Applications, and Future Directions », *Sensors*, vol. 23, no. 17, p. 7545, 2023.

[71] R. Ji, S. Wang, Q. Liu, and W. Lu, « High-Speed Visible Light Communications: Enabling Technologies and State of the Art », *Applied Sciences*, vol. 8, no. 4, p. 589, 2018.

[72] M. Kavehrad, « Broadband Room Service by Light », *Scientific American*, vol. 297, no. 1, pp. 82–87, Jul. 2007.

[73] C. Medina, M. Zambrano, and K. Navarro, « LED Based Visible Light Communication: Technology, Applications and Challenges – A Survey », *International Journal of Advances in Engineering & Technology*, vol. 8, no. 4, pp. 482–495, 2015.

[74] M. A. Arfaoui, M. D. Soltani, I. Tavakkolnia, *et al.*, « Physical Layer Security for Visible Light Communication Systems: A Survey », *IEEE Communications Surveys & Tutorials*, vol. 22, no. 3, pp. 1887–1908, 2020.

[75] Hao Ma, L. Lampe, and S. Hranilovic, « Integration of indoor visible light and power line communication systems », *in IEEE 17th International Symposium on Power Line Communications and Its Applications*, Johannesburg, South Africa: IEEE, Mar. 2013, pp. 291–296.

[76] H. S. Oh, J. H. Joo, J. H. Lee, J. H. Baek, J. W. Seo, and J. S. Kwak, « Structural Optimization of High-Power AlGaInP Resonant Cavity Light-Emitting Diodes for Visible Light Communications », *Japanese Journal of Applied Physics*, vol. 47, no. 8, p. 6214, 2008.

[77] H. Zhao, Y. Liu, K. Huang, X. Ji, and D. Wang, « A Study on Networking Scheme of Indoor Visible Light Communication Networks », *in IEEE 79th Vehicular Technology Conference (VTC Spring)*, Seoul, South Korea, May 2014, pp. 1–5.

[78] G. D. H. Niranga, A. R. Devidas, and M. V. Ramesh, « NeoCommLight: A Visible Light Communication System for RF-Restricted NICUs », *IEEE Access*, vol. 12, pp. 12 827–12 842, 2024.

[79] P. Dwivedy, V. Dixit, and A. Kumar, « A Survey on Visible Light Communication for 6G: Architecture, Application and Challenges », *in International Conference on Computer, Electronics & Electrical Engineering & Their Applications (IC2E3)*, Srinagar Garhwal, India, Jun. 2023, pp. 1–6.

[80] M. Obeed, A. M. Salhab, M.-S. Alouini, and S. A. Zummo, « On Optimizing VLC Networks for Downlink Multi-User Transmission: A Survey », *IEEE Communications Surveys & Tutorials*, vol. 21, no. 3, pp. 2947–2976, 2019.

[81] H. Sadat, M. Abaza, A. Mansour, and A. Alfalou, « A Survey of NOMA for VLC Systems: Research Challenges and Future Trends », *Sensors*, vol. 22, no. 4, p. 1395, 2022.

[82] Y. Almadani, D. Plets, S. Bastiaens, *et al.*, « Visible Light Communications for Industrial Applications—Challenges and Potentials », *Electronics*, vol. 9, no. 12, p. 2157, 2020.

[83] L. E. M. Matheus, A. B. Vieira, L. F. M. Vieira, M. A. M. Vieira, and O. Gnawali, « Visible Light Communication: Concepts, Applications and Challenges », *IEEE Communications Surveys & Tutorials*, vol. 21, no. 4, pp. 3204–3237, 2019.

[84] S. Rehman, S. Ullah, P. Chong, S. Yongchareon, and D. Komosny, « Visible Light Communication: A System Perspective—Overview and Challenges », *Sensors*, vol. 19, no. 5, p. 1153, 2019.

[85] In Hwan Park, Y. H. Kim, and J. Y. Kim, « Interference mitigation scheme of visible light communication systems for aircraft wireless applications », *in IEEE International Conference on Consumer Electronics (ICCE)*, Las Vegas, USA: IEEE, Jan. 2012, pp. 355–356.

[86] M. C. Ilter, A. A. Dowhuszko, K. K. Vangapattu, J. Hämäläinen, and R. Wichman, « Visible light communication-based positioning for indoor environments using supervised learning », *in GLOBECOM 2020 - 2020 IEEE Global Communications Conference*, Taipei, Taiwan, Dec. 2020, pp. 1–6.

[87] D. Karunatilaka, F. Zafar, V. Kalavally, and R. Parthiban, « LED Based Indoor Visible Light Communications: State of the Art », *IEEE Communications Surveys & Tutorials*, vol. 17, no. 3, pp. 1649–1678, 2015.

[88] L. Zhang, W. Zhang, and J. Sun, « VLC system implementation with white LEDs », *in IEEE International Conference on Communications in China (ICCC)*, Qingdao, China, Oct. 2017, pp. 1–6.

[89] S. Schmid, T. Richner, S. Mangold, and T. R. Gross, « EnLighting: An Indoor Visible Light Communication System Based on Networked Light Bulbs », *in IEEE International Conference on Sensing, Communication, and Networking (SECON)*, London, UK, Jun. 2016, pp. 1–9.

[90] P. H. Pathak, X. Feng, P. Hu, and P. Mohapatra, « Visible Light Communication, Networking, and Sensing: A Survey, Potential and Challenges », *IEEE Communications Surveys Tutorials*, vol. 17, no. 4, pp. 2047–2077, 2015.

[91] C.-H. Yeh and C.-W. Chow, « Phosphor-LED-Based Wireless Visible Light Communication (VLC) and Its Applications », *in Optoelectronics - Advanced Device Structures*, Jul. 2017.

[92] M. Galal, W. Ng, R. Binns, and A. Aziz, « Experimental Characterization of RGB LED Transceiver in Low-Complexity LED-to-LED Link », *Sensors*, vol. 20, p. 20, 2020.

[93] M. Katz and I. Ahmed, « Opportunities and Challenges for Visible Light Communications in 6G », *in 6G Wireless Summit (6G SUMMIT)*, Levi, Finland, Mar. 2020, pp. 1–5.

[94] D. C. O'Brien, L. Zeng, H. Le-Minh, G. Faulkner, J. W. Walewski, and S. Randel, « Visible light communications: Challenges and possibilities », *in International Symposium on Personal, Indoor and Mobile Radio Communications*, Cannes, France, Sep. 2008, pp. 1–5.

[95] Y. Chen, A. Bayesteh, Y. Wu, *et al.*, « Toward the Standardization of Non-Orthogonal Multiple Access for Next Generation Wireless Networks », *IEEE Communications Magazine*, vol. 56, no. 3, pp. 19–27, 2018.

[96] N. A. Alhaj, M. F. Jamlos, S. A. Manap, A. A. Bakhit, and R. Mamat, « A Review of Multiple Access Techniques and Frequencies Requirements towards 6G », *in International RF and Microwave Conference (RFM)*, Kuala Lumpur, Malaysia, Dec. 2022, pp. 1–4.

[97] A. W. Scott and R. Frobenius, « Multiple Access Techniques: FDMA, TDMA, AND CDMA », *in RF Measurements for Cellular Phones and Wireless Data Systems*, Hoboken, NJ, USA: Wiley, 2008, pp. 413–429.

[98] M. Shahjalal, M. M. Islam, M. K. Hasan, M. Z. Chowdhury, and Y. M. Jang, « Multiple Access Schemes for Visible Light Communication », *in International Conference on Ubiquitous and Future Networks (ICUFN)*, Zagreb, Croatia, Jul. 2019, pp. 115–117.

[99] H. Mathur and T. Deepa, « A Survey on Advanced Multiple Access Techniques for 5G and Beyond Wireless Communications », *Wireless Personal Communications*, vol. 118, no. 2, pp. 1775–1792, May 2021.

[100] Z. Ding, M. Peng, and H. V. Poor, « Cooperative Non-Orthogonal Multiple Access in 5G Systems », *IEEE Communications Letters*, vol. 19, no. 8, pp. 1462–1465, Aug. 2015.

[101] P. N. Thakre and S. B. Pokle, « A survey on Power Allocation in PD-NOMA for 5G Wireless Communication Systems », *in International Conference on Emerging Trends in Engineering and Technology - Signal and Information Processing (ICETET-SIP-22)*, Nagpur, India, Apr. 2022, pp. 1–5.

[102] J. Dai, K. Niu, and J. Lin, « Code-Domain Non-Orthogonal Multiple Access for Visible Light Communications », *in Globecom Workshops (GC Wkshps)*, Abu Dhabi, United Arab Emirates, Dec. 2018, pp. 1–6.

[103] Z. Ding, X. Lei, G. K. Karagiannidis, R. Schober, J. Yuan, and V. K. Bhargava, « A Survey on Non-Orthogonal Multiple Access for 5G Networks: Research Challenges and Future Trends », *IEEE Journal on Selected Areas in Communications*, vol. 35, no. 10, pp. 2181–2195, Oct. 2017.

[104] M. Moltafet, N. M. Yamchi, M. R. Javan, and P. Azmi, « Comparison Study Between PD-NOMA and SCMA », *IEEE Transactions on Vehicular Technology*, vol. 67, no. 2, pp. 1830–1834, Feb. 2018.

[105] S. S. Bawazir, P. C. Sofotasios, S. Muhaidat, Y. Al-Hammadi, and G. K. Karagiannidis, « Multiple Access for Visible Light Communications: Research Challenges and Future Trends », *IEEE Access*, vol. 6, pp. 26 167–26 174, 2018.

[106] M. W. Eltokhey, M.-A. Khalighi, and Z. Ghassemlooy, « Multiple Access Techniques for VLC in Large Space Indoor Scenarios: A Comparative Study », *in International Conference on Telecommunications (ConTEL)*, Graz, Austria, Jul. 2019, pp. 1–6.

[107] M. Guerra-Medina, O. González, B. Rojas-Guillama, J. Martín-González, F. Delgado, and J. Rabadan, « Ethernet-OCDMA system for multi-user visible light communications », *Electronics Letters*, vol. 48, pp. 227–228, Feb. 2012.

[108] S. Jawad, « Code division multiple-access techniques in optical fiber networks. I. Fundamental principles », *IEEE Transactions on Communications*, pp. 824–833, Jan. 1989.

[109] R. Róka, « Performance Analysis of Wavelength Division Multiplexing-Based Passive Optical Network Protection Schemes by Means of the Network Availability Evaluator », *Applied Sciences*, vol. 12, no. 15, p. 7911, 2022.

[110] H. Chun, S. Rajbhandari, G. Faulkner, *et al.*, « LED Based Wavelength Division Multiplexed 10 Gb/s Visible Light Communications », *Journal of Lightwave Technology*, vol. 34, no. 13, pp. 3047–3052, Jul. 2016.

[111] H. Harkat, P. Monteiro, A. Gameiro, F. Guiomar, and H. Farhana Thariq Ahmed, « A Survey on MIMO-OFDM Systems: Review of Recent Trends », *Signals*, vol. 3, no. 2, pp. 359–395, Jun. 2022.

[112] W. Gappmair, « On Parameter Estimation for Bandlimited Optical Intensity Channels », *Computation*, vol. 7, no. 1, p. 13, 2019.

[113] S. Hranilovic, « Minimum-Bandwidth Optical Intensity Nyquist Pulses », *IEEE Transactions on Communications*, vol. 55, no. 3, pp. 574–583, Mar. 2007.

[114] J. Dang and Z. Zhang, « Comparison of optical OFDM-IDMA and optical OFDMA for uplink visible light communications », *in International Conference on Wireless Communications and Signal Processing (WCSP)*, Huangshan, China, Oct. 2012, pp. 1–6.

[115] S. Dimitrov and H. Haas, « Information Rate of OFDM-Based Optical Wireless Communication Systems With Nonlinear Distortion », *Journal of Lightwave Technology*, vol. 31, no. 6, pp. 918–929, Mar. 2013.

[116] J. Carruthers and J. Kahn, « Multiple-subcarrier modulation for nondirected wireless infrared communication », *IEEE Journal on Selected Areas in Communications*, vol. 14, no. 3, pp. 538–546, 1996.

[117] J. Armstrong and A. Lowery, « Power efficient optical OFDM », *Electronics Letters*, vol. 42, no. 6, p. 370, 2006.

[118] M.-A. Khalighi, S. Long, S. Bourennane, and Z. Ghassemlooy, « PAM- and CAP-Based Transmission Schemes for Visible-Light Communications », *IEEE Access*, vol. 5, pp. 27 002–27 013, 2017.

[119] Y. Yang, C. Chen, P. Du, X. Deng, and J. Luo, « Low complexity ofdm vlc system enabled by spatial summing modulation », *Optics Express*, vol. 27, no. 21, pp. 30 788–30 795, 2019.

[120] Y. Dong, X. Cao, Z. Sun, Y. Huang, and X. Deng, « Two-dimensional adaptive-bandwidth bit and power loading for mimo-ofdm vlc communications », *Optics Express*, vol. 32, no. 25, pp. 44 031–44 048, 2024.

[121] X. Deng, Mardanikorani, G. Zhou, and J.-P. Linnartz, « DC-bias for Optical OFDM in Visible Light Communications », *IEEE Access*, vol. 7, pp. 98 319–98 330, Jul. 2019.

[122] Z. Chen, D. A. Basnayaka, and H. Haas, « Space Division Multiple Access for Optical Attocell Network Using Angle Diversity Transmitters », *Journal of Lightwave Technology*, vol. 35, no. 11, pp. 2118–2131, 2017.

[123] R. C. Kizilirmak, *Non-Orthogonal Multiple Access (NOMA) for 5G Networks. In Towards 5G Wireless Networks—A Physical Layer Perspective*. London, UK: Intechopen Limited, Dec. 2016.

[124] Z. Ding, P. Fan, and H. V. Poor, « Impact of User Pairing on 5G Nonorthogonal Multiple-Access Downlink Transmissions », *IEEE Transactions on Vehicular Technology*, vol. 65, no. 8, pp. 6010–6023, 2016.

[125] K. Higuchi and A. Benjebbour, « Non-orthogonal Multiple Access (NOMA) with Successive Interference Cancellation for Future Radio Access », *IEICE Transactions on Communications*, vol. E98.B, pp. 403–414, Mar. 2015.

[126] A. Assaidah, O. C. Satya, H. Satria, Y. Adnan, K. Saleh, and C.-W. Chow, « NOMA or MIMO Effects Severer BER in VLC Network Performance? », *in International Workshop on Artificial Intelligence and Image Processing (IWAIIP)*, Yogyakarta, Indonesia, Dec. 2023, pp. 289–293.

[127] A. Akbar, S. Jangsher, and F. A. Bhatti, « NOMA and 5G emerging technologies: A survey on issues and solution techniques », *Computer Networks*, vol. 190, p. 107 950, May 2021.

[128] R. Abbas, « VLC systems using NOMA techniques: An overview », *Physical Communication*, vol. 60, p. 102 144, Aug. 2023.

[129] T. Cover, « Broadcast channels », *IEEE Transactions on Information Theory*, vol. 18, no. 1, pp. 2–14, Jan. 1972.

[130] H. Marshoud, P. C. Sofotasios, S. Muhaidat, G. K. Karagiannidis, and B. S. Sharif, « On the Performance of Visible Light Communication Systems With Non-Orthogonal Multiple Access », *IEEE Transactions on Wireless Communications*, vol. 16, no. 10, pp. 6350–6364, Oct. 2017.

[131] H. Sadat, M. Abaza, S. M. Gasser, and H. ElBadawy, « Performance Analysis of Cooperative Non-Orthogonal Multiple Access in Visible Light Communication », *Applied Sciences*, vol. 9, no. 19, p. 4004, 2019.

[132] L. Yin, W. O. Popoola, X. Wu, and H. Haas, « Performance Evaluation of Non-Orthogonal Multiple Access in Visible Light Communication », *IEEE Transactions on Communications*, vol. 64, no. 12, pp. 5162–5175, Dec. 2016.

[133] Z. Ding, Z. Yang, P. Fan, and H. V. Poor, « On the Performance of Non-Orthogonal Multiple Access in 5G Systems with Randomly Deployed Users », *IEEE Signal Processing Letters*, vol. 21, no. 12, pp. 1501–1505, Dec. 2014.

[134] O. Maraqa, A. S. Rajasekaran, S. Al-Ahmadi, H. Yanikomeroglu, and S. M. Sait, « A Survey of Rate-Optimal Power Domain NOMA With Enabling Technologies of Future Wireless Networks », *IEEE Communications Surveys & Tutorials*, vol. 22, no. 4, pp. 2192–2235, 2020.

[135] H. Marshoud, V. M. Kapinas, G. K. Karagiannidis, and S. Muhaidat, « Non-Orthogonal Multiple Access for Visible Light Communications », *IEEE Photonics Technology Letters*, vol. 28, no. 1, pp. 51–54, Jan. 2016.

[136] G. Wang, Y. Shao, L.-K. Chen, and J. Zhao, « Subcarrier and Power Allocation in OFDM-NOMA VLC Systems », *IEEE Photonics Technology Letters*, vol. 33, no. 4, pp. 189–192, Feb. 2021.

[137] J. Li, T. Gao, B. He, W. Zheng, and F. Lin, « Power Allocation and User Grouping for NOMA Downlink Systems », *Applied Sciences*, vol. 13, no. 4, p. 2452, 2023.

[138] L. Lei, D. Yuan, C. K. Ho, and S. Sun, « Power and Channel Allocation for Non-Orthogonal Multiple Access in 5G Systems: Tractability and Computation », *IEEE Transactions on Wireless Communications*, vol. 15, no. 12, pp. 8580–8594, 2016.

[139] B. Di, L. Song, and Y. Li, « Sub-Channel Assignment, Power Allocation, and User Scheduling for Non-Orthogonal Multiple Access Networks », *IEEE Transactions on Wireless Communications*, vol. 15, no. 11, pp. 7686–7698, Nov. 2016.

[140] Z. Yang, W. Xu, and Y. Li, « Fair Non-Orthogonal Multiple Access for Visible Light Communication Downlinks », *IEEE Wireless Communications Letters*, vol. 6, pp. 66–69, 2016.

[141] T. V. Pham and A. T. Pham, « Max-Min Fairness and Sum-Rate Maximization of MU-VLC Local Networks », *in IEEE Globecom Workshops (GC Wkshps)*, San Diego, USA, Dec. 2015, pp. 1–6.

[142] M. Kashef, M. Ismail, M. Abdallah, K. Qaraqe, and E. Serpedin, « Power allocation for maximizing energy efficiency of mixed RF/VLC wireless networks », *in European Signal Processing Conference (EUSIPCO)*, Nice, France, Aug. 2015, pp. 1441–1445.

[143] Q.-V. Pham and C. S. Hong, « Power Control for Harmonic Utility in Non-Orthogonal Multiple Access based Visible Light Communications », *arXiv preprint arXiv:1801.04655*, Aug. 2018. arXiv: 1801.04655 [cs].

[144] R. Jiang, Q. Wang, H. Haas, and Z. Wang, « Joint User Association and Power Allocation for Cell-Free Visible Light Communication Networks », *IEEE Journal on Selected Areas in Communications*, vol. 36, no. 1, pp. 136–148, Jan. 2018.

[145] M. F. Hanif, Z. Ding, T. Ratnarajah, and G. K. Karagiannidis, « A Minorization-Maximization Method for Optimizing Sum Rate in the Downlink of Non-Orthogonal Multiple Access Systems », *IEEE Transactions on Signal Processing*, vol. 64, no. 1, pp. 76–88, Jan. 2016.

[146] H. Shen, Y. Wu, W. Xu, and C. Zhao, « Optimal power allocation for downlink two-user non-orthogonal multiple access in visible light communication », *Journal of Communications and Information Networks*, vol. 2, no. 4, pp. 57–64, Dec. 2017.

[147] R. Mitra and V. Bhatia, « Precoded Chebyshev-NLMS-Based Pre-Distorter for Nonlinear LED Compensation in NOMA-VLC », *IEEE Transactions on Communications*, vol. 65, no. 11, pp. 4845–4856, Nov. 2017.

[148] Y. Yapici and I. Guvenc, « Non-Orthogonal Multiple Access for Mobile VLC Networks with Random Receiver Orientation », *arXiv preprint arXiv:1801.04888*, Feb. 2019. arXiv: 1801.04888 [cs, math].

[149] M. Mounir, M. B. El_Mashade, and A. Mohamed Aboshosha, « On The Selection of Power Allocation Strategy in Power Domain Non-Orthogonal Multiple Access (PD-NOMA) for 6G and Beyond », *Transactions on Emerging Telecommunications Technologies*, vol. 33, no. 6, e4289, 2022.

[150] S. Tao, H. Yu, Q. Li, and Y. Tang, « Performance analysis of gain ratio power allocation strategies for non-orthogonal multiple access in indoor visible light communication networks », *EURASIP Journal on Wireless Communications and Networking*, vol. 2018, no. 1, p. 154, 2018.

[151] S. Tao, H. Yu, Q. Li, and Y. Tang, « Strategy-Based Gain Ratio Power Allocation in Non-Orthogonal Multiple Access for Indoor Visible Light Communication Networks », *IEEE Access*, vol. 7, pp. 15 250–15 261, 2019.

[152] M. W. Baidas, Z. Bahbahani, and E. Alsusa, « User association and channel assignment in downlink multi-cell NOMA networks: A matching-theoretic approach », *EURASIP Journal on Wireless Communications and Networking*, vol. 2019, no. 1, p. 220, 2019.

[153] R. P. Devi and N. Prabakaran, « Rate Performance and Spectral Efficiency of Non-Orthogonal Multiple Access for 5G Communication », *International Journal of Recent Technology and Engineering (IJRTE)*, vol. 8, no. 2, pp. 3337–3341, Jul. 2019.

[154] F. Wei, T. Zhou, T. Xu, and H. Hu, « BER Analysis for Uplink NOMA in Asymmetric Channels », *IEEE Communications Letters*, vol. 24, no. 11, pp. 2435–2439, Nov. 2020.

[155] W. Xia, Y. Zhou, G. Yang, and R. T. Chen, « Optimal Minimum Euclidean Distance-Based Precoder for NOMA With Finite-Alphabet Inputs », *IEEE Access*, vol. 7, pp. 45 123–45 136, 2019.

[156] Y. Saito, A. Benjebbour, Y. Kishiyama, and T. Nakamura, « System-level performance evaluation of downlink non-orthogonal multiple access (NOMA) », *in International Symposium on Personal, Indoor, and Mobile Radio Communications (PIMRC)*, London, UK, Sep. 2013, pp. 611–615.

[157] M. M. El-Sayed, A. S. Ibrahim, and M. M. Khairy, « Power allocation strategies for Non-Orthogonal Multiple Access », *in International Conference on Selected Topics in Mobile & Wireless Networking (MoWNeT)*, Cairo, Egypt, Apr. 2016, pp. 1–6.

[158] Z. Yang, Z. Ding, P. Fan, and N. Al-Dhahir, « A General Power Allocation Scheme to Guarantee Quality of Service in Downlink and Uplink NOMA Systems », *IEEE Transactions on Wireless Communications*, vol. 15, no. 11, pp. 7244–7257, Nov. 2016.

[159] W. Bai, T. Yao, H. Zhang, and V. C. M. Leung, « Research on Channel Power Allocation of Fog Wireless Access Network Based on NOMA », *IEEE Access*, vol. 7, pp. 32 867–32 873, 2019.

[160] M. B. Janjua, D. B. da Costa, and H. Arslan, « User Pairing and Power Allocation Strategies for 3D VLC-NOMA Systems », *IEEE Wireless Communications Letters*, vol. 9, no. 6, pp. 866–870, Jun. 2020.

[161] X. Liu, H. Yu, Y. Zhu, and E. Zhang, « Power Allocation Algorithm of Optical MIMO NOMA Visible Light Communications », *in International Conference on Electronics Information and Emergency Communication (ICEIEC)*, Beijing, China, Jul. 2019, pp. 1–5.

[162] C. Chen, W.-D. Zhong, H. Yang, and P. Du, « On the Performance of MIMO-NOMA-Based Visible Light Communication Systems », *IEEE Photonics Technology Letters*, vol. 30, no. 4, pp. 307–310, Feb. 2018.

[163] H. Wang, F. Wang, and R. Li, « Enhancing power allocation efficiency of NOMA aided-MIMO downlink VLC networks », *Optics Communications*, vol. 454, p. 124 497, 2020.

[164] A. Li, A. Harada, and H. Kayama, « A Novel Low Computational Complexity Power Assignment Method for Non-orthogonal Multiple Access Systems », *IEICE Transactions on Fundamentals of Electronics, Communications and Computer Sciences*, vol. E97.A, no. 1, pp. 57–68, 2014.

[165] B. Narottama and S. Y. Shin, « Dynamic Power Allocation for Non-Orthogonal Multiple Access with User Mobility », *in Information Technology, Electronics and Mobile Communication Conference (IEMCON)*, Vancouver, Canada, Oct. 2019, pp. 0442–0446.

[166] M. Ahmed, R. Yasmin, H. Homyara, and M. Hasan, « Generalized Power Allocation (GPA) Scheme for Non-Orthogonal Multiple Access (NOMA) Based Wireless Communication System », *International Journal of Computer Science, Engineering and Information Technology*, vol. 08, pp. 01–09, Dec. 2018.

[167] N. Otao, Y. Kishiyama, and K. Higuchi, « Performance of Non-orthogonal Multiple Access with SIC in Cellular Downlink Using Proportional Fair-Based Resource Allocation », *IEICE Transactions on Communications*, vol. E98.B, no. 2, pp. 344–351, 2015.

[168] Q. Zhao, J. Jiang, Y. Wang, and J. Du, « A low complexity power allocation scheme for NOMA-based indoor VLC systems », *Optics Communications*, vol. 463, p. 125 383, May 2020.

[169] I. A. Elewah, F. Jasman, and S. Ng, « Performance enhancement for a non-orthogonal multiple access system using 4 × 4 multiple-input multiple-output visible-light communication », *Optical Engineering*, vol. 59, no. 12, p. 126 104, 2020.

[170] C. Chen, S. Fu, X. Jian, M. Liu, X. Deng, and Z. Ding, « NOMA for Energy-Efficient LiFi-Enabled Bidirectional IoT Communication », *IEEE Transactions on Communications*, vol. 69, no. 3, pp. 1693–1706, Mar. 2021.

[171] Z. Tahira, H. M. Asif, A. A. Khan, S. Baig, S. Mumtaz, and S. Al-Rubaye, « Optimization of Non-Orthogonal Multiple Access Based Visible Light Communication Systems », *IEEE Communications Letters*, vol. 23, no. 8, pp. 1365–1368, Aug. 2019.

[172] Y. S. Eroglu, C. K. Anjinappa, İ. Guvenc, and N. Pala, « Slow Beam Steering and NOMA for Indoor Multi-User Visible Light Communications », *IEEE Transactions on Mobile Computing*, vol. 20, no. 4, pp. 1627–1641, Apr. 2021.

[173] M. Wafik Eltokhey, M.-A. Khalighi, and Z. Ghassemlooy, « Power Allocation Optimization in NOMA-Based Multi-Cell VLC Networks », *in International Symposium on Wireless Communication Systems (ISWCS)*, Berlin, Germany, Sep. 2021, pp. 1–5.

[174] A. S. Sadiq, A. A. Dehkordi, S. Mirjalili, and Q.-V. Pham, « Nonlinear marine predator algorithm: A cost-effective optimizer for fair power allocation in NOMA-VLC-B5G networks », *Expert Systems with Applications*, vol. 203, p. 117 395, 2022.

[175] Q. Li, T. Shang, and T. Tang, « Adaptive optimal power allocation scheme based on intelligent user association for NOMA-VLC systems », *Optical Switching and Networking*, vol. 47, p. 100 714, Feb. 2023.

[176] X. Zhang, Q. Gao, C. Gong, and Z. Xu, « User Grouping and Power Allocation for NOMA Visible Light Communication Multi-Cell Networks », *IEEE Communications Letters*, vol. 21, no. 4, pp. 777–780, Apr. 2017.

[177] Y. Fu, Y. Hong, L.-K. Chen, and C. W. Sung, « Enhanced Power Allocation for Sum Rate Maximization in OFDM-NOMA VLC Systems », *IEEE Photonics Technology Letters*, vol. 30, no. 13, pp. 1218–1221, Jul. 2018.

[178] S. Ma, Y. He, H. Li, S. Lu, F. Zhang, and S. Li, « Optimal Power Allocation for Mobile Users in Non-Orthogonal Multiple Access Visible Light Communication Networks », *IEEE Transactions on Communications*, vol. 67, no. 3, pp. 2233–2244, Mar. 2019.

[179] Z. Dong, T. Shang, Q. Li, and T. Tang, « Adaptive Power Allocation Scheme for Mobile NOMA Visible Light Communication System », *Electronics*, vol. 8, no. 4, p. 381, 2019.

[180] S. Feng, T. Bai, and L. Hanzo, « Joint Power Allocation for the Multi-User NOMA-Downlink in a Power-Line-Fed VLC Network », *IEEE Transactions on Vehicular Technology*, vol. 68, no. 5, pp. 5185–5190, May 2019.

[181] Q. Li, T. Shang, T. Tang, and Z. Dong, « Optimal Power Allocation Scheme Based on Multi-Factor Control in Indoor NOMA-VLC Systems », *IEEE Access*, vol. 7, pp. 82 878–82 887, 2019.

[182] H. Liu, P. Zhu, Y. Chen, and M. Huang, « Power Allocation for Downlink Hybrid Power Line and Visible Light Communication System », *IEEE Access*, vol. 8, pp. 24 145–24 152, 2020.

[183] Z. Dong, T. Shang, Q. Li, and T. Tang, « Differential evolution-based optimal power allocation scheme for NOMA-VLC systems », *Optics Express*, vol. 28, no. 15, p. 21 627, 2020.

[184] H. Marshoud, P. C. Sofotasios, S. Muhaidat, and G. K. Karagiannidis, « Multi-user techniques in visible light communications: A survey », *in International Conference on Advanced Communication Systems and Information Security (ACOSIS)*, Marrakesh, Morocco, Oct. 2016, pp. 1–6.

[185] A. Nuwanpriya, S.-W. Ho, and C. S. Chen, « Indoor MIMO Visible Light Communications: Novel Angle Diversity Receivers for Mobile Users », *IEEE Journal on Selected Areas in Communications*, vol. 33, no. 9, pp. 1780–1792, Sep. 2015.

[186] C. Chen, W.-D. Zhong, H. Yang, S. Zhang, and P. Du, « Reduction of SINR Fluctuation in Indoor Multi-Cell VLC Systems Using Optimized Angle Diversity Receiver », *Journal of Lightwave Technology*, vol. 36, no. 17, pp. 3603–3610, Sep. 2018.

[187] M. K. Aljohani, O. Z. Aletri, K. D. Alazwary, *et al.*, « NOMA Visible Light Communication System with Angle Diversity Receivers », *in International Conference on Transparent Optical Networks (ICTON)*, Bari, Italy, Jul. 2020, pp. 1–5.

[188] V. Dixit and A. Kumar, « Performance analysis of angular diversity receiver based MIMO–VLC system for imperfect CSI », *Journal of Optics*, vol. 23, no. 8, p. 085 701, 2021.

[189] T. Fath and H. Haas, « Performance Comparison of MIMO Techniques for Optical Wireless Communications in Indoor Environments », *IEEE Transactions on Communications*, vol. 61, no. 2, pp. 733–742, Feb. 2013.

[190] A. Mansour, J. Youssef, and K.-C. Yao, « Underdetermined BSS of MISO OSTBC Signals », *Lecture Notes in Computer Science*, pp. 678–685, 2009.

[191] M. Safari and M. Uysal, « Do We Really Need OSTBCs for Free-Space Optical Communication with Direct Detection? », *IEEE Transactions on Wireless Communications*, vol. 7, no. 11, pp. 4445–4448, Nov. 2008.

[192] U. F. Siddiqi, O. Narmanlioglu, M. Uysal, and S. M. Sait, « Joint bit and power loading for adaptive MIMO OFDM VLC systems », *Transactions on Emerging Telecommunications Technologies*, vol. 31, no. 7, 2020.

[193] X. Guo, Y. Yuan, C. Pan, and J. Xiao, « Interleaved superposed-64QAM-constellation design for spatial multiplexing visible light communication systems », *Optics Express*, vol. 29, no. 15, pp. 23 341–23 356, Jul. 2021.

[194] A. K. Gupta and A. Chockalingam, « Performance of MIMO Modulation Schemes With Imaging Receivers in Visible Light Communication », *Journal of Lightwave Technology*, vol. 36, no. 10, pp. 1912–1927, May 2018.

[195] Z. Ding, R. Schober, and H. V. Poor, « A General MIMO Framework for NOMA Downlink and Uplink Transmission Based on Signal Alignment », *IEEE Transactions on Wireless Communications*, vol. 15, no. 6, pp. 4438–4454, Jun. 2016.

[196] B. Lin, Z. Ghassemlooy, X. Tang, Y. Li, and M. Zhang, « Experimental demonstration of optical MIMO NOMA-VLC with single carrier transmission », *Optics Communications*, vol. 402, pp. 52–55, Nov. 2017.

[197] J. Shi, Y. Hong, J. He, R. Deng, and L.-K. Chen, « Experimental Demonstration of OQAM-OFDM based MIMO-NOMA over Visible Light Communications », *in Optical Fiber Communication Conference (OFC)*, San Diego, USA, Mar. 2018, pp. 1–3.

[198] A. K. Mishra and A. Trivedi, « Performance analysis of MIMO-NOMA-Based Indoor Visible Light Communication in Single Reflection Environment », *in Conference on Information and Communication Technology*, Allahabad, India, Dec. 2019, pp. 1–5.

[199] V. S. Rajput, D. R. Ashok, and A. Chockalingam, « MU-MIMO NOMA with Linear Precoding Techniques in Indoor Downlink VLC Systems », *in Vehicular Technology Conference (VTC2020-Spring)*, Antwerp, Belgium, May 2020, pp. 1–6.

[200] R. Raj and A. Dixit, « Performance Evaluation of Power Allocation Schemes for Non-Orthogonal Multiple Access in MIMO Visible Light Communication Links », *in International Conference on Signal Processing and Communications (SPCOM)*, Bangalore, India, Jul. 2020, pp. 1–5.

[201] M. K. Jha, N. Kumar, and Y. V. S. Lakshmi, « NOMA MIMO Visible Light Communication with ZF-SIC and MMSE-SIC », *in PhD Colloquium on Ethically Driven Innovation and Technology for Society (PhD EDITS)*, Bangalore, India, Nov. 2020, pp. 1–2.

[202] Q. Zhao, B. Bai, J. Jiang, S. Ma, and J. Zhu, « User pairing and power allocation scheme for NOMA-based indoor VLC systems », *in International Conference on Optoelectronic and Microelectronic Technology and Application*, vol. 11617, Nanjing, China: SPIE, Dec. 2020, pp. 434–437.

[203] S. M. R. Islam, M. Zeng, O. A. Dobre, and K.-S. Kwak, « Resource Allocation for Downlink NOMA Systems: Key Techniques and Open Issues », *IEEE Wireless Communications*, vol. 25, no. 2, pp. 40–47, Apr. 2018.

[204] T. Dogra and M. R. Bharti, « User pairing and power allocation strategies for downlink NOMA-based VLC systems: An overview », *AEU - International Journal of Electronics and Communications*, vol. 149, p. 154 184, May 2022.

[205] S. Mounchili and S. Hamouda, « New User Grouping Scheme for Better User Pairing in NOMA Systems », *in International Wireless Communications and Mobile Computing (IWCMC)*, Limassol, Cyprus, Jun. 2020, pp. 820–825.

[206] E. M. Almohimmah, M. T. Alresheedi, A. F. Abas, and J. Elmirghani, « A Simple User Grouping and Pairing Scheme for Non-Orthogonal Multiple Access in VLC System », *in International Conference on Transparent Optical Networks (ICTON)*, Bucharest, Romania, Jul. 2018, pp. 1–4.

[207] M. B. Shahab, M. Irfan, M. F. Kader, and S. Shin, « User Pairing Schemes for Capacity Maximization in Non-orthogonal Multiple Access Systems », *Wireless Communications and Mobile Computing*, vol. 16, pp. 2884–2894, Sep. 2016.

[208] H. Liu, B. Huang, J. Yang, *et al.*, « Joint user grouping and power allocation in VLC-NOMA system », *Physical Communication*, vol. 54, p. 101 841, 2022.

[209] Y. Han, X. Zhou, L. Yang, and S. Li, « A Bipartite Matching Based User Pairing Scheme for Hybrid VLC-RF NOMA Systems », *in International Conference on Computing, Networking and Communications (ICNC)*, Maui, USA, Mar. 2018, pp. 480–485.

[210] L. Zhu, J. Zhang, Z. Xiao, X. Cao, and D. O. Wu, « Optimal User Pairing for Downlink Non-Orthogonal Multiple Access (NOMA) », *IEEE Wireless Communications Letters*, vol. 8, no. 2, pp. 328–331, 2019.

[211] H. You, Z. Pan, N. Liu, and X. You, « User Clustering Scheme for Downlink Hybrid NOMA Systems Based on Genetic Algorithm », *IEEE Access*, vol. 8, pp. 129 461–129 468, 2020.

[212] L. Yin, X. Wu, and H. Haas, « On the performance of non-orthogonal multiple access in visible light communication », *in International Symposium on Personal, Indoor, and Mobile Radio Communications (PIMRC)*, Hong Kong, China, Aug. 2015, pp. 1354–1359.

[213] V. Dixit and A. Kumar, « Performance analysis of non-line of sight visible light communication systems », *Optics Communications*, vol. 459, p. 125 008, Mar. 2020.

[214] J. Barry, J. Kahn, W. Krause, E. Lee, and D. Messerschmitt, « Simulation of multipath impulse response for indoor wireless optical channels », *IEEE Journal on Selected Areas in Communications*, vol. 11, no. 3, pp. 367–379, Apr. 1993.

[215] V. Dixit and A. Kumar, « Performance analysis of L-PPM modulated NLOS-VLC system with perfect and imperfect CSI », *Journal of Optics*, vol. 23, no. 1, p. 015 702, 2020.

[216] T. Komine and M. Nakagawa, « Fundamental analysis for visible-light communication system using LED lights », *IEEE Transactions on Consumer Electronics*, vol. 50, no. 1, pp. 100–107, 2004.

[217] H. S. Ibrahim, M. Abaza, A. Mansour, and A. Alfalou, « Power Allocation Techniques for Non-orthogonal Multiple Access Based MIMO Visible Light Communication Systems », *in International Conference on Signal and Image Processing (ICSIP)*, Wuxi, China, Jul. 2023, pp. 930–934.

[218] W. J. Ryu, J. W. Kim, and D.-S. Kim, « On the Reliability Evaluation in Downlink VLC NOMA Systems », *in International Conference on Information and Communication Technology Convergence (ICTC)*, Oct. 2021, pp. 989–993.

[219] X. Liu, Y. Wang, F. Zhou, S. Ma, R. Q. Hu, and D. W. K. Ng, « Beamforming Design for Secure MISO Visible Light Communication Networks With SLIPT », *IEEE Transactions on Communications*, vol. 68, no. 12, pp. 7795–7809, Dec. 2020.

[220] V. Dixit and A. Kumar, « An Exact Error Analysis of Multi-User RC/MRC Based MIMO-NOMA-VLC System With Imperfect SIC », *IEEE Access*, vol. 9, pp. 136 710–136 720, 2021.

[221] A. Gorcin and H. Arslan, « An ofdm signal identification method for wireless communications systems », *IEEE Transactions on Vehicular Technology*, vol. 64, no. 12, pp. 5688–5700, 2015.

[222] F. Fang, L. Zhang, Z. Wu, and J. Jiang, « Energy Consumption Minimization for Multi-carrier NOMA Visible Light Communication Downlinks », *in International Conference on Communications in China (ICCC)*, Jul. 2021, pp. 876–880.

[223] H. Li, Z. Huang, Y. Xiao, S. Zhan, and Y. Ji, « A Power and Spectrum Efficient NOMA Scheme for VLC Network Based on Hierarchical Pre-Distorted LACO-OFDM », *IEEE Access*, vol. 7, pp. 48 565–48 571, 2019.

[224] P. Song, F. Gong, and L. Cai, « User Pairing and Power Allocation for FTN-based SC-NOMA and MIMO-NOMA Systems Considering User Fairness », *arXiv preprint arXiv:2207.02653*, Jul. 2022. arXiv: 2207.02653.

[225] H. Bany Salameh, H. Al-Obiedollah, M. Al-Hayek, S. Abdel-Razeq, and A. Al-ajlouni, « A two-dimensional OMA-NOMA user-pairing and power-minimization approach for opportunistic B5G-enabled IoT networks », *Cluster Computing*, vol. 26, no. 2, pp. 1113–1124, Apr. 2023.

[226] K. Kandasamy and M. Selvaraj, « Scaled selection combining receiver for cooperative noma-based 5g cellular systems », *AEU - International Journal of Electronics and Communications*, vol. 177, p. 155 251, Aug. 2024.

[227] V. Kumar, B. Cardiff, and M. Flanagan, « Performance analysis of noma with generalised selection combining receivers », *Electronics Letters*, vol. 55, no. 25, pp. 1364–1367, Aug. 2019.

[228] V. Dixit and A. Kumar, « An exact BER analysis of NOMA-VLC system with imperfect SIC and CSI », *AEU - International Journal of Electronics and Communications*, vol. 138, p. 153 864, Aug. 2021.

COLLEGES SCIENCES
BRETAGNE POUR L'INGENIEUR
LOIRE ET LE NUMERIQUE

ENSTA BRETAGNE

Titre : Amélioration des communications optiques sans fil à l'aide de techniques hybrides et d'accès multiple

Mots-clés : Communication par lumière visible (VLC), intégration de l'accès multiple non-orthogonal (NOMA), techniques d'allocation de puissance, algorithmes de couplage d'utilisateurs

Résumé : La communication par lumière visible (VLC) est une technologie prometteuse pour la connectivité sans fil en intérieur, offrant une transmission de données à haute vitesse tout en atténuant la congestion du spectre. Cette thèse explore l'intégration de l'accès multiple non-orthogonal (NOMA) et des techniques à entrées multiples et sorties multiples (MIMO) pour améliorer l'efficacité des systèmes VLC. Nous examinons différentes techniques d'allocation de puissance, notamment l'allocation de puissance fixe (FPA), selon le ratio de gain (GRPA) et selon la différence de gain normalisée (NGDPA), afin d'optimiser la répartition des ressources entre les utilisateurs. Divers algorithmes de couplage d'utilisateurs, tels que l'algorithme de couplage à différence la plus proche (NLUPA) et celui de la différence de gain uniforme (UCGD), sont également étudiés. Le débit total réalisable dans des scénarios avec un nombre pair et impair d'utilisateurs est évalué et comparé aux performances du NOMA sans couplage et de l'OFDMA. De plus, l'analyse du taux d'erreur binaire (BER) est réalisée sous différentes techniques de diversité (SC, EGC, MRC). Nous dérivons également une expression analytique du BER pour un nombre arbitraire d'utilisateurs, fournissant des informations précieuses sur les performances des systèmes NOMA-MIMO-VLC.

Title: Enhancement of Optical Wireless Communications Using Hybrid and Multiple Access Techniques

Keywords: Visible light communication (VLC), non-orthogonal multiple access (NOMA), power allocation techniques, user pairing algorithms

Abstract: Visible light communication (VLC) is a promising technology for indoor wireless connectivity, offering high-speed data transmission and alleviating spectrum congestion. This thesis explores the integration of non-orthogonal multiple access (NOMA) and multiple-input multiple-output (MIMO) techniques to improve VLC system efficiency. We investigate various power allocation techniques, including fixed power allocation (FPA), gain ratio power allocation (GRPA), and normalized gain difference power allocation (NGDPA), to enhance resource distribution among users. Different user pairing algorithms, such as next-largest-difference user-pairing algorithm (NLUPA) and uniform channel gain difference (UCGD), are also examined. The achievable sum rate for NOMA-MIMO-VLC systems is analyzed in scenarios with even and odd user numbers, and results are compared with NOMA without pairing and orthogonal frequency division multiple access (OFDMA). Furthermore, we assess the bit error rate (BER) performance under diversity techniques, such as selection combining (SC), equal gain combining (EGC), and maximum ratio combining (MRC). Finally, we derive an analytic expression for BER for an arbitrary number of users. Overall, our comprehensive study provides valuable insights into NOMA-MIMO-VLC systems for indoor wireless communication.